

Contents lists available at [ScienceDirect](https://www.sciencedirect.com)

## Progress in Materials Science

journal homepage: [www.elsevier.com/locate/pmatsci](http://www.elsevier.com/locate/pmatsci)

## Recent advances in scalable synthesis and performance of Janus polymer/inorganic nanocomposites

Yijiang Liu<sup>a</sup>, Jialin Wang<sup>a</sup>, Yue Shao<sup>b</sup>, Renhua Deng<sup>c</sup>, Jintao Zhu<sup>c</sup>, Zhenzhong Yang<sup>b,\*</sup><sup>a</sup> College of Chemistry, Xiangtan University, Xiangtan 411105, Hunan Province, China<sup>b</sup> Department of Chemical Engineering, Tsinghua University, Beijing 100084, China<sup>c</sup> School of Chemistry and Chemical Engineering, Huazhong University of Science and Technology, Wuhan 430074, China

## ARTICLE INFO

## Keywords:

Polymer/inorganic nanocomposites  
 Janus materials  
 Compartmentalization  
 Scalable synthesis  
 Properties  
 Applications

## ABSTRACT

Janus nanomaterials composed of two compartments with dissimilar compositions and/or functionalities have garnered considerable interest over the past several decades owing to their diverse nanostructures and intriguing properties arising from the two constituents and microstructures. Janus polymer/inorganic nanocomposites represent a class of unique materials that afford synergistic features of polymers and inorganic substance, rendering appealing properties and promising applications. Various synthetic routes have been developed to craft a host of Janus materials with tunable composition, morphology and microstructures. This review focuses on the recent advances in rational design, precision synthesis, and performance of a set of Janus polymer/inorganic nanocomposites. Four main synthetic strategies are discussed, including Pickering emulsion interfacial synthesis, conventional emulsion interfacial synthesis, confined self-assembly of block copolymers, and seeded swelling emulsion polymerization. The detailed synthetic methods and strictly Janus characteristics are highlighted. This review aims to attract broad interests in the polymer and nanomaterial communities by directing the research focus on judicious design and synthesis as well as large-scale production of Janus polymer/inorganic nanocomposites, thereby imparting the further exploration of their extraordinary attributes and practical applications.

## 1. Introduction

The concept of Janus, a Roman God with two faces placed back to back, was coined by de Gennes in his Nobel lecture in 1991 to designate a family of particles with two different compositions and thus physical properties compartmentalized on the same particles [1]. Notably, Lee et al. firstly used the term of Janus to describe the asymmetric latex of polystyrene/poly(methyl methacrylate) (PS/PMMA) via seeded emulsion polymerization in 1985 [2]. Diverse synthetic strategies have been developed to attain a large family of Janus particles with tunable shapes, including sphere-like [3-6], dumbbell-like [7,8], cylindrical [9,10], and sheet-like (disk-shaped) [11,12]. Janus particles find promising applications as colloidal surfactants [13,14], building blocks for superstructures [15,16], self-propelled nanomotors [17,18], optical detection and display [19,20], and biomedicine [21-23]. Janus nanoparticles could form Jamming structures at the emulsion interface, thereby providing a powerful tool to process liquid droplets for deformation and

\* Corresponding author.

E-mail address: [yangzhenzhong@tsinghua.edu.cn](mailto:yangzhenzhong@tsinghua.edu.cn) (Z. Yang).<https://doi.org/10.1016/j.pmatsci.2021.100888>

Received 21 March 2021; Received in revised form 21 October 2021; Accepted 4 November 2021

Available online 11 November 2021

0079-6425/© 2021 Elsevier Ltd. All rights reserved.

printing [24]. Janus materials have witnessed increasingly growing development over the past several decades, and a variety of new Janus materials have been crafted and displayed unique properties and diverse potential applications. In order to meet the requirements for practical applications, it is key to developing methods for the large-scale fabrication of Janus materials with tunable morphology, size and composition [25].

In this review, we concentrate on the recent advances in interfacial synthesis of Janus materials, which carry the potential to easily scale up produce the Janus materials. The review is composed of two main parts: (1) recent advances in synthesis of Janus polymer/inorganic nanocomposites, and (2) representative performances and potential applications of the Janus materials. The ability to delicately exploit the interfacial characteristics is crucial to effectively synthesize Janus materials with anisotropic shape and asymmetric composition as depicted in Fig. 1. Interfacial synthesis represents a simple yet robust route to simultaneously protect and compartmentalize the constituents to yield Janus structures. In both Pickering emulsion interfacial synthesis and conventional emulsion interface synthesis, the Janus emulsion interface plays a key role in providing a highly effective way for protection and selective modification (Fig. 1a) as noted above. A temporal template is provided for self-organized materialization by either sol-gel process or biphasic polymerization to achieve a Janus shell (Fig. 1b). On the other hand, in the case of Janus nanomaterials formed via solvent evaporation of a copolymer emulsion droplet, the generation of a neutral interface is vital for self-assembly and thus the shape of the derived Janus materials (Fig. 1c). For the seeded emulsion polymerization, the ability to control the interfacial interactions is key to render a distinctly compositional compartmentalization of Janus materials with well-defined shape and microstructure (Fig. 1d). Notably, some exciting applications of Janus materials, dictated by the size, shape, microstructure, and compartmentalization of compositions and functions, are then discussed. Finally, the challenges and opportunities for the reliable crafting of Janus materials with more fascinating architectures and tailored functionality, and developing Janus materials in newly emerging fields are outlined.

## 2. Pickering emulsion interfacial synthesis

When a colloidal particle is immobilized at a fluidic interface, the particle is automatically divided into two parts immersing in the two immiscible phases. The aspect ratio of the two parts is determined by the contact angle. Selective modifications of the two parts are allowed in the orthogonal mode. In the case of two-dimensional (2D) planar interface, the sequential modification is general to achieve the asymmetric structure by utilizing various physical or chemical approaches while the particles are partially embedded in a solid matrix. The modification techniques involve masking [26-29], micro-contact printing [30-33], e-beam sputtering [34-36], chemical vapor deposition [37,38], and contact with reactive media [39,40]. The features of this strategy have been well summarized in the previous review papers. It is noted that the 2D protection synthesis is less efficient with a small quantity of Janus materials.

Compared with the 2D synthesis, three-dimensional (3D) interfacial synthesis is advantageous to large-scale synthesize Janus particles due to the significantly increased interface area. When the particles are entrapped at a liquid/liquid interface, a Pickering emulsion is formed [41]. The immobilization is thermodynamically controlled depending on the contact angle between the particle and the liquids, ensuring the emulsion interface covered by the particle monolayer. The aspect ratio of the two parts immersing in the two immiscible phases is determined by wettability of the particle in the phases thus contact angle. Wettability of the particle is controlled by proper modifications. After the two parts are sequentially modified, a Janus particle is achieved whose Janus balance is tunable. The term of Janus balance is analogous to the concept of hydrophilic-lipophilic balance of a surfactant, describing more

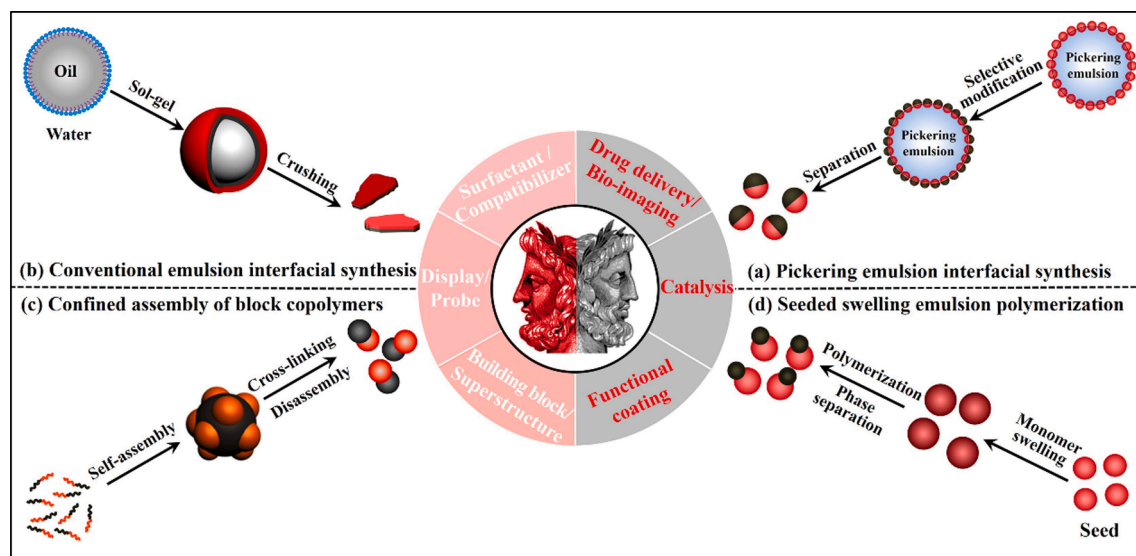
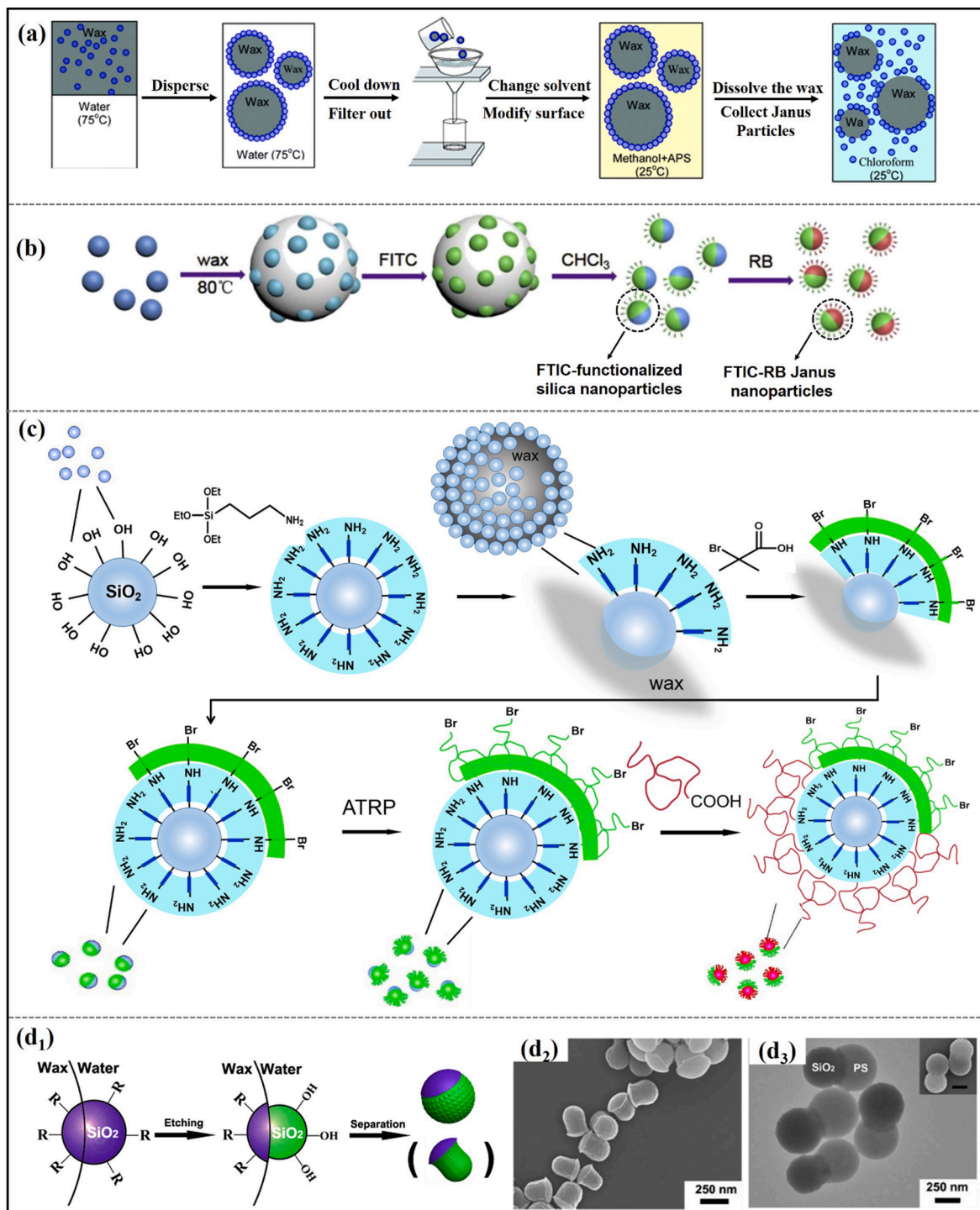


Fig. 1. Representative synthetic approaches to Janus polymer/inorganic nanocomposites and the representative performances. (a) Pickering emulsion interfacial synthesis. (b) Conventional emulsion interfacial synthesis. (c) Confined self-assembly of block copolymers. (d) Seeded swelling emulsion polymerization.



**Fig. 2.** (a) Schematic synthesis of the Janus particle at a frozen wax Pickering emulsion interface. Adapted with permission from Ref. [42]. Copyright 2006 American Chemical Society. (b) Schematic synthesis of the fluorescent Janus silica particle and detection of pH in a cell. Adapted with permission from Ref. [45]. Copyright 2019 Elsevier. (c) The bi-component Janus particle by a combined method of “grafting from” and “grafting to”. Adapted with permission from Ref. [47]. Copyright 2008 American Chemical Society. (d<sub>1</sub>) Schematic synthesis of the Janus silica particle by selective etching the particle at the frozen wax Pickering emulsion interface, (d<sub>2</sub>) the non-spherical Janus silica particle after a further etching, (d<sub>3</sub>) the Janus silica/PS colloidal dimers by polymerization of styrene onto the vinyl-group side of the Janus silica particle. Adapted with permission from Ref. [51]. Copyright 2009 The Royal Society of Chemistry.

hydrophilic or lipophilic feature of the Janus materials.

### 2.1. Frozen Pickering emulsion interfacial synthesis

At a liquid/liquid fluid Pickering emulsion interface, the colloidal particle is rotatable which usually leads to failure in distinct compartmentalization of the particle. It is reasonable that the rotation can be prohibited when the Pickering emulsion interface is frozen. Selective modification becomes easier to achieve Janus structures. Wax is usually selected as the oil phase, which becomes solidified at a lower temperature. Accordingly, the elegant strategy is proposed to synthesize Janus materials at a frozen wax/water Pickering emulsion interface upon cooling below the melt temperature of wax (Fig. 2a) [42,43]. As a consequence, rotation of the particles is prohibited at the emulsion interface. The free particles left in the continuous phase can be easily separated from the solidified wax spheres by either filtration or centrifugation. All the derived particles will become Janus after the selective modification. The continuous phase can be exchanged with other poor solvents for example methanol, providing suitable media for further reactions. Selective modification of the exposed side of the particle toward the aqueous phase is allowed by aminopropyltriethoxysilane (APS) to introduce hydrophilic amine- group while the other side is protected by embedding within the solid wax phase. After liberating the asymmetric silica particles from the wax spheres by dissolution, the opposite side is exposed for another modification by using octadecanetriethylchlorosilane (OTS) to introduce the hydrophobic group. Distinct compartmentalization of the two groups is guaranteed to derive the Janus particles. Composition and performance of the two opposite sides are broadly varied. Wettability of the particle is easily adjusted by feeding surfactants besides surface modification. As the result, penetration depth of the particle at a Pickering emulsion interface is tunable. Janus balance of the derived particle is adjustable after the modifications. The penetration depth is also affected by feeding electrolytes thus influencing the Janus balance. At a given penetration depth, Janus balance can be further controlled by using different agents for example silanes with either more hydrophobic or hydrophilic groups to modify the silica particle [44]. Functional groups can be easily conjugated onto the desired sides of a Janus silica particle along the frozen Pickering emulsion interfacial synthesis. As an example, a fluorescent Janus silica particle is obtained with fluorescein isothiocyanate (FITC) green-emissive and rhodamine B (RB) red-emissive dyes distinctly compartmentalized onto the opposite sides of the Janus particle (Fig. 2b) [45]. The Janus probe displays dual emission bands at 530 and 580 nm upon excitation at 488 nm, which is promising in bioanalysis and bioimaging. When the mesoporous silica particles are immobilized at the frozen wax/water emulsion interface, hyaluronic acid (HA) is conjugated onto the exposed side in the presence of EDC-HCl/NHS. 2,3-Dimethylmaleic anhydride (DMMA) is conjugated onto the opposite side of HA-containing Janus particle. After a further loading of doxorubicin hydrochloride (DOX) within the mesopore, the Janus particle is capable for tumor-targeting therapy. The Janus particle demonstrates the synergistic effect of active targeting and charge reversal, which can effectively deliver drug in the tumor cells for killing [46]. While the amine- group capped silica particle is anchored at the frozen Pickering emulsion interface, the atom transfer radical polymerization (ATRP) initiator can be grafted onto the exposed side by amination [47]. Two polymers are sequentially conjugated by “grafting from” via ATRP and “grafting to” via coupling reaction with carboxylic acid capped polymers (Fig. 2c). When the polymers are responsive, phase behavior of the Janus particle can be triggered according to external stimuli [48]. Similarly, a Janus silica particle is synthesized with poly(acrylic acid) (PAA) and PS brushes onto the opposite sides. Catalytic metallic NPs can be *in situ* grown at PAA to derive functional Janus particles [49]. Other polymerizations for example UV-induced surface initiated polymerization can be used to graft polymers to achieve the Janus composite particles [50].

Although growth of materials onto the exposed side of the anchored particles at a Pickering emulsion interface is effective for compartmentalization, excess growth may cause coalescence among the particles. After release from the interface, some aggregates may coexist with the Janus particles. Alternatively, selective etching the exposed side of the particle at the Pickering emulsion interface provides another effective way for the compartmentalization. As an example, the fresh silanol group is exposed after the functional corona is etched from the exposed side with ammonium fluoride ( $\text{NH}_4\text{F}$ ). A Janus structure is thus achieved. Starting from the fresh surface, a favorable growth is allowed by using various silanes with desired functional groups. The corona is generated by modification with 3-aminopropyltriethoxysilane (APS) or 3-methacryloxypropyltrimethoxysilane (MPS) [51]. After etching with  $\text{NH}_4\text{F}$ , the amine- or vinyl- group is eliminated while the functional group at the opposite side is protected within the wax phase (Fig. 2d). Shape of the silica particle is tunable with etching, evolving into mushroom-like shape. By growing polymers from the residual vinyl- group, a variety of non-spherical Janus composite particles are yielded with polymer caps. Microstructure of the cap is tunable from smooth to nanoscale roughness under varied polymerization conditions.

The Janus titania particle is achieved after degrading the functional corona from the exposed side by UV irradiation when the particle is anchored at the frozen Pickering emulsion interface [52]. After coupling with phosphonate agents, new Janus particles with desired functional groups are derived [53]. The etching strategy can be extended to derive a huge family of Janus materials. Against the  $\text{Fe}_3\text{O}_4$ @silica core/shell particle, the exterior surface of the silica shell can be selectively modified to introduce ionic liquid (IL) moieties while the interior surface is protected. After the inward etching of the  $\text{Fe}_3\text{O}_4$  core, the interior surface of the silica shell is exposed for another modification, such as grafting a thermal responsive poly(N-isopropylacrylamide) (PNIPAM). The functional Janus cage is promising in interfacial catalysis [54]. By stepwise etching, the sphere of  $\text{AlSi}_{10}$  metallic alloy can be divided into multi-layered compartments with varied compositions. A Janus porous sphere is achieved with the coral-like architecture [55]. The coral-like structure is conducive to promote mass transfer by the magnified capillary force.

When the homogeneous particle is too small below tens nanometers, the absorption energy at the interface becomes comparable with thermal energy. It is difficult to form monolayer of nanoparticles at the interface. Aggregates appear and cover the interface, making the Pickering emulsion interfacial synthesis invalid. It is necessary to introduce functional groups at the emulsion interface to induce the formation of monolayer with smaller particles. As one example, PAA-*b*-PS is used to stabilize the paraffin/water emulsion

interface with PAA groups exposed toward the aqueous phase. A monolayer of the amine- group capped  $\text{Fe}_3\text{O}_4@/\text{SiO}_2$  core/shell nanoparticle is formed by preferential absorption onto the paraffin sphere surface *via* hydrogen bonding with the exposed PAA block. Afterwards, poly(ethylene oxide) with aldehyde group (PEO-CHO) is used to modify the exposed side of the absorbed nanoparticle *via* Schiff's base bonding [56]. After detaching from the wax surface, the Janus nanoparticle of PS- $\text{Fe}_3\text{O}_4@/\text{SiO}_2$ -PEO composite is derived. The Janus nanoparticle is amphiphilic which can be driven with a magnet. In the reverse water/oil emulsion stabilized with PAA-b-PS, the emulsion interface becomes robust after crosslinking the interior surface with PAA. A Janus colloidosome is derived and can be easily functionalized by favorable growth of metallic NPs at the interior surface [57].

## 2.2. Fluidic Pickering emulsion interfacial synthesis

Although frozen Pickering emulsion interface is effective to synthesize Janus materials, a problem remains if a fluidic Pickering emulsion interface is suitable to synthesize Janus material. It is key to restrict rotation of the particles at the fluidic liquid/liquid interface. Synchronous grafting different polymers onto the opposite sides of the particles thus introducing amphiphilicity provides the effective way to restrict the rotation at the fluidic interface. This strategy makes the synthesis of Janus particles feasible at the liquid/

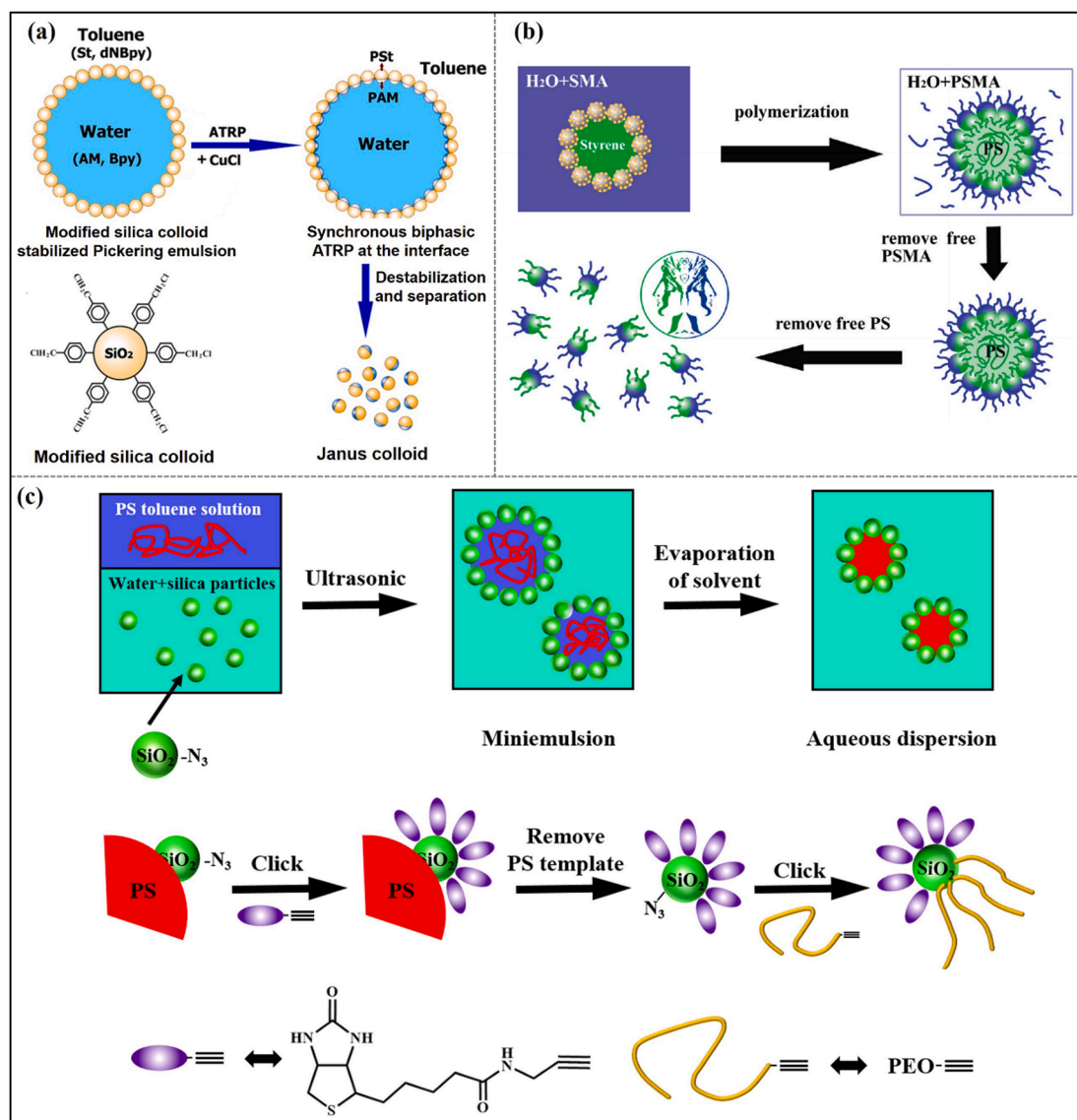


**Fig. 3.** (a) Janus particle by the synchronous biphasic ATRP grafting at a Pickering emulsion interface. Adapted with permission from Ref. [58]. Copyright 2008 Wiley. (b) Janus silica particle by surface-initiated free radical polymerization at a Pickering emulsion interface. Adapted with permission from Ref. [59]. Copyright 2009, American Chemical Society. (c) Bio-conjugated Janus particle by click reaction. Adapted with permission [60]. Copyright 2009 American Chemical Society.

liquid interface. The ATRP initiator covered silica particle is used to stabilize a Pickering emulsion. Since the particle is more hydrophobic, the continuous phase is oil, while water is the dispersed phase. In the internal aqueous phase, an example hydrophilic monomer of acrylamide (AAM) and the ligand of 2,2'-bipyridine (Bpy) are fed for the ATRP grafting of hydrophilic PAAm at the side exposed toward the aqueous phase. Similarly, in the external toluene phase, styrene (St) and oily ligand of 4,4'-di-5-nonyl-2,2'-bipyridine (dNBpy) are fed for the grafting of hydrophobic PS at the other side. Upon feeding CuBr, the concurrent ATRP grafting polymerizations are initiated onto the corresponding sides in the two phases (Fig. 3a). The particle becomes amphiphilic at the beginning stage. Grafting degrees of the two polymers are increased with prolonging polymerization time. The Janus particle is achieved by simple centrifugation without dissolution of the dispersed phase [58]. Along with the similar approach, the Janus particle is synthesized by the common free radical polymerization (Fig. 3b). [59] After introducing amine-group onto the silica particle by using 3-triethoxysilylpropylamine, the free radical initiator of 4S, 4'S-bis(N-hydroxysuccinimidy)-4,4'-((E)-diazene-1,2-diyl) bis(4-cyanopentanoate) (derived from 4,4'-azobis(4-cyanopentanoic acid)) is conjugated after activation with N-hydroxysuccinimide. Upon immobilization at the Pickering emulsion interface, poly(sodium methacrylate) (PSMA) and PS are synchronously grafted at the corresponding hemispheres in the two phases. It is noted that some free polymers are found in the two phases by this common free radical polymerization, separation is required to purify the Janus particles by removal of the polymers. When the azide-modified silica particle is used to stabilize the PS/toluene solution in water, the particle is anchored at the PS sphere surface after evaporation of the solvent. After the alkynated biotin is fed in aqueous phase, biotin is conjugated onto exposed side of the silica particle by azide-alkyne click reaction. After the biotin-conjugated silica particle is detached from the PS sphere by dissolution, PEO is tethered onto the opposite side of the biotin-conjugated Janus silica particle by using alkynated PEO. A Janus particle of PEO-silica-biotin is achieved (Fig. 3c) [60]. At the CuO particle stabilized Pickering emulsion interface, CuS is formed at the exposed side when adding thioacetamide in the continuous aqueous phase. The corresponding Janus CuO/CuS particle is achieved [61]. A Janus microgel is synthesized by selective amidation of the exposed side of the poly(N-isopropylacrylamide-co-acrylic acid) (Poly(NIPAM-co-AA)) at the Pickering emulsion interface [62].

### 2.3. Janus platelets by Pickering emulsion interfacial synthesis

When a sheet-like (or disk-like) platelet is anchored at the liquid-liquid Pickering emulsion interface, flipping is dynamically restricted [63]. Janus platelet is thus achieved by the selective modifications. A PS sphere with a positively charged surface is synthesized by ATRP emulsion polymerization using the ATRP initiator of 11'-(N,N,N-trimethylammonium bromide)-undecyl-2-bromo-2-methyl propionate. The negatively charged Laponite disk is preferentially absorbed onto the sphere surface by electrostatic interaction. The two sides are compartmentalized after the selective modifications. Upon feeding poly(2-dimethylaminoethylmethacrylate) (PDEAEMA), the exposed side of the Laponite is covered with PDEAEMA. A Janus Laponite disk with two different polymers at the opposite sides is derived after dissolution of PS sphere. The Janus Laponite disk is amphiphilic, which can be stacked into superstructures in selective solvents [64]. It is noted that both polymers are connected with the particle via electrostatic interaction, which may be disintegrated upon varying pH or adding electrolytes. Covalent binding can guarantee a permanent adhesion. The ATRP-initiator of  $\alpha$ -bromoisobutyrylbromide modified Kaolinite particle is used to form a Pickering emulsion. The water phase contains water-soluble monomer of N-isopropylacrylamide, or 2-dimethylaminoethylmethacrylate, copper (II) bromide and N,N,N',N',N''-pentamethyldiethylenetriamine as the catalyst,  $\alpha$ -bromoisobutyric acid as the initiator, and ascorbic acid as the reducing agent. The oil phase is consisted of lauryl methacrylate as the monomer, copper (II) bromide and tris(2-pyridylmethylamine) as the catalyst, ethyl  $\alpha$ -bromoisobutyrate as the initiator, and tin 2-ethylhexanoate as the reducing agent. After the simultaneous "grafting from" of hydrophilic and hydrophobic polymers onto the opposite sides, a Janus Kaolinite particle is derived (Fig. 4a) [65].

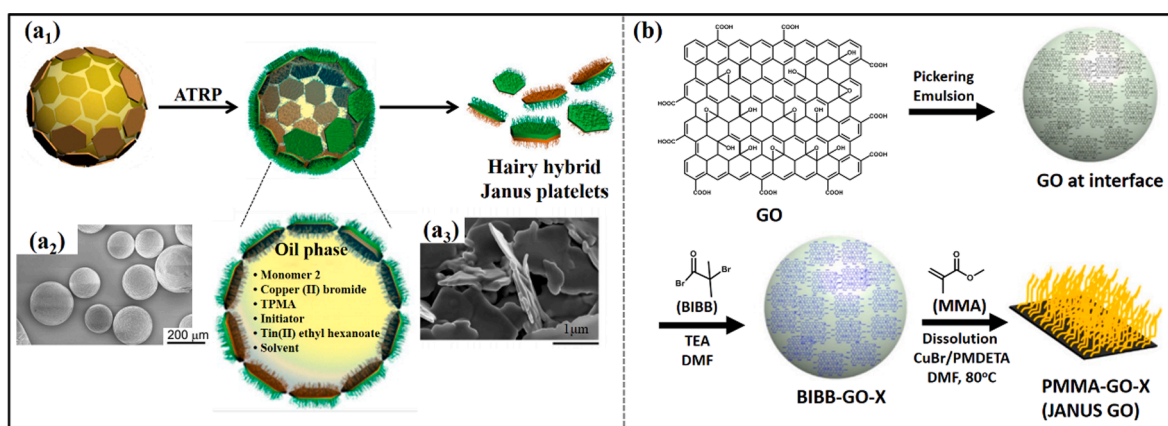


**Fig. 4.** (a<sub>1</sub>) Schematic synthesis of Janus platelet of Kaolinite/polymer composite, (a<sub>2</sub>) SEM images of the wax sphere with the Br modified Kaolinite and (a<sub>3</sub>) the Janus platelet with two polymers at the opposite sides. Adapted with permission from Ref. [65]. Copyright 2014 American Chemical Society. (b) Schematic synthesis of the Janus platelet of PMMA-GO-X. Adapted with permission from Ref. [67]. Copyright 2017 American Chemical Society.

The liquid/liquid Pickering interface is an ideal skeleton to divide one object into two distinct regions for selective modifications, which is advantageous to achieve Janus two-dimensional materials [66]. The coverage degree by the nanosheet should be sufficiently low to ensure monolayer of the nanosheet. Otherwise, the nanosheets will be overlapped at the edge, making the compartmentalization less distinct after the modification. When a graphene oxide (GO) nanosheet is anchored at the Pickering emulsion interface, the exposed side can be modified by a selective amidation with 2-bromoisobutryl bromide (BIBB) for grafting of PMMA (Fig. 4b) [67]. After detaching from the emulsion droplet surface, the Janus PMMA-GO nanosheet is derived. Similarly, poly(2-acryloyloxyethylferrocenecarboxylate) (PMAEFC) and polydopamine (PDA) can be selectively grafted onto opposite sides of the GO nanosheet, thus yielding a Janus structure [68].

Due to the precise controllability and relatively high yield, Pickering emulsion interfacial synthesis has been widely utilized for the preparation of Janus materials. As summarized in Table 1, Janus materials with various composition and diverse morphology can be generated by using this method. A prominent feature of the Janus materials by Pickering emulsion interfacial synthesis is the facilely tunable Janus balance. However, the synthesis is time consuming involving many tedious steps from the formation of emulsion, solidification, selective modification, dissolution, to filtration for separation.

### 3. Conventional emulsion interfacial synthesis

#### 3.1. Conventional emulsion interfacial materialization

After realizing that a conventional emulsion interface is temporally Janus with an asymmetric nanostructure, Yang et al. reported a new method to generate a Janus shell by materialization of the Janus interface. Silanes with different pendant groups are dissolved in the oil phase as precursors for the materialization. At the emulsion interface, a self-organized sol/gel process is induced by the functional group of the emulsifier. A Janus silica membrane is thus formed [13,69]. The hydrophilic pendant amine-group from aminopropyltrimethoxysilane (APTMS) is exposed toward the aqueous phase, while the hydrophobic phenyl-group from phenyltriethoxysilane (PTES) is exposed toward the oil phase. Tetraethoxysilane (TEOS) is used to chemically connect the two layers. Acidic group from the hydrolyzed styrene-maleic anhydride copolymer (HSMA) emulsifier at the emulsion interface is decisive to the self-organization by specific interactions. After removal of the core by dissolution, a Janus hollow sphere is obtained (Fig. 5a). This method provides a general way to large-scale fabricate Janus hollow spheres with tunable composition and microstructure. A Janus nanosheet of silica composite is achieved by simply crushing the Janus hollow sphere, whose thickness is tunable. The Janus silica nanosheet is too rigid to adapt curvature of an example toluene/water emulsion interface. As the result, the droplets are large with a diameter around 0.1–0.3 mm. Oil/water separation from the emulsion stabilized with the Janus nanosheet becomes easier. When feeding the example toluene-in-water emulsion through a porous mica membrane, the continuous aqueous phase elutes while toluene droplets are left. The droplets are stable in air, implying that the Janus nanosheet stabilized emulsion interface is robust. By favorable growth of materials onto the desired side, composition and microstructure of the Janus nanosheet is adjusted. After Fe<sub>3</sub>O<sub>4</sub> nanoparticles are preferentially grown at the amine-group terminated side of the Janus nanosheet, the emulsion droplets stabilized with the

**Table 1**  
Janus materials synthesized by using Pickering emulsion interfacial synthesis.

Composition	Synthetic Method	Shape	Size <sup>d</sup>	Property/Application	Ref.
Janus SiO <sub>2</sub>	FPEIS <sup>a</sup>	Sphere	1.5 μm	Amphiphilicity	[42,43]
Janus TiO <sub>2</sub>			~ 160 nm	Amphiphilicity	[52,53]
SiO <sub>2</sub> + fluorescent dye	FPEIS		233 nm	Fluorescence probe	[45]
SiO <sub>2</sub> (DOX) + target molecule	FPEIS		110 nm	Tumor-targeting therapy	[46]
SiO <sub>2</sub> + polymer	FPEIS + SIP <sup>b</sup>		depending on SiO <sub>2</sub>	Stimuli-responsive, catalysis	[47-50]
SiO <sub>2</sub> + polymer	FPEIS + Selective etching	Non-spherical	variable	Functional composite	[51]
Ionic liquid and PNIPAM grafted SiO <sub>2</sub>		Porous cage	~ 300–400 nm	Magnetic, catalysis	[54]
PEG–AlSi <sub>10</sub> –PNIPAM (PDEAEMA)		Coral-like porous sphere	2 μm	Responsive, container	[55]
PS-Fe <sub>3</sub> O <sub>4</sub> @SiO <sub>2</sub> -PEO	FPEIS	Core-shell	~ 240 ± 30 nm	Magnetic responsive surfactant	[56]
PAAm-SiO <sub>2</sub> -PS	Fl-PEIS <sup>c</sup> + Biphasic	Sphere	450 nm	Amphiphilicity	[58]
PSMA-SiO <sub>2</sub> -PS	grafting		~ 150 nm	Amphiphilicity	[59]
PEO-silica-biotin	Fl-PEIS + Click reaction		~ 150 nm	Biocompatibility	[60]
CuO/CuS	Fl-PEIS		4.2 μm	Solid surfactant	[61]
PS-Laponite-PDMAEMA	Fl-PEIS + Biphasic grafting	Sheet-like	28 nm	Self-assembly	[64]
PDMAEMA-Kaolinite-PLMA			irregular, μm	Surfactant, anti-icing coating	[65]
Janus PMMA-GO				Amphiphilicity	[67]
PMAEFC-GO-PDA				Self-healing	[68]

a: FPEIS: Frozen Pickering emulsion interface synthesis.

b: SIP: Surface initiated polymerization.

c: Fl-PEIS: Fluidic Pickering emulsion interfacial synthesis.

d: Size of the Janus materials is tunable, only one example is listed in the tables (Same in the following tables).

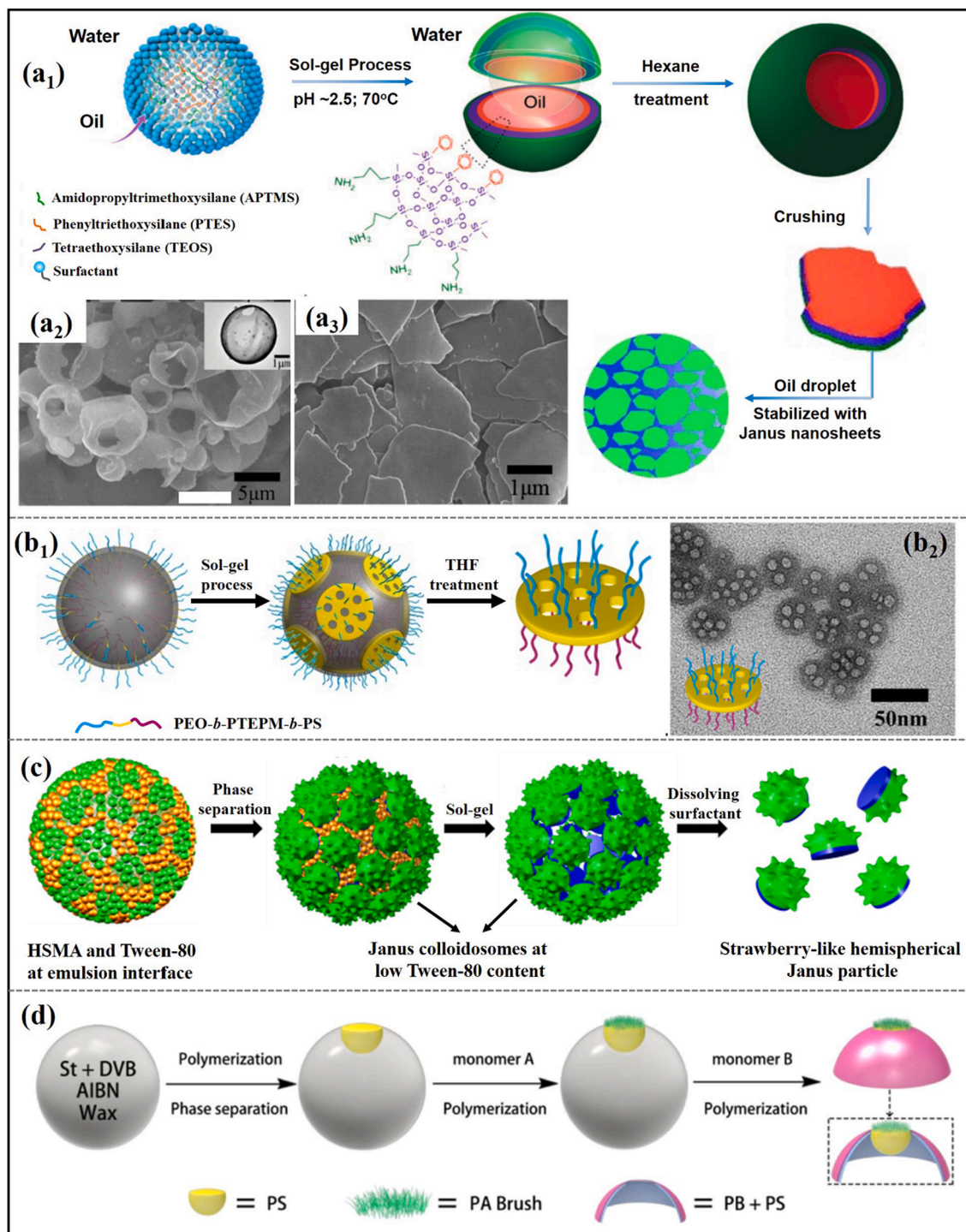


**Fig. 5.** (a<sub>1</sub>) Illustrative fabrication of the Janus hollow sphere by emulsion interfacial self-organized sol-gel process and the corresponding nanosheet by crushing, (a<sub>2</sub>) SEM images of the Janus hollow sphere and (a<sub>3</sub>) the Janus nanosheet. Adapted with permission from Ref. [13,69] Copyright 2011 The Royal Society of Chemistry and Copyright 2011 Wiley. (b<sub>1</sub>) Illustrative synthesis of the tri-layered composite Janus mesoporous disc and (b<sub>2</sub>) the TEM image. Adapted with permission from Ref. [80] Copyright 2016 American Chemical Society. (c) Schematic fabrication of the strawberry-like Janus hemispherical particle. Adapted with permission from Ref. [85] Copyright 2015 Nature Publishing Group. (d) Illustrative synthesis of the Jellyfish-like Janus cage. Adapted with permission from Ref. [88] Copyright 2020 American Chemical Society.

Janus composite nanosheet can be withdrawn by a magnet [69]. This performance is attractive for efficient treatment of emulsified contaminants. A polymer-inorganic bi-layered Janus composite nanosheet is obtained when a polymerizable silane of MPS is used to introduce vinyl-group onto the interior surface of the shell [70]. A further polymerization of NIPAM is performed to conjugate a thermal responsive polymer onto the interior surface [71]. By covalent linking of the ATRP or (RAFT) initiator onto the amine-group terminated side of the Janus silica nanosheet, pH-responsive PDEAEMA or thermal responsive PNIPAM is easily grafted onto the corresponding side [72]. Similarly, a light-triggered Janus composite nanosheet is derived by polymerizing spiropyran-containing monomer (SPMA). The hydrophobic-hydrophilic reversible transformation is achieved *via* reversion from spiropyran to the zwitterionic merocyanine under UV irradiation [73]. After sequential grafting by selective ATRP, a dually-responsive Janus composite nanosheet is generated with a sandwiched structure of PNIPAM-silica-PDEAEMA [74]. Janus performance can be triggered within a broad window by changing pH or (and) temperature. A pH responsive polymeric Janus container is achieved with a biodegradable poly ( $\epsilon$ -caprolactone) (PCL) at the interior surface while pH-responsive PDEAEMA at the outer surface [75]. An ionic liquid functionalized Janus nanosheet is derived from the Janus hollow sphere with the triethoxy-3-(2-imidazolin-1-yl)propyl ionic liquid group onto the interior surface when using the corresponding silane for the self-organized interfacial materialization [76]. These Janus nanosheets can serve as solid emulsifiers to stabilize emulsion droplets, which are useful to collect target chemicals. The example Janus silica nanosheet integrating with the artificial receptors is capable to efficiently capture 2,6-dichlorophenol (DCP) and Pb (II), which is promising for environmental remedy and detoxification [77]. When a reactive amphiphilic polymer is self-assembled forming a monolayer at the emulsion interface, a polymeric Janus nanosheet is derived by crosslinking the monolayer [78]. Hydrophilic and hydrophobic segments of the polymer are distinctly compartmentalized at the corresponding phases. When using the amine-group capped silica nanoparticle to crosslink the carboxyl- group containing segment in the external aqueous phase, microstructure and performance of the Janus membrane are tunable [79]. When poly(ethylene oxide)-*block*-poly(3-triethoxysilylpropylmethacrylate)-*block*-polystyrene (PEO-*b*-PTEPM-*b*-PS) is used as the emulsifier, a tri-layered Janus shell is achieved after crosslinking the self-assembled monolayer by the sol-gel process at the emulsion interface. When another “inert” amphiphilic copolymer of PEO-*b*-PS is present at the emulsion interface, a phase separation occurs at the interface. When PEO-*b*-PS is dispersed within the membrane of PEO-*b*-PTEPM-*b*-PS, a Janus mesoporous disc is derived after dissolving PEO-*b*-PS (Fig. 5b) [80]. The mesoporous Janus disc is promising for intensified mass transfer in interfacial catalysis. When using poly(ethyleneglycol)-*block*-poly(L-lysine)-*block*-polystyrene (PEG-*b*-PLL-*b*-PS) to stabilize the toluene/water emulsion, the intermediate layer of the interfacial membrane is positively charged under acidic conditions. After feeding silicic acid, the silica layer is formed thereby. As a result, a Janus silica nanosheet with two polymer brushes onto the opposite sides is prepared after crushing the composite membrane [81]. A responsive Janus nanosheet is derived from the self-assembled monolayer of PTEPM-*b*-PS after the sol-gel process of TEOS at a water/toluene emulsion interface, which is further grafted with the responsive polymer by surface-initiated ATRP [82]. Strength and thickness of the Janus nanosheet are tunable by varying block length of the copolymer and the concentration. In combination with polymerization of various monomers, morphology and composition of the Janus nanosheets are greatly extended.

A patchy microstructure is easily achieved at the emulsion interface when two surfactants experience a phase separation, which is beneficial to control morphology of the Janus materials. As an example, the patchy microstructure is fabricated at *n*-decane/water emulsion interface in the presence of the binary surfactant mixture of hydrolyzed styrene-maleic anhydride copolymer (HSMA) and Tween-80 [71]. After the self-organized sol-gel process of APTES and TEOS, the HSMA occupied emulsion interface is materialized. A porous silica shell is achieved when the HSMA phase is continuous after removal the disperse phase of Tween-80. After a further growth onto the interior surface, the interior surface becomes coarsening. The coarsening interior surface gives rise to a magnified capillary force which is beneficial for intensified mass transfer through the transverse pores [83,84]. This Janus cage is highly efficient to collect oil from the aqueous surroundings. When the interior surface is grafted with responsive polymers for example the thermal responsive PNIPAM, the Janus cage can capture oil at high temperature, and release outwardly upon decreasing temperature. When HSMA is a disperse phase at the emulsion interface, a strawberry-like hemispherical particle is generated after the interfacial materialization. The concaved surface is coarsening and the bottom surface is flat (Fig. 5c) [85]. The coarsening microstructure is arisen from newly formed micelles of Tween-80 at the surface during the sol-gel process. The particle is Janus with amine- group at the concaved surface while silanol- group at the flat bottom surface. Functional group for example a curing agent can be selectively conjugated onto the flat bottom surface, while the amine-group terminated surface is grafted with a hydrophobic polymer for example PS. In mimicking amphiphilic surfactants, the derived Janus particle can form a self-assembled monolayer at substrates with the hydrophobic concaved part facing toward air. This approach is highly effective to fabricate a lotus mimic yet robust superhydrophobic coating. At the patchy emulsion interface, a cone-like Janus particle is prepared by polymerization induced phase separation under an outward convex interfacial tension mismatch [86]. The cone-like shape is originated from squeezing the deformable PS particle at the triple-phase contact line region while the as-polymerized particle is immigrated toward the interface due to the Pickering effect. The cone part is exposed to the external aqueous phase while the flat side is directed toward the wax phase. Along the stepwise modifications, the cone surface and flat side of the particle can be selectively conjugated with desired materials. Similarly, a robust coating is easily fabricated by using the cone-like Janus particle as a building block. The coating is highly adhesive to water droplets which are tightly pinned when the substrate is turned downwardly. In the case of an emulsion interface solely stabilized by HSMA, a ball-on-disk Janus structure is achieved by the copolymerization between the hydrophobic monomer of styrene in the oil phase and the hydrophilic monomer of acrylamide in the aqueous phase [87]. The exposed part of the deformable particle is elongated at the triple-phase contact line region by the interfacial tension difference. By extending this approach, a Jellyfish-like Janus cage is achieved with a PS/PAM lobe as the “head” part and PS/PAA as the “belly” part. In the first step, a PS lobe is generated *via* the free radical polymerization of styrene/divinylbenzene (St/DVB) in the paraffin emulsion droplet, which is anchored at the emulsion interface after immigration owing to the Pickering effect. The exposed side of the crosslinked PS hemisphere is covered with polyacrylamide (PAM) after the polymerization of

acrylamide (AM) in the aqueous phase. In the second step, the bi-layered belly of PS/PAA is achieved by the copolymerization of hydrophobic styrene/divinylbenzene in the oil phase with the hydrophilic acrylic acid (AA) in the aqueous phase. Elimination of the residual free radicals at the PS/PAM head surface prior to the second interfacial polymerization is crucial to generate the Jellyfish-like structure (Fig. 5d) [88]. It is noted that the “head” and “belly” parts are covalently connected at their boundary.

### 3.2. Janus cages by interfacial materialization

Besides conventional emulsion interfaces stabilized by molecular surfactants, Pickering emulsion interfaces can also be used to derive Janus hollow spheres. Against the silica particle stabilized Pickering emulsion, a bi-layered polymeric shell is generated by the interfacial copolymerization of the hydrophobic and hydrophilic monomers in the two corresponding phases. The silica particle spans across the whole shell. After dissolving the silica particle, a robust polymeric Janus cage is derived with the transverse macroscopic pores. The pores are uniform with the same size as the silica particle [89]. The porous Janus cage can collect large organic species for example hydrophobic colloids. In addition, Janus hollow spheres can be synthesized by materialization of the air/liquid interface of a bubble. By spraying a mixture of ethyl-2-cyanoacrylate (ECA) and other polymeric or (and) inorganic precursors, shell of PECA is formed via the rapid cationic polymerization at the bubble surface while flowing with catalytic ammonia [90]. In the stage of solvent evaporation, materials are grown onto the interior surface of the PECA shell by precipitation. The Janus hollow sphere is composed of multiple layers with varied compositions. Upon incorporation of functional materials for example a photocatalytic titania nanoparticle P25, the Janus hollow sphere can act as a micro-reactor to decompose organic pollutants upon UV irradiation after selective capturing the compounds from the aqueous media [91].

Janus hollow spheres and the derivative Janus nanosheets can be synthesized against the liquid/solid interfaces. As an example, the amphiphilic silane can self-assemble into a monolayer onto a solid surface via specific interactions. After the sol-gel process, the monolayer is converted into a robust thin silica composite membrane. After removal of the solid core by dissolution under sonication, the corresponding Janus nanosheet is achieved with the molecular scale thickness. The example amphiphilic silane of 3-butyldianhydridemercaptopropyltrimethoxysilane (BDMPS) is used to prove the concept. A self-assembled monolayer of BDMPS is formed onto the CaCO<sub>3</sub> particle surface by coordination interaction. The acid anhydride group is adhered to the particle surface via the coordination, while the tail group faces toward the external oil phase. A robust Janus monolayer is derived by the surface sol-gel process. Selective modification of the exterior silica surface by other silanes allows to conjugate other groups, for example hydrophobic alkyl-group from octadecyltrichlorosilane. The derived nanosheet is flexible, which can wrap the guest species with an individual nanosheet [92]. The method is general to derive a huge family of flexible functional Janus nanosheets. The example Janus nanosheet is achieved with carboxylic acid and amine- groups onto the opposite sides. Self-assembly and disassembly of the Janus nanosheet can be triggered by altering pH values in water [93]. This performance can be used in encapsulation and controlled release of guest materials. A magnetic

**Table 2**  
Janus materials synthesized by using conventional emulsion interfacial synthesis.

Composition	Synthetic Method	Shape	Size	Property/Application	Ref.
Janus SiO <sub>2</sub>	CEIM <sup>a</sup>	Hollow sphere	8 μm	Water/oil separation	[13]
Janus SiO <sub>2</sub>	CEIM	Nanosheet	65 nm (thickness)	Water/oil separation	[69]
C <sub>8</sub> -SiO <sub>2</sub> -PEG	CEIM	Porous Janus cage	1.2 μm	containers	[91]
SiO <sub>2</sub> + polymers	CEIM + SIP <sup>b</sup>	Nanosheet	depending on SiO <sub>2</sub>	Responsive, solid emulsifier	[70-75]
SiO <sub>2</sub> + Ionic liquid	CEIM + selective modification	Nanosheet	depending on SiO <sub>2</sub>	Solid emulsifier, catalysis	[76,77]
PS-SiO <sub>2</sub> -imidazole		Hemispherical	~300 nm	Superhydrophobic coating	[85]
C <sub>8</sub> H <sub>17</sub> -PS-NH <sub>2</sub>		Cone-like	~500 nm	Superhydrophobic coating	[86]
Crosslinked HSMA	CEIM + crosslinking	Nanosheet	6 nm (thickness)	Solid surfactants	[78]
PS-SiO <sub>2</sub> -PEO		Cage	3–20 μm	Oil container	[79]
PEO-b-PTEPM-b-PS		Porous disc	5 nm (thickness)	Solid surfactant	[80]
PEG/silica-polylysine/PS		Hollow sphere	~ 20 nm	Solid surfactant	[81]
PDMAEMA(PNIPAM)-SiO <sub>2</sub> -PS	CEIM + crosslinking + SIP	Nanosheet	N/A	Responsive solid surfactant	[82]
PAM-PS	Conventional emulsion interfacial polymerization	ball-on-disk	μm	Solid surfactant	[87]
PAA-PS@PAM		Jellyfish-like Janus cage	Tunable, μm	Container	[88]
PAM-PDVB		porous Janus cage	Tunable, μm	Container	[89]
PS-PECA	Aerosol-assisted solvent evaporation	Janus cage	10 μm	N/A <sup>c</sup>	[90]
Janus SiO <sub>2</sub>	Solid-liquid interfacial materialization	Nanosheet	Ultrathin (3.5 nm)	Responsive solid surfactant	[92,93]
Fe <sub>3</sub> O <sub>4</sub> -SiO <sub>2</sub> -Ionic liquid			0.93 nm (thickness)	Catalysis	[94]

a: CEIM: Conventional emulsion interfacial materialization.

b: SIP: Surface initiated polymerization.

c: N/A: not available.

responsive Janus nanosheet with  $\text{Fe}_3\text{O}_4$  nanoparticle and  $\text{PW}_{12}\text{O}_{40}^{3-}$ -based ionic liquid group onto the opposite sides is synthesized at the solid/liquid interface [94]. When using the amine- group capped  $\text{Fe}_3\text{O}_4$ @ $\text{SiO}_2$  core/shell particle as the core, triethoxysilylbutyraldehyde (TESBA) is conjugated *via* the dynamic Schiff's base bonding. The aldehyde group is adhered onto the core surface. After the sol-gel process, a Janus silica composite membrane with a molecular thickness is generated. By breaking the Schiff's base bonding under acidic conditions, the Janus silica nanosheet is derived with silanol/aldehyde functional groups onto the opposite sides. The amine- group capped  $\text{Fe}_3\text{O}_4$ @ $\text{SiO}_2$  core/shell particle can be recycled. After modification with chitosan-capped  $\text{Fe}_3\text{O}_4$  NP and  $\text{PW}_{12}\text{O}_{40}^{3-}$ -based ionic liquid onto the aldehyde and silanol sides, respectively, the Janus nanosheet is capable of effectively decomposing sulfur contained compounds. After the reaction, the Janus composite nanosheets can be recycled with a magnet. This performance is promising for production of clean fuels.

Apparently, interfacial materialization is a direct way to prepare Janus materials with tunable shape and microstructure through duplicating the self-assembled and/or cross-linked liquid/liquid, liquid/solid and liquid/gas interfaces. Table 2 lists the Janus materials prepared by using the interfacial materialization. The synthetic procedure is relatively simple compared with Pickering emulsion interfacial synthesis, yet the lateral size of Janus nanosheet derived by crushing corresponding Janus hollow sphere is random.

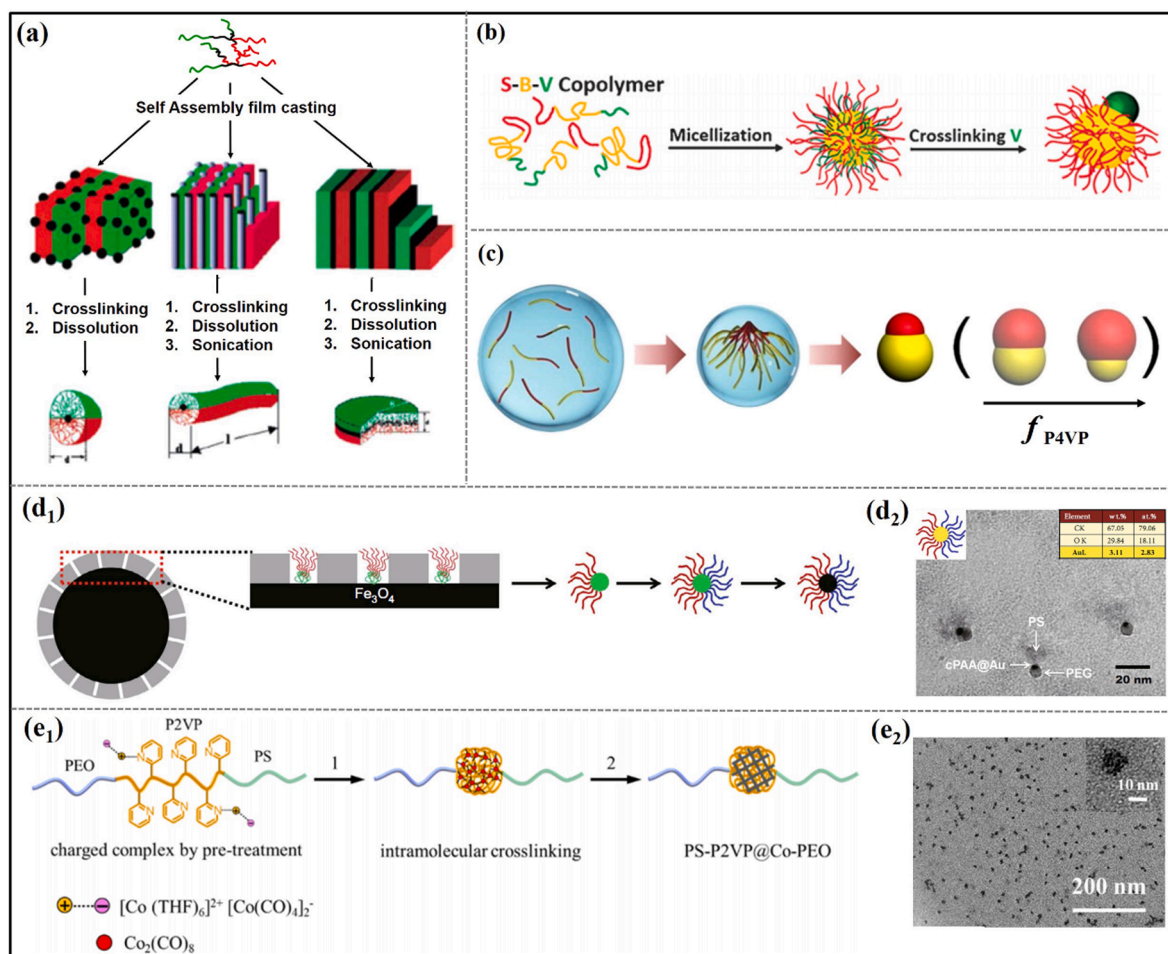


**Fig. 6.** (a) Schematic synthesis of the Janus nanoparticle from a terpolymer supramolecular structure. Adapted with permission from Ref. [95]. Copyright 2013 American Chemical Society. (b) Schematic synthesis of the Janus nanoparticle by direct self-assembly of diblock copolymer. Adapted with permission from Ref. [101]. Copyright 2016 Wiley. (c) Illustrative synthesis of the Janus NPs by solvent evaporation induced assembly of P4VP-based diblock copolymers in emulsion droplets, size of the P4VP head (red) and thus Janus balance are tunable by varying P4VP fraction. Adapted with permission from Ref. [110]. Copyright 2016 American Chemical Society. (d<sub>1</sub>) Synthesis of the tri-segmental Janus nanoparticle by confined self-assembly of a diblock copolymer within the mesoporous  $\text{SiO}_2$  channel, (d<sub>2</sub>) TEM image of the PS-cPAA@Au-PEG Janus composite nanoparticle. Adapted with permission from Ref. [111]. Copyright 2015 Science China Press and Springer-Verlag Berlin Heidelberg. (e<sub>1</sub>) Illustrative synthesis of the single-chain Janus composite nanoparticle of PS-P2VP@Co-PEO and (e<sub>2</sub>) the TEM image. Adapted with permission from Ref. [119]. Copyright 2013 American Chemical Society.

## 4. Janus materials by Self-Assembly

### 4.1. Janus materials by self-assembly of block copolymers

Block copolymers (BCPs) are inherently compartmentalized by different blocks at molecular scale, providing a huge library for Janus materials. Methodological development is key to process the BCPs into Janus materials by condensation and fixation. Selective-disassembly of self-assembled supramolecular structures is effective to fabricate Janus polymeric materials with tunable morphologies. Janus materials can be derived from phase-separated ABC-triblock terpolymers. When the middle block of B is crosslinked, A and C blocks are present in the form of polymer brushes onto the two sides of the crosslinked B phase [95]. In 2001, Müller and co-workers firstly reported the pioneering work on preparation of Janus particles by disassembling a film of ABC-triblock terpolymer [96]. Both A and C blocks are self-assembled into lamellae structure, while the B block forms the spherical micro-domains. Then B micro-domains are crosslinked ahead of disassembly of the film in a good solvent, and Janus micelles are obtained. Morphology of the Janus materials is tunable from sphere to cylinder to disc by adjusting block ratio (Fig. 6a) [97-99]. Following this approach, a kind of Janus nanoparticle is derived from multicompartment micelles of the ABC triblock terpolymers [100]. Size of the Janus nanoparticle is determined by the molecular weight, while Janus balance of the nanoparticle is dependent on the lengths of A and C blocks. Besides disassembly of the selectively-crosslinked supramolecular structures, Janus nanoparticles can be generated in a direct way by self-assembly of triblock terpolymers [101]. As an example, polystyrene-*block*-polybutadiene-*block*-poly(2-vinylpyridine) (PS-*b*-PB-*b*-P2VP) can form micelles in DMF with PB as the core, while PS and P2VP form the mixed shell. During the selective crosslinking of P2VP with 1,4-dibromobutane, the intermicellar crosslinking is prohibited owing to the steric hindrance from the PS chains. The PB core is highly elastic enabling the crosslinked P2VP to protrude as a lobe (Fig. 6b) [101]. A Janus structure is thus achieved. After self-assembly of poly(methylmethacrylate)-*block*-poly(2-cinnamoyloxyethylmethacrylate)-*block*-poly(2-dimethylaminoethyl-methacrylate) (PMMA-*b*-PCEMA-*b*-PDMAEMA) in water, well-defined micellar dimers are formed. The partial crosslinking is performed by UV irradiation. Janus nanoparticles are generated after following disassembly in acetone [102]. Worm-like Janus micelles can be produced by self-assembly of triblock terpolymer, in which a crystallizable PE is applied as the middle block, while PS and PEO serve as two highly incompatible corona blocks. In toluene, the self-assembly is driven by the crystallization of PE, resulted in the formation of worm-like Janus micelles with a crystalline PE core [103]. Additionally, Janus nanotubes can be obtained from self-assembled cyclic peptide-polymer conjugates. Two different polymers such as poly(*n*-butyl acrylate, PBA) and PS can be sequentially tethered onto the cyclic peptide by copper-catalyzed azide-alkyne cycloaddition followed by a thiol-ene reaction. The peptide-polymer conjugates can be regarded as a kind of triblock copolymer, where the cyclic peptide serves as the intermediate block. Janus nanotubes with interior cyclic peptide and segregated exterior PBA and PS chains are achieved after self-assembly in bulk or solution [104].

Compared to triblock terpolymers, diblock copolymers are more attractive because of their easier synthesis. A type of Janus nanoparticle is achieved by non-covalent crosslinking the PAA core of micelles with mixed shell *via* co-assembly of PEO-*b*-PAA and poly(2-vinylnaphthalene)-*block*-PAA (P2VN-*b*-PAA) [105]. After crosslinking the PAA core with 1,2-propanediamine (PDA) in DMF, P2VN in the mixed shell is collapsed into many separated microdomains at pH = 7. It is noticed that the mixed-shell micelles (MSMs) are stable as individuals while the P2VN microdomains are protected by water-soluble PEO chains. By lowering pH value to ~ 3.1, the intramicellar complexation occurs between PEO and PAA, resulting in the asymmetric intramicellar phase separation between hydrophilic PEO/PAA complex and hydrophobic P2VN. UFO disk-shaped Janus micelles are prepared *via* co-assembly of water soluble copolymers of PAA-*b*-PAAm and poly(2-methylvinylpyridinium iodide)-*block*-poly(ethylene oxide) (P2MVP-*b*-PEO) [106]. Similarly, a kind of ellipsoidal Janus micelle is prepared by co-assembly of two fully water-soluble block copolymers of PAA-*b*-PAAm and P2MVP-*b*-PEO [107]. Formation of Janus micelles is driven by the delicate interplay between two opposed forces: an attraction between the oppositely charged core blocks and a subtle repulsion between the neutral water-soluble corona blocks. Janus-type DNA structure assembled from DNA-peptide conjugates (DP) has been developed recently. DP is firstly synthesized by the click reaction between azide-terminated peptide and alkyne-modified DNA. By adding the DP-1,1,1,3,3,3-hexafluoroisopropanol (HFIP) dispersion into a phosphate buffered saline (PBS), the self-assembly is triggered by H-bonding and  $\pi$ - $\pi$  interaction of phenylalanine-rich peptide block. When the peptides adopt a parallel  $\beta$ -sheet assembly, Janus nanosheets with distinct DNA and peptide faces are derived [108]. Undoubtedly, Janus nanosheets with two different DNA sequences on opposite faces can be achieved by self-assembly of triblock DNA1-peptide-DNA2 conjugates.

By using a micelle assembled from diblock copolymers, a hybrid Janus nanoparticle of polymer/Au is produced by a further favorable complexation. The non-covalently crosslinked micelle core plays a decisive role in forming the Janus architecture, where nucleation and growth of Au nanoparticles are restricted within the central area of the micelle core [109]. The micelle of PEG<sub>113</sub>-*b*-P4VP<sub>75</sub> (EV) is formed in a methanol/water (1/9, v/v) mixture, where polyethylene glycols (PEG) acts as the shell and P4VP as the core. AIBN is mainly localized within the hydrophobic P4VP core. In the presence of H<sub>2</sub>AuCl<sub>4</sub> and Na<sub>2</sub>PdCl<sub>4</sub>, Au nanoparticle is favorably formed by reduction at 76 °C. It is noted that non-covalent crosslinking of the P4VP core with PdCl<sub>4</sub> *via* complexation is dominant, nucleation and growth of Au nanoparticles occur predominantly at the core/shell interface. Meanwhile, copolymerization of N-isopropylacrylamide (NIPAM) and N,N'-methylenebisacrylamide (MBA) occurs at the same interface with the poly(NIPAM-*co*-MBA) shell covering the core. The Au nanoparticles are anchored at the polymer shell. Upon dissolution of the micelle at a low pH, the Janus-like nanoparticle of Au/polymer is derived. It is well known that diblock copolymers tend to form core-shell structures rather than Janus nanoparticles. It is important to develop new methods to prepare Janus nanoparticles from diblock copolymers. Deng et al. firstly reported on the synthesis of robust Janus nanoparticles *via* confined self-assembly under neutral interface. Poly(vinyl alcohol) (PVA) is applied as the surfactant to construct a neutral interface for emulsion droplet containing PS-*b*-P4VP, and a Janus particle is generated after removal of the solvent from the droplet (Fig. 6c) [110]. Janus balance can be easily tuned by adjusting block ratio of the

copolymers.

The confined self-assembly of diblock copolymers within a porous solid mold represents an advantageous strategy to construct Janus materials. As a proof of the concept, a Janus composite colloid with two different polymers conjugated onto the opposite two sides is generated against the mesoporous shell onto the  $\text{Fe}_3\text{O}_4$  core [111]. The mesopores are transverse and perpendicular to the core surface. The diblock copolymer of PS-*b*-PAA is absorbed within the mesoporous channel, where the coordination between PAA and  $\text{Fe}_3\text{O}_4$  induces the formation of a Janus cluster. The PS part is orientated outwardly while the PAA part is adhered to the core surface. After selective crosslinking of the PAA block with tetraethylenepentamine (TEPA), an ordered array of Janus nanomaterials is generated at the core particle surface after the silica layer is etched at ambient temperature. A kind of spiky corona is formed around the core. The Janus colloid of PS-*c*PAA is released after detaching from the core upon breaking the specific interaction at high temperature. Onto the opposite side of PS-*c*PAA, another polymer for example amine-capped PEG can be conjugated by amination. A tri-segmental composite Janus colloid is derived. The crosslinked *c*PAA domain acts as a nanoreactor, where functional materials for example Au nanoparticle can be preferentially grown (Fig. 6d) [111]. The derived Janus composite colloid of PS- $\text{Fe}_3\text{O}_4$ -PEO is amphiphilic, which can be manipulated with a magnet. Similarly, another segmental Janus nanoparticle of polymer/metal composite such as PNIPAM-Au@*c*P4VP-PS is obtained against the C8-SiO<sub>2</sub> patchy sphere mold. P4VP is previously grown at the isolated patchy regions, which can induce the favorable growth of Au nanoparticle. Afterwards, a thiol-capped polymer for example PNIPAM-SH is conjugated onto the exposed part of the Au nanoparticle [112].

Many polymer chains or clusters are present onto the opposite sides of the abovementioned Janus colloids. It is interesting to achieve such Janus colloids with polymer single-chain conjugated onto one side or two different chains onto the opposite sides. Intramolecular crosslinking of copolymers is a straightforward way to synthesize the single-chain Janus nanoparticles. Starting from an example copolymer of poly(ethylene oxide)-*block*-poly(2-cinnamoyloxyethylmethacrylate) (PEO-*b*-PCEMA), a tadpole-like Janus nanoparticle is achieved by intramolecular crosslinking of the PCEMA block while the PEO block remains linear [113]. The intramolecular crosslinking is general toward single-chain Janus nanoparticles with tunable composition and microstructure. Another tadpole-like Janus nanoparticle is synthesized by intramolecular crosslinking of the P4VP block of PMMA-*b*-P4VP with propargyl bromide [114]. A tadpole-like Janus nanoparticle is prepared by hydrolysis and intramolecular polycondensation of the silane moiety of poly(ethylene oxide)-*block*-poly[(methyl methacrylate)-*co*-poly(3-trimethoxysilylpropyl methacrylate)] (PEO-*b*-P(MMA-*co*-TMSPMA)) [115]. A single chain of PEO is tethered onto the silica-like head. In a mixed solvent of THF/water, the Janus nanoparticle can self-assemble into spherical micelles, vesicles, and large compound micelles. The morphology is dependent on the size of the silica head and the initial concentration. Different from the linear BCP counterpart, the self-assembly is surfactant-alike owing to rigidity of the hydrophobic silica head. A CO<sub>2</sub> responsive polymer single-chain Janus nanoparticle is synthesized by photo irradiated intrachain crosslinking [116]. Polystyrene-*block*-poly{(N,N-dimethylaminoethyl methacrylate)-*co*-4-methyl-[7-(methacryloyl) oxyethyloxy] coumarin} is used to derive the Janus nanoparticle. The responsive performance is arisen from the reversible protonation/deprotonation of tertiary amine group.

However, the intramolecular crosslinking approaches toward the single-chain Janus nanoparticles are usually performed under extremely dilute concentration when the polymer coils are isolated. It remains challenging to large scale synthesize single-chain nanoparticles in concentrated solutions. Yang et al. proposed a new conceptual method of electrostatic-mediated intramolecular crosslinking of polymers in concentrated solutions [117]. Prior to the intramolecular crosslinking with a multiple-valent agent, the crosslinkable block is modified with a mono-valent to introduce electrostatic interaction. In the case of poly(vinylpyridine) contained polymers, iodoethane and 1,5-diiodopentane are used as the modification agent and crosslinker. In the case of PAA contained polymers, 1-methylimidazole and 1,6-hexanedithiocyanate are used for the electrostatic-mediated intramolecular crosslinking. In the case of polyisoprene contained polymers, they resemble PAA contained polymers after the click reaction with mercaptoacetic acid. The modification and intramolecular crosslinking can adopt either physical or (and) chemical interaction. Intramolecular crosslinking of polystyrene-*block*-poly(4-vinylpyridine)-*block*-poly(ethylene oxide) (PS-*b*-P4VP-*b*-PEO) can be achieved at an unprecedentedly high concentration of 300 mg/mL. In contrast, the intramolecular crosslinking occurs at an extremely low concentration of mg/mL scale in the absence of the electrostatic interaction. This new method paves the avenue to large scale produce a huge family of functional Janus single-chain composite nanoparticles. The example Janus nanoparticle of PS<sub>5,2k</sub>-*c*PAA<sub>4k</sub> contains a single chain of PS conjugated onto the crosslinked colloid of *c*PAA. The residual PAA at the *c*PAA colloid renders PS<sub>5,2k</sub>-*c*PAA<sub>4k</sub> pH responsive when used as an emulsifier. At a low pH below pKa of PAA (~4.6), the Janus colloid is nearly neutral and less amphiphilic. Above the pKa, the Janus colloid becomes highly negatively charged. As the result, the Janus nanoparticle displays amphiphilic. Residual PAA of PS<sub>5,2k</sub>-*c*PAA<sub>4k</sub> can induce a favorable growth of functional materials such as  $\text{Fe}_3\text{O}_4$  within the *c*PAA domain. The Janus composite colloid of PS<sub>5,2k</sub>-*c*PAA<sub>4k</sub>@ $\text{Fe}_3\text{O}_4$  is paramagnetic, which can be entirely collected with a magnet. When the initiator of 2,2'-azobis(2-methylpropionamide) dihydrochloride (AIBA, V-50) is incorporated into the *c*PAA head by amidation, a thermal-responsive polymer of PNIPAM can be further grafted onto the *c*PAA head, forming dually responsive tadpole-like composite Janus nanoparticles toward temperature and magnetic stimuli [118]. Another reactive Janus single-chain colloid of PS-*c*P4VP@silane-PEO is derived which can form a self-assembled monolayer (SAM) at water/cyclohexane interfaces. The SAM becomes robust after a sol-gel process of the *c*P4VP@silane colloid upon altering pH ~ 3 in the aqueous phase. The membrane is homogeneous and the thickness is ~13.5 nm, which is comparable with the size of PS-*c*P4VP@silane-PEO. PEO and PS are distinctly compartmentalized onto the opposite sides of the Janus membrane. Along with the electrostatic-mediated intramolecular crosslinking, a magnetic Janus single-chain composite nanoparticle is derived *via* complexation of P2VP with octacarbonyl cobalt, where the P2VP/Co core is conjugated with PS and PEO single chains onto the opposite sides (Fig. 6e) [119]. Along with the similar approach, a Janus colloidal dimer is achieved by the two-step orthogonal intramolecular crosslinking of the diblock copolymer of poly(isoprene)-*block*-poly(vinylpyridine) (PI-*b*-P4VP) in a highly concentrated solution in DMSO [120]. The first colloid is achieved by intramolecular crosslinking of the PI block with 1,6-

hexanediisothiocyanate after the modification with 2-mercaptoethylamine hydrochloride to introduce the electrostatic interaction. The Janus single-chain nanoparticle of cPI-P4VP is derived. In the sequential step, the other colloid is achieved by intramolecular crosslinking of the P4VP block with 1,5-diiodopentane after the modification with iodoethane. The cPI colloid contains residual amine and cyanate groups while the cP4VP contains residual pyridine and quaternized groups. The Janus colloidal dimer can be synthesized at a high concentration of 100 mg/mL. Functional colloidal dimers are expected by selective loading materials within the desired domains. Another Janus polymeric colloidal dimer is achieved by intramolecular crosslinking of poly(oligo(ethylene glycol) mono-methyl ether methacrylate-co-anthracene-9-carboxyl)ethylmethacrylate)-block-poly(oligo( $\epsilon$ -caprolactone) methyl methacrylate-co-hydroxyethylmethacrylate) [121]. UV irradiation and atom transfer radical coupling (ATRC) are used for the orthogonal crosslinking. The dimer displays an ellipse-shape under TEM. It is noted that the intramolecular crosslinking is performed at a low concentration of 0.5 mg/mL. Multichain particles are inevitably co-existent during the synthesis of the single-chain Janus nanoparticle by double crosslinking of poly(2-(methacryloyloxy)ethyl pent-4-ynoate)-*r*-poly(hydroxyethylmethacrylate))-block-poly(2 (dimethylamino) ethylmethacrylate) ((PMAEP-*r*-PHEMA)-*b*-PDMAEMA) [122]. Under well-controlled conditions, the single-chain Janus nanoparticles in the mixture are self-sorted to form regularly structured macroscopic assemblies (MAs) with a crystal-like precipitate from the suspension. After dissociation of the MAs, single-chain Janus nanoparticle is purified which is uniform in size and shape. Notably, by the termination of the corresponding anionic living single polymer chains onto the chlorine-capped and amine capped inorganic nanoparticle (i.e.,  $\text{Fe}_3\text{O}_4$ ), single-chain/colloid composite Janus nanoparticles are generated, respectively [123,124]. The molecular weight of polymer is crucial for the formation of single-chain/colloid composite Janus nanoparticles, which can be formed only when the hydrodynamic size of the polymer is larger than the  $\text{Fe}_3\text{O}_4$  NP diameter [123]. Starting from a thermoresponsive poly(2-(2-methoxyethoxy) ethyl methacrylate) (PMEOMA) single polymer chain, the resulting single-chain/colloid composite Janus nanoparticle integrates thermal response, paramagnetic and photothermal effects [124]. This finding provides a new way to achieve pure single-chain Janus nanoparticles and build superstructures thereby.

Interestingly, Janus materials by assembled from two different kinds of homopolymer have been reported recently. The 10-nm scale Janus nanorods are prepared by self-assembly of ureas-functionalized polymers of poly(N,N-dimethylacrylamide) (PDMAc) and poly(N-acryloylmorpholine) (PNAM) in water. The self-assembly is driven by the interactions between unsymmetrical and complementary hydrogen bonding [125]. Besides H-bonding, donor-acceptor interaction is another fascinating driving force to fabricate Janus structure. Poly(2-hydroxyethyl acrylate) (PHEA) containing electron-rich dialkoxynaphthalene (DAN) moiety and PEO containing electron-deficient naphthalene diimide (NDI) can form Janus nanocylinders in DMSO upon slow addition of water [126]. The co-assembly of two polymers is driven by cooperative hydrogen bonding and charge transfer complexation between DAN and NDI.

#### 4.2. Janus materials via confined self-assembly and disassembly of block copolymers

Janus nanoparticles from block copolymers (BCPs) with a covalent linkage are robust to keep the integrity under harsh conditions for example at high temperature and in good solvents. Although some Janus nanoparticles have been reported by direct synthesis *via*

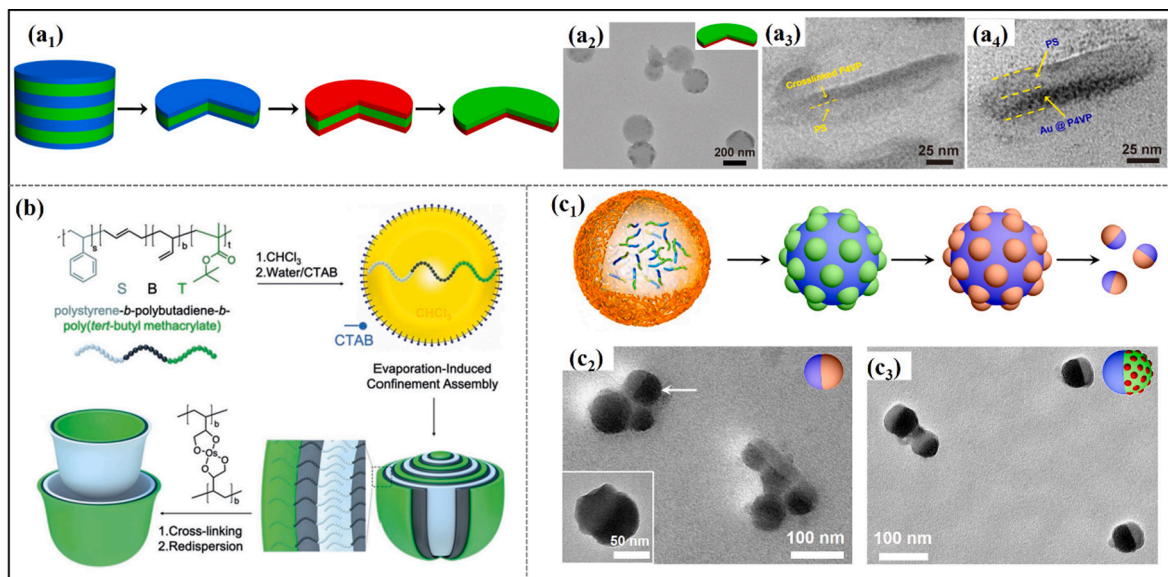


**Fig. 7.** (a<sub>1</sub>) Illustrative synthesis of the Janus nanodisc, (a<sub>2</sub>) the TEM image, (a<sub>3</sub>, a<sub>4</sub>) side view TEM images of the Janus nanodisc and after a favourable growth of Au nanoparticles. Adapted with permission from Ref. [129]. Copyright 2014 Wiley. (b) Schematic synthesis of the Janus nanocup by evaporation-induced assembly of the ABC triblock terpolymer. Adapted with permission from Ref. [131]. Copyright 2018 Wiley. (c<sub>1</sub>) Illustrative synthesis of the Janus nanoparticle, (c<sub>2</sub>, c<sub>3</sub>) TEM images of the Janus nanoparticle and after a favourable growth of Au nanoparticles. Adapted with permission from Ref. [132]. Copyright 2015 American Chemical Society.

self-assembly of BCPs, the thermodynamic consideration suggests that multiple-compartmental micelles (MCMs) or core-shell structures are inevitably coexistent with the Janus nanoparticles [127]. Multi-compartmental particles can be easily obtained through confined self-assembly of block copolymers. When the self-assembly is performed under a sufficient confinement, formation of Janus nanoparticles is favored [128]. However, some other particles are coexistent with the Janus one. Tedious separation is required to achieve pure Janus nanoparticles. On the other hand, starting from the multi-compartmental particles, Janus nanoparticles can be derived by disassembly when one block is crosslinked. Janus disc of P4VP-PS is prepared by stepwise disassembly of the disc-stacked particles (DSPs) of PS-*b*-P4VP (Fig. 7a) [129]. The DSPs are consisted of alternative lamellar layers of PS and P4VP, which are formed by emulsion droplet confined assembly. A symmetric PS-*b*-P4VP is chosen in order to form the lamellar structure. Poly(vinyl alcohol) (PVA) is used as the stabilizer, which is neutral to PS and P4VP chains that results in the ellipsoidal pupa-like shape with alternative block layers rather other morphologies for example onion-like. Using a P4VP selective solvent such as ethanol, the DSPs are partially disassembled and form the P4VP/PS/P4VP sandwiched nanodisc. Both the top and bottom P4VP layers are then crosslinked with 1, 5-diiodopentane (DIP), followed by disassembly of the intermediate PS layer in a good solvent for example chloroform. Crosslinking with DIP renders the P4VP layer positive charge, facilitating a further growth of functional materials. Composition, microstructure and property of the Janus nanodisc are broadly tunable. In a following study, Janus nanodiscs are prepared by one-step disassembly of triblock terpolymer DSPs, where the middle B block is selectively crosslinked [130]. This approach can be extended to achieve other morphologies. For example, Janus nanocup of triblock terpolymer of polystyrene-*block*-polybutadiene-*block*-poly(*tert*-butylmethacrylate) (SBT) has been reported (Fig. 7b) [131]. Stability of the nanocup is improved with the crosslinkable middle block length.

A patchy particle with the P4VP protuberances on the PS core surface is achieved from the CHCl<sub>3</sub>/water emulsion stabilized with PVA. Janus nanoparticles of PS-*b*-P4VP is derived by disassembly after the P4VP part at the patchy particle protuberances is cross-linked. Functional materials can be preferentially grown at the P4VP region, enriching composition and functionality of the Janus nanoparticle (Fig. 7c) [132]. The neutral emulsion interface is determinative to form the Janus nanoparticle, allowing both blocks to expose at the interface at an equal probability. At a strong confinement degree, colloidal molecules with tunable geometry are

**Table 3**  
Janus materials synthesized by self-assembly.

Composition	Synthetic Method	Shape	Size	Property/Application	Ref.		
ABC triblock polymer	Disassembly	Sphere, cylinder, disc	Tunable, nm	Amphiphilicity	[97-99]		
PS- <i>c</i> PB-PMAA	Self-assembly	Particle	Tunable, nm	Amphiphilicity, Self-assembly	[100]		
PS- <i>c</i> PB-PVP		Snowman-like	42 nm	Self-assembly	[101]		
PMMA- <i>c</i> PCEMA-PDMAEMA		Particle	~ 20 nm	Amphiphilicity	[102]		
PS-PE-PEO		Worm-like micelle	700 nm (length)	Surfactant	[103]		
PS-peptide-PBA	Confined self-assembly and disassembly	nanotube	70–200 nm	Self-assembly	[104]		
P2VN-PEO/PAA		Particle	N/A	Self-assembly	[105]		
PEO-P2MVP/PAA-PAM		Disc	20 nm (core)	Self-assembly	[106]		
PEO-P2MVP/PAA-PAAM		Ellipsoidal	20 ± 2 nm	Self-assembly	[107]		
DNA-peptide		Nanosheet	N/A	molecular recognition	[108]		
PNM/Au		Snowman-like	~50 nm	N/A <sup>a</sup>	[109]		
P4VP-PS		Confined self-assembly	Snowman-like	tunable	Surfactant, self-assembly	[110]	
PS- <i>c</i> PAA		Confined self-assembly and disassembly	Parachute	5–7 (head)	Surfactant	[111]	
PNIPAM-Au@ <i>c</i> P4VP-PS		Particle	Particle	4–5 nm (Au core)	Responsive	[112]	
<i>c</i> PCEMA-PEO		Electrostatic-mediated intramolecular crosslinking	Tadpole-like	4.7 nm (head)	Self-assembly	[113]	
<i>c</i> P4VP-PMMA	4 nm (head)			Self-assembly	[114]		
Silica-PEO	19.7 ± 3.1 nm			Self-assembly	[115]		
PS- <i>c</i> P(DMAEMA- <i>co</i> -CMA)	7.7 nm			CO <sub>2</sub> responsive	[116]		
<i>c</i> PAA-PS, PS- <i>c</i> P4VP, PS- <i>c</i> P4VP-PEO, etc.	Tunable			Multifunctional (Paramagnetic, pH responsive)	[117]		
PS- <i>c</i> PAA@(Fe <sub>3</sub> O <sub>4</sub> -PNIPAM)	Intramolecular cross-linking			Tadpole-like	25 nm	Thermal, magnetic responsive	[118]
PEO-P2VP@Co-PS					8 nm	catalysis	[119]
<i>c</i> PI- <i>c</i> P4VP					6.4 nm	N/A	[120]
poly(OEGMA- <i>co</i> -AnMA)- <i>b</i> -poly(OCLMA- <i>co</i> -HEMA)	6 nm			Surfactant	[121]		
Fe <sub>3</sub> O <sub>4</sub> -PVBC	Coupling			Tadpole-like	Tunable	Surfactant	[123]
Fe <sub>3</sub> O <sub>4</sub> - <i>c</i> PMEO <sub>2</sub> MA		10–29 nm, tunable	Multi-responsive surfactant		[124]		
PDMAc-PNAM	Self-assembly (H-bonding)	Nanorod	12 nm (diameter)	surfactant	[125]		
PEO-NDI/DAN-U <sub>2</sub> -PHEA	Self-assembly (charge transfer complexation)	Nanocylinders	13 nm (diameter)	N/A	[126]		
<i>c</i> P4VP-PS	Self-assembly and disassembly	Disc	31 nm (thickness)	Surfactant, self-assembly	[129]		
PS- <i>c</i> PI-P2VP	Confined self-assembly in emulsion droplet	Nanodisc	N/A	surfactant	[130]		
PS- <i>c</i> PB-PBA		Nanocup	N/A	container	[131]		
PS- <i>c</i> P4VP		Sphere	~70 nm	self-assembly	[132]		

a: Not available.

generated by the confined self-assembly. The emulsion droplet should be small sufficiently to achieve pure Janus nanoparticles. Otherwise, multiple-compartmental particles would be present. This process is also confirmed by computer simulation [133].

As discussed above, self-assembly and disassembly of supramolecular structures is effective to fabricate Janus polymeric materials with tunable morphologies and compositions. Inorganic species (i.e., Au) can be selectively grown at the functional polymer domains. The coexistence of multiple-compartmental micelles (MCMs) or core-shell structures with the Janus nanoparticles is the major problem by using solution self-assembly. This problem can be addressed by confined self-assembly and disassembly of block

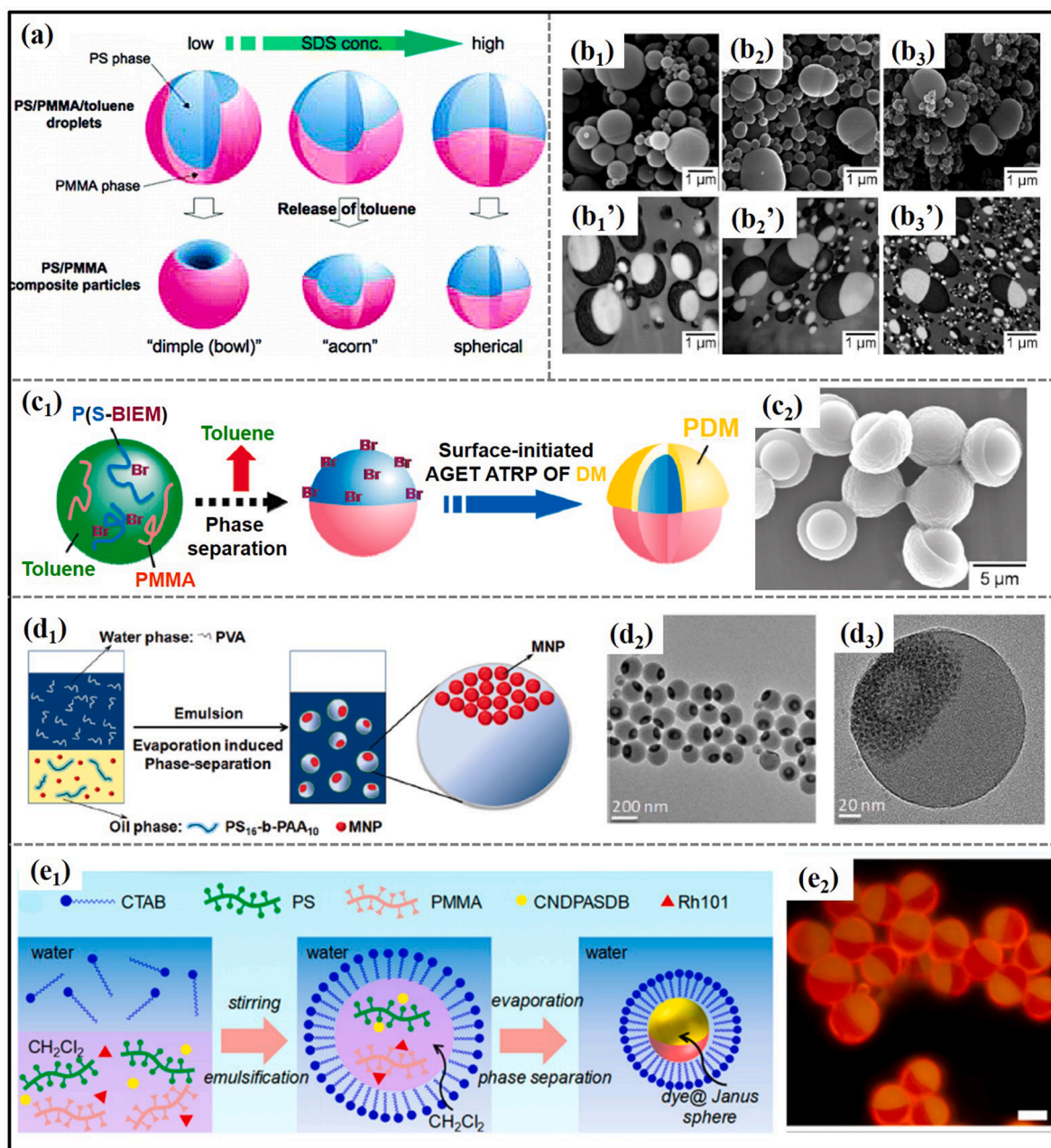


**Fig. 8.** (a) Schematic morphological evolution of the particles with increasing SDS surfactant concentration. Adapted with permission from Ref. [134]. Copyright 2006 American Chemical Society. (b<sub>1</sub>-b<sub>3</sub>) SEM images of the Janus particles with increasing molecular weight, the TEM images (b<sub>1</sub>'-b<sub>3</sub>'). Adapted with permission from Ref. [135]. Copyright 2008 American Chemical Society. (c<sub>1</sub>) Schematic synthesis of the mushroom-like Janus particle by emulsion solvent evaporation and ATRP polymerization, (c<sub>2</sub>) SEM image of the particle. Adapted with permission from Ref. [138]. Copyright 2010 American Chemical Society. (d<sub>1</sub>) Schematic synthesis of the multifunctional composite by emulsion evaporation induced phase separation, (d<sub>2</sub>, d<sub>3</sub>) TEM images of the magneto-optical composite. Adapted with permission from Ref. [145]. Copyright 2010 American Chemical Society. (e<sub>1</sub>) Schematic preparation of the fluorescent Janus particle, (e<sub>2</sub>) PL image of the dye-loaded Janus particle. Adapted with permission from Ref. [147]. Copyright 2019 American Chemical Society.

copolymers in emulsion droplets with neutral emulsion interfaces and small size. Table 3 demonstrates the Janus materials fabricated by using self-assembly strategy.

## 5. Seeded swelling polymerization synthesis

### 5.1. Polymer seeded synthesis

#### 5.1.1. Evaporation of polymer emulsion droplets

Phase separation of multiple component polymers is effective to control microstructure and property of materials in a confined space, which is driven by either solvent evaporation or polymerization. When the phase separation occurs in a small confined space for example an emulsion droplet, a Janus particle may be prepared. A typical approach reported by Okubo *et al* is based on solvent evaporation induced phase separation in an emulsion droplet [134]. Morphology of the Janus materials is tunable by controlling the surfactant type and concentration (Fig. 8a). The mixture of PS/PMMA in toluene is selected as the oil phase. In the case of PVA, a single dimple is present at particle surface. In the case of sodium dodecyl sulfate (SDS), the composite particle is evolved from dimple *via* acorn to spherical with increasing SDS concentration. The eccentric core-shell and hemisphere morphological change is arisen from contraction of the PS phase after hardening of the PMMA phase by phase separation during toluene evaporation. The droplet morphologies are not consistent with theoretical predictions based on interfacial free energy consideration. The discrepancy is explained that each polymer phase contains a small amount of the other polymer thus affecting the interfacial tension. Molecular weight of the polymer is another key parameter to control the morphology (Fig. 8b) [135,136], which is defined by  $(M_{wPS} + M_{wPMMA})/2$  at the equal weight fraction. Toluene is used as the solvent and the nonionic surfactant of poly(oxyethylene nonylphenylether) (Emulgen 911) is used as the surfactant. After evaporation of the solvent from the emulsion droplet, the spherical droplet becomes a snowman-like particle with a Janus structure. The non-spherical shape is highly dependent on the molecular weight. The interfacial tension between PS and PMMA increases with the molecular weight, driving the formation of snowman-like shape to decrease the interfacial area between the two phases. A functional Janus nanocomposite is achieved by introducing reactive groups at the corresponding polymers. As an example, a thermal responsive polymer brush is grafted onto hemispherical surface of the PS/P(MMA-CMS) composite particle when the PMMA chain contains chloromethylstyrene (CMS) [137]. When the ATRP initiator group is exposed on one side of the mushroom-like Janus particle by emulsion evaporation, a pH responsive Janus particle is derived by selective ATRP of functional monomers (Fig. 8c) [138,139]. A PS/PMMA particle with the Janus-like morphology is achieved by evaporation of dichloromethane (DCM) from the polymer/hexadecane (HD)/DCM-in-water emulsion droplet. By adjusting composition and the interfacial tension, morphology of the polymer particles is greatly tailored [140,141]. A Janus-like morphology of PS/PMMA is achieved *via* the internal phase separation followed by extraction of hexadecane (HD). The internal phase separation is driven by evaporation of DCM from the emulsion droplet. The particle changes from bowl-like to hemisphere and truncated sphere with increasing SDS content. With increasing PMMA/PS ratio, the particle changes from capped acorn to 'ball-in-bowl' morphology. Similarly, a pH-responsive biphasic Janus particle of PS/P2VP is synthesized by slow evaporation of chloroform from the PS and P2VP contained oil phase after a UV crosslinking of the benzophenone units at the backbones of both polymers [142]. By adjusting pH of the aqueous phase or controlling mass ratio of PS/P2VP, a pH triggered emulsion inversion is achieved when using the PS-P2VP Janus particle as the stabilizer. The approach is valid to generate polymeric Janus particles from the asymmetric bottlebrush block copolymer emulsion [143]. In contrast to linear block copolymers, a bottlebrush block copolymer can well keep the Janus architecture due to the densely grafted side chains. For example, a self-engulfed Janus nanoparticle from the azobenzene liquid crystalline mesogen contained block copolymer (PMAAz) is prepared *via* the solvent evaporation from the emulsion. The azobenzene-containing PMAAz undergoes the transition from ordered LC state to a disordered expanding state upon visible light irradiation, which is promising for remote controlled release under light irradiation [144].

Emulsion evaporation induced phase separation is applicable to fabricate functional Janus nanocomposites. For example, when a hydrophobic magnetic nanoparticle and the amphiphilic block copolymer of PS-*b*-PAA are mixed in chloroform in the presence of PVA, an emulsion is formed under ultrasonication [145]. After slow evaporation of the organic solvent, the nanoparticles are segregated into clusters and located eccentrically at one side of the composite particle. A Janus nanocomposite is thus achieved (Fig. 8d). The approach is useful for selective encapsulation of therapeutic and diagnostic agents such as DOX within biocompatible polymers. The Janus particle of polymeric-based composite is promising for theranostic applications [146]. As an example, the fluorescent PS-PMMA Janus microstructure containing two isolated emissive dyes of hydrophobic 1,4-bis( $\alpha$ -cyano-4-diphenylamino-styryl)-2,5-diphenylbenzene and hydrophilic rhodamine-101 within the PS and PMMA hemispheres are prepared by evaporation of DCM/water emulsion droplets (Fig. 8e) [147]. The Janus material displays different color under two different wavelength channels. In another example, the optical active Janus particle of chiral helical polyacetylene is constructed by emulsion polymerization combined with solvent evaporation induced phase separation [148]. In the emulsion polymerization, PMMA experiences the phase separation from polyacetylene domains along with the polymerization of acetylenic monomers and evaporation of the solvent. Mushroom- and bowl-like Janus particles are obtained. The optical activity is originated from the helical polyacetylene chains.

#### 5.1.2. By seeded swelling emulsion polymerization

Seeded emulsion polymerization is effective toward polymeric Janus materials with various morphologies. In the first step, the seed particle is prepared by conventional emulsion polymerization. In the second step, after the seed is swelled with monomer, polymerization induced phase separation drives the formation of lobes protruded from the seed surface. According to different protrusion degree, morphology of the particle can be tunable from snowman, acorn to dumbbell. An example snowman-like Janus particle is

fabricated *via* the seeded emulsion polymerization of butyl methacrylate (*n*BMA) against the micrometer-sized PS particle in an ethanol/water (80/20, w/w) medium (Fig. 9a) [149]. With increasing ethanol content in the medium, number of the *n*BMA protuberance increases. Similarly, the protuberance number increases with increasing AIBN concentration for the polymerization. The composite particles with well-defined number of the poly(*n*BMA) protuberances may serve building blocks to construct superstructures. Similarly, a golf ball-like particle with numerous dimples at the surface is prepared against the seed particle of polystyrene/poly(styrene-*co*-sodium styrene sulfonate) by polymerization of *n*-BMA in the presence of dodecane droplets in a methanol/water (80/20, w/w) medium [150]. The dimples at the surface are formed by the volume reduction of poly(*n*-BMA)/dodecane domains with evaporating dodecane. Size and number of the dimples decrease with the sodium styrene sulfonate content. A biphasic dumbbell- or peanut-shaped particle is prepared which contains distinct lobes of “soft” PBA and “hard” PS [151,152]. The particle is made by seeded swelling emulsion polymerization of *n*BA against the PS particle (Fig. 9b). A “hard-soft” Janus composite particle of PS/PEHMA/*n*-paraffin is achieved *via* the seeded emulsion polymerization of 2-ethylhexylmethacrylate (EHMA) against the PS bead in the presence of *n*-paraffin droplet [153]. Paraffin plays a key role in driving the asymmetric distribution of PEHMA on the surface, leading to the Janus composite particle. A magnetic patchy Janus microsphere is synthesized by seeded swelling polymerization, which is composed of the Fe<sub>2</sub>O<sub>3</sub>-functionalized PS-*co*-PVA and the hydrophobic poly(tetradecyl acrylate) (PTA) bulbs (Fig. 9c) [154]. After the PS-*co*-PVA seed is prepared by dispersion polymerization, swelling with tetradecylacrylate (TA) is performed. By using UV irradiation to initiate the polymerization of TA, the amphiphilic Janus microsphere is achieved by the phase separation between PS-*co*-PVA and PTA. After the PS-*co*-PVA bulb is modified with poly(ethyleneimine) (PEI), Fe<sub>2</sub>O<sub>3</sub> is further decorated by electrostatic interaction. Size of each bulb is controllable by changing the monomer swelling ratio. Functional materials for example catalytic nanoparticles such as Pd and Ag are further grown [155]. Similarly, Janus dimers with different size are fabricated by emulsion polymerization, which is controlled by monomer ratio and polymerization temperature [156]. By the two-step dispersion polymerization, a functional Janus particle of Br@PS-poly(propargylacrylate) with distinct surface chemistry is achieved [157]. The aspect size ratio between the two patches is tunable by controlling the volume ratio between the feeding monomers. The distinct patches carry chemical handles, facilitating orthogonal surface modification using ATRP and thiol-yne click chemistry for the brominated and alkyne-containing patches, respectively. Many bifunctional colloidal particles with tailored directional properties are derived from the mother Janus particles.

In fact, the first synthesis of asymmetric particles by seeded emulsion polymerization can be traced back to early 1985 [2]. The asymmetric Janus particle is composed of two immiscible polymeric lobes of PS and PMMA. This approach is further developed to achieve an amphiphilic dumbbell-like particle by the seeded emulsion polymerization [158,159]. By regulating the crosslinking density gradient of the seed particles to overcome the effect of surface tension (Fig. 10a), directionality of the phase separation is well controlled to tune the microstructure from rod-like, cone-like to triangle diamond-like. Synthesis of “rods” and “triangles” against a

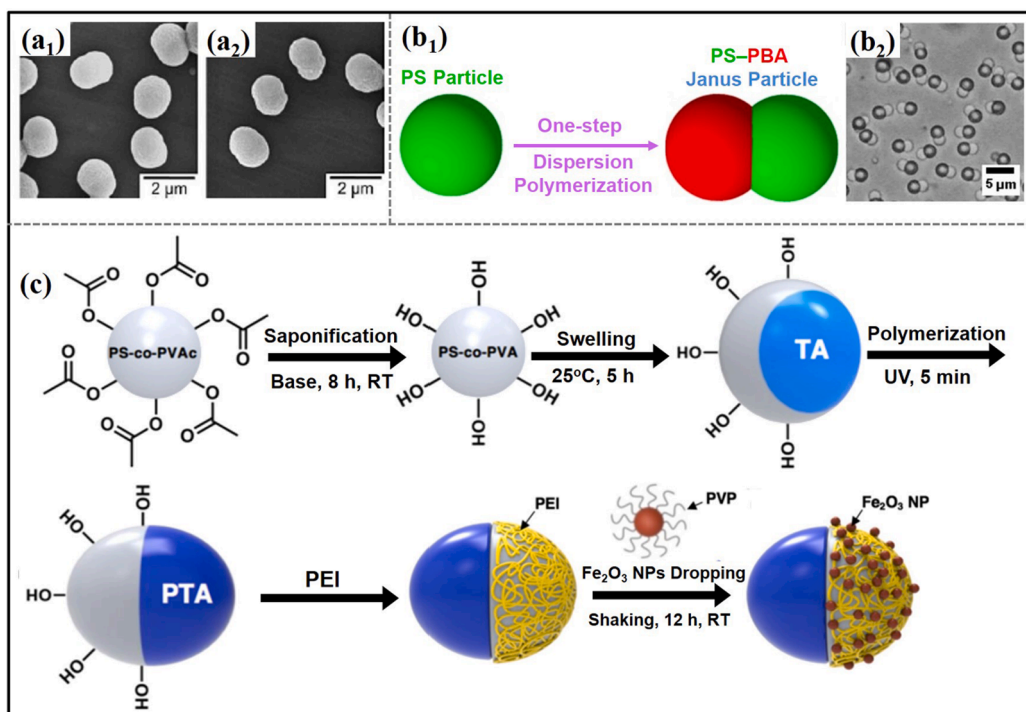


**Fig. 9.** (a<sub>1</sub>, a<sub>2</sub>) SEM images of the two PS/*n*BMA particles by seeded dispersion polymerization at various AIBN concentrations. Adapted with permission from Ref. [149]. Copyright 2005 Springer. (b<sub>1</sub>) Schematic synthesis of the PS/PBA Janus particle by seeded dispersion polymerization, (b<sub>2</sub>) optical image of the hard-soft Janus particle of PS/PBA. Adapted with permission from Ref. [151]. Copyright 2014 American Chemical Society. (c) Schematic formation of the magnetic Janus microsphere. Adapted with permission from Ref. [154]. Copyright 2018 American Chemical Society.

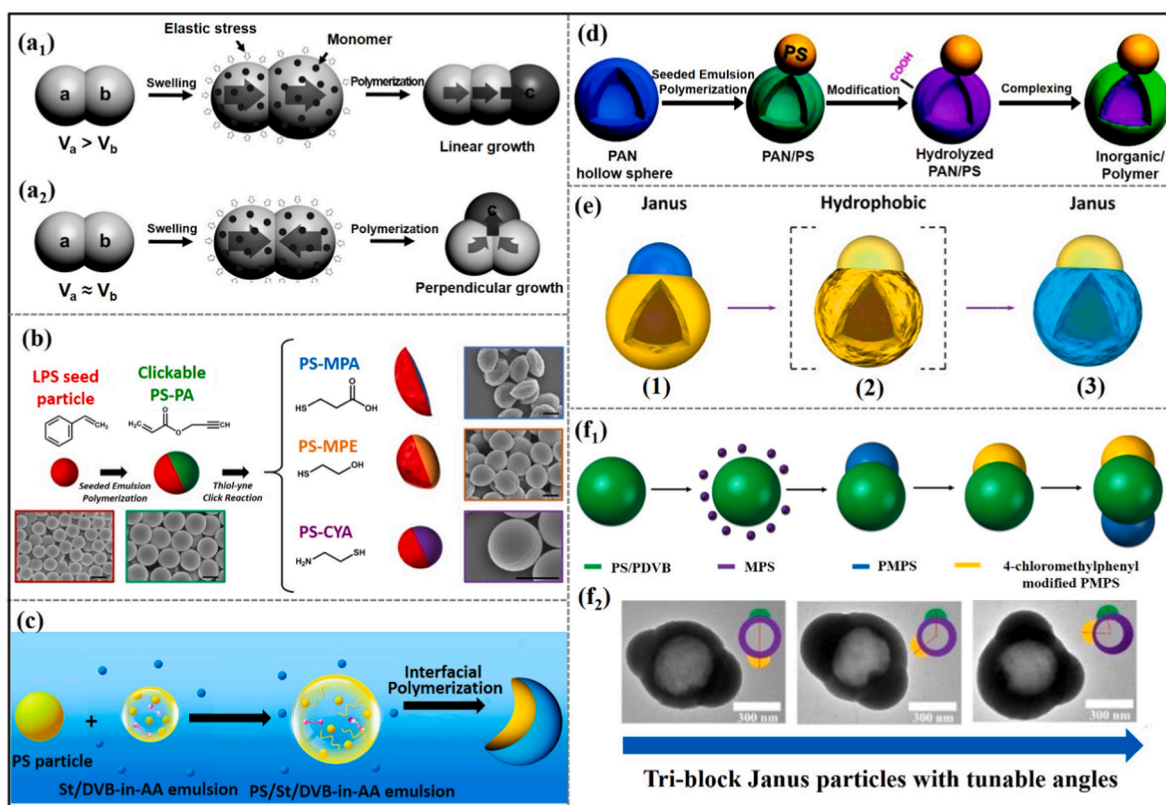


**Fig. 10.** (a<sub>1</sub>) Rod-like particle derived against the dimer with different crosslinking degree thus the phase separation direction along the axis, (a<sub>2</sub>) a triangle particle derived by perpendicular growing the third lobe against the dimer with the equal crosslinking degree. Adapted with permission from Ref. [159]. Copyright 2010 Wiley. (b) Schematic synthesis and the corresponding SEM images of the clickable PS-PA Janus particle and subsequent modification *via* different thiol-yne click reactions. Adapted with permission from Ref. [161]. Copyright 2016 American Chemical Society. (c) Schematic synthesis of the Janus colloid *via* emulsion interfacial polymerization. Adapted with permission from Ref. [162]. Copyright 2018 American Chemical Society. (d) Schematic synthesis of the Janus inorganic/polymer composite colloids. Adapted with permission from Ref. [165]. Copyright 2010 American Chemical Society. (e) Illustrative synthesis of the robust reactive Janus snowman-like composite particles: (1) silica@PDVB, (2) N-octyltriethoxysilane-silica@PDVB, (3) N-octyltriethoxysilane-silica@PDVB-PAA. Adapted with permission from Ref. [166]. Copyright 2015 American Chemical Society. (f<sub>1</sub>) Illustrative synthesis of the triblock Janus particle by seeded emulsion polymerization, (f<sub>2</sub>) SEM images of the triblock Janus particles with varied configuration. Adapted with permission from Ref. [168]. Copyright 2019 American Chemical Society.

dimer are compared to illustrate the effect of crosslinking degree on particle morphology. When the two bulbs possess slightly different degrees of crosslinking, a rod-like structure is derived after the swelling polymerization. When the two bulbs possess the same crosslinking degree, a triangle particle is derived after the polymerization. Starting from a crosslinked PS latex, a dimer is synthesized, containing the second lobe with tunable crosslinking degree. Generation of the lobe is attributed to the extrusion of newly formed polymer upon releasing the internal elastic stress arisen from crosslinking. Morphological evolution of the Janus particles is monitored during the seeded emulsion polymerization by using experimental and computational tools [160]. A slightly crosslinked PS seed is synthesized by dispersion polymerization, which is further swollen in *tert*-butyl acrylate and styrene monomers. Along with the polymerization, the dumbbell structure is achieved from the multi-lobe morphology. This nucleation-growth model has been verified by computer simulation. A clickable polystyrene-poly(propargyl acrylate) (PS-PA) Janus particle is synthesized by using acetylene pendant group contained PA as a monomer. Other functional Janus particles are derived after selective modifications *via* thiol-yne click reaction. The linear polystyrene (LPS) particle (~850 nm diameter) is prepared *via* dispersion polymerization. The LPS particle is swollen with a monomer mixture of styrene, propargyl acrylate and divinylbenzene. The click-active PS-PA Janus particle is achieved after the polymerization induced phase separation. It is found that the PS side contains a minority of PA while the PA side contains PS. Three thiols of 3-mercaptopropionic acid (MPA), 2-mercaptoethanol (MPE), and cysteamine (CYA) are used for the clicking reactions. After the thiol-yne click reactions, a distinct boundary is observed between smooth and rough faces of the particles (Fig. 10b) [161]. By using a non-crosslinked PS particle, a Janus particle can be constructed *via* the emulsion interfacial polymerization. Since the PS seed can be dissolved in the St/DVB-in-AA emulsion, the newly formed PS/PDVB nucleus should be covered by the dissolved PS chains inside the oil droplet. When the PS/PDVB nucleus is anchored at the interface, the reactive site of the PS/PDVB nucleus is exposed toward the aqueous phase due to the hydrophobic PS. The polymerization at the interface occurs faster than within the oil phase. An asymmetric Janus particle of PS/PDVB-PAA is derived (Fig. 10c) [162]. Dumbbell-like particle bearing different charges onto the two

lobes is depicted as another example [163]. It is key that the surface groups are covalently bound at the crosslinked seed, which cannot migrate to cover monomer after the polymerization induced phase separation in the second polymerization step. Using different surface-active monomers in each step gives the dumbbell-like particle with different surface chemistry at each part. The seed part contains negatively charged sulfate groups from the potassium persulfate initiator and tertiary amine groups from 2-(diethylamino) ethyl methacrylate after the polymerization, while the protrusion is stabilized with the positively charged cetyltrimethylammonium bromide (CTAB). After polymerization at a low pH, the tertiary amine groups are protonated thus positively charged. Both parts of the Janus particle are positively charged. When the tertiary amine groups become deprotonated with increasing pH, negative charge from the sulfate groups is dominant at the seed part. Meanwhile, the protrusion remains positively charged from the CTAB. The Janus particle is assembled into strings and circles. An acorn-shaped Janus polymeric particle is derived by two-step emulsion polymerization [164]. One part is composed of PMMA/n-butylacrylate (nBA) while the other part is composed of poly(nBA)/pentafluorostyrene (p-PFS). In the first step of emulsion polymerization, a spherical colloidal seed of poly(nBA)/poly(p-PFS) is prepared. In the second step polymerization for PMMA/P(nBA), the acorn morphology is achieved due to the lowest energy interfacial contact. Selection of proper monomers for the polymers with similar glass transition temperatures and precise control of interfacial energetic conditions during the polymerization are key to generate the unique acorn-shaped microstructure.

Although the seeded emulsion polymerization is highly efficient to achieve asymmetric structures, distinct compartmentalization of different compositions remains a problem. Since the phase separation is incomplete especially in a highly viscoelastic matrix, one major phase should contain another dispersed minor phase. The conventional Janus particles are asymmetric in shape, yet compartmentalization of different compositions is less strict. In order to address this key issue, an effective approach is proposed by further modification of the as-synthesized asymmetric particle to derive strict Janus particles in terms of asymmetric shape and distinct compositional compartmentalization. The example snowman-like asymmetric particle of poly(acrylonitrile) (PAN)/PS is achieved by seeded emulsion polymerization of styrene against the crosslinked PAN hollow sphere [165]. It is noted that the PAN shell should contain some amount of PS while no PAN is present in the PS lobe since the PAN shell has been highly crosslinked. After a selective hydrolysis of PAN shell to introduce functional groups for example carboxylic acid (-COOH), preferential growth of functional materials such as titania and/or metal oxides are thus induced to coat the whole outer surface of the shell. Effect of the residual PS within the shell is fully screened by the new grown materials. In terms of shape and surface wettability, the particle is strict Janus, which can be well dispersed in both water and solvents (Fig. 10d). Composition of the shell is broadly extended. It is curious if there are some new strategies to drive the phase separation more completely for a "strict" Janus structure in one step. A functional monomer of MPS with a silane pendant group is used for the straightforward one-step synthesis of a snowman-like Janus particle of silica@PDVB against the PDVB hollow sphere seed (Fig. 10e) [166]. The seed PDVB/PS composite hollow particle is dispersed in water in the presence of SDS. Monomer MPS is emulsified in water containing initiator KPS, forming a monomer/water emulsion at ambient temperature. By feeding the monomer emulsion into the seed dispersion under stirring, the seed emulsion polymerization is performed at 70 °C to generate the snowman-like Janus particle. pH value and sufficient reaction time are significant for the sol-gel process toward the well grown silica bulge. The effects of hydrophilic transition of the growing species by hydrolysis and condensation and the polymerization induced phase separation are coupled to drive the complete phase separation achieving the strict Janus particle. Size of the silica bulge is tunable with MPS feeding content. After dissolution of linear PS from the PDVB/PS part, the PDVB side becomes nanoscale coarsening while the silica bulge remains smooth. Both the silica head and PDVB belly are highly crosslinked, which are covalently linked at the connection. The Janus particle is robust against solvents under stirring. The particle is well dispersible both in water and solvents after removal of the surfactant from the exterior surface, implying the Janus particle is amphiphilic. Aspect ratio of the two sides is tunable across 1:1, implying that Janus balance is tunable from more hydrophobic to hydrophilic. The PDVB belly is hollow with tunable cavity size for further control of density. Both sides of the silica@PDVB Janus particle are reactive for selective growth of desired materials in an orthogonal way. A huge family of Janus particles can be derived with tunable Janus balance and functionality. Onto the silica head, the imidazole group is selectively conjugated by using the functional silane of triethoxy-3-(2-imidazolyl-1-yl)propylsilane. After quaternization of the imidazole group with 1-chlorobutane, the head is thus functionalized with the ionic liquid group. After the anion exchange from Cl<sup>-</sup> to PW<sub>12</sub>O<sub>40</sub><sup>3-</sup>, the Janus particle displays highly catalytic activity while preserving the amphiphilic performance. The example water soluble dye of methyl orange (MO) is easily decomposed upon feeding H<sub>2</sub>O<sub>2</sub> to the Janus particle stabilized oil/water emulsion, while the decomposed products such as monomethylaniline and N,N-dimethylaniline are captured by the internal oil phase, thereby highly promoting the reaction [167]. Against the snowman-like Janus particle of PDVB/silica as the seed, a triblock Janus particle is derived after growing another silica bulge (Fig. 10f). [168] It is found that both silica bulges grow at the eccentricity transition zone of the hollow seed particle, where the internal stress in the seed is highly accumulated. The axis angle between the two bulges is dependent on the eccentricity degree. Against the concentric hollow particle of a linear PS, the two silica bulges are located at the opposite poles. When using a slightly eccentric hollow particle of crosslinked PS, the two silica bulges are arrayed with an obtuse angle of 116 ± 12°. The angle becomes acute about 84 ± 9° when using a highly eccentric hollow particle. When the eccentricity degree is extremely high, the angle is too small that the two silica bulges are coalesced and form a large bulge. The surfactant SDS concentration is another key variable to control structure of the triblock Janus particles. At a low SDS concentration level for example 0.40 mg/mL, the surfactant is insufficient to fully cover the particle during the second seeded emulsion polymerization. As the result, the partially hydrolyzed silica species growing from the polymer shell serve as temporal "surfactant" to stabilize the particle, forming the second silica bulge by further coalescence. The triblock Janus particle is obtained. At an extremely low SDS concentration for example 0.20 mg/mL, a number of smaller silica particles are present in the serum while the second silica bulge forms onto the polymer shell. At a high SDS concentration above 0.60 mg/mL, the silica appears on the whole surface of the diblock Janus particle. A core-shell structure is formed. The two silica bulges can be selectively modified in the orthogonal mode to further tune the composition [168].

Bio-functional Janus particles have been reported by seeded emulsion polymerization after the thiol-click reaction. A duple

particle of PS is synthesized as the seed to derive a Janus particle of PS/PVBC after the seed swelling polymerization of vinylbenzylchloride (VBC). Bio-functionalization of the Janus particle is performed with glucose by the thiol-chloride “click” reaction, which exhibits region-selective binding of proteins. The Janus particle is promising in target drug delivery [169]. Various triblock Janus particles are fabricated by the combination of seeded emulsion polymerization of PtBA and thiol-ene click reaction [170].

Another approach is proposed to achieve the anisotropic Janus particles by protruding the core from core-shell structures. In the case of a polyelectrolyte coated PS core/shell sphere, the PS core is swollen to protrude from the shell at the initial stage of dissolving upon immersing in a core good solvent. When the dissolution is terminated, the PS protrusion is fixated, giving the anisotropic Janus particle [171]. Onto the negatively charged PS particle core, cationic poly(allylamine hydrochloride) (PAH) and anionic sodium poly(styrene sulfonate) (PSS) are alternately deposited, forming the polyelectrolyte multilayer (PEM) shell. When a PS good solvent for example THF is added to the PEM-coated PS aqueous dispersion at a THF/water volume ratio of 0.5:1, a small protrusion appears which is progressively evolved into a large spherical lobe. The protrusion can be terminated by adding excess water at a given stage. Morphology of the Janus particle is tunable by changing the dissolution degree. Starting with a PS sphere core, the core-shell particle is synthesized by seeded emulsion polymerization. The shell is a random copolymer of styrene (St) and trimethoxysilylpropylacrylate (TMSPA). During the swelling polymerization with styrene, the PS core is locally squeezed through the hydrophilic shell to achieve highly uniform dumbbell shape. Relative size of the two lobes is tunable by varying the swelling degree. The uniform Janus particles may serve as new building blocks for three-dimensional photonic crystals [172]. The example dumbbell-like particle with an overall length of 422 nm and the same lobe with a diameter of 267 nm is used to construct the photonic crystal. The length/diameter aspect ratio is calculated to be 1.58. The unique crystal is formed under an external electric field to align the assembled structure from the dumbbell-like particle. The new optical property of partial photonic band gap with birefringence can be modulated by an external field or quenched by solvent evaporation [173]. A snowman-like Janus composite particle is prepared by  $\gamma$ -ray initiated seeded emulsion polymerization after a hydrolytic condensation on the surface of second monomer swollen P(St-DVB-AA) seed [174]. By using the special facility, the polymerization can be performed at room temperature. Phase separation due to the polymerization induced elastic-retractile force gives the snowman-like asymmetric particle. The Janus particle becomes robust after the  $\gamma$ -ray radiation polymerization at ambient temperature [175]. By the polymerization of 3-methacryloxypropyl trimethoxysilane/styrene against the seed particle of P(St-DVB-AA), the snowman-like asymmetric particle is achieved by changing the amount of second monomer. The snowman-like particle serves as a solid surfactant to stabilize water/styrene emulsion to derive a hierarchical porous material after the  $\gamma$ -ray radiation polymerization. A Janus spherical particle composed of PS and PMMA hemispheres is synthesized from a core-shell structure by a simple solvent-absorption/release method from the core-shell particle [176]. The PS hemisphere is covered with PAA, while the PMMA hemisphere is covered with poly(vinylpyrrolidone) (PVP). The PS<sub>PAA</sub>/PMMA<sub>PVP</sub> composite particle is prepared by seeded dispersion polymerization of MMA using PVP as the stabilizer against the PAA stabilized PS seed particle. The Janus particle can self-organize into a colloidal chain *via* hydrogen bonding interaction between the two stabilizers at pH  $\sim$  4.0 below pKa (4.8) of the carboxyl group. Recently, Xia *et al.* have reported the synthesis of Janus particles by simply breaking the symmetry of spherical core-shell particles by swelling, where the PS sphere is covered with a rigid silica shell [177]. In the PS good solvents, the rigid shell is perforated by the osmotic pressure. The swollen PS is squeezed out from the shell, generating a Janus particle comprised of two distinct components.

Although the abovementioned swelling methods are elegant to achieve Janus particles, the Janus particles are inevitably aggregated during the swelling process at a higher concentration. In order to solve this problem, Yang *et al.* proposed a new strategy to prepare Janus particles by using monomer (or solvent) emulsion to swell the core/shell particle rather than the mixed solvents [178]. It is key that the protruded lobe is well protected by the surfactant to avoid the aggregation. Oil-in-water emulsions are employed to swell the example core/shell particle of PS/titania. The protrusion is initiated from the cracking open hole within the shell owing to the osmotic pressure. The swelling induced protrusion occurs in a confined compartment enveloped with the surfactant on the exterior surface of the titania shell. No coalescence among the polymer lobes is guaranteed by the protection with the surfactant layer. The aspect ratio of PS/titania parts can be greatly controlled with the swelling extent. The synthesis can be successfully performed at a higher particle concentration up to 5 wt%. After the surfactant is washed from the particle surface, the strict Janus particle is achieved with two different parts in both chemistry and structure. When monomers are used as the oil solvents for the emulsions, a further crosslinking can strengthen the polymer lobe, making the Janus particle stable in organic solvents. By tuning polymerization time and monomer/particle ratio, aspect size ratio of the polymer/inorganic parts thus Janus balance of the composite particle is continuously tunable from more hydrophilic to more lipophilic. By using a crosslinked block copolymer micelle as the stabilizer in the emulsion polymerization, the corresponding Janus particles are formed [179]. A polymer nanogel is synthesized by crosslinking the core of  $\omega$ -end unsaturated poly(methyl methacrylate/methacrylic acid)-*block*-poly(*n*-butyl methacrylate) (P(MMA/MAA)-*b*-P(*n*-BMA)) copolymer micelle. The reactive nanogel as a macromolecular surfactant with carboxylic acid groups is clustered into patches to avoid spreading, which are strongly locked at the latex surface after the emulsion polymerization. Anisotropic Janus or patchy colloids are synthesized thereby. Surface density thus number of the patches are tunable by varying pH during the emulsion polymerization. The Janus particle with one patch is achieved at a high pH  $\sim$  8.8. By swelling polymerization against a crosslinked block copolymer micelle, a Janus nanoparticle is formed after generating a new lobe [180]. Both shape of the anisotropic bulge and the polymer composition can be controlled. The monodisperse surfactant-free anisotropic Janus nanoparticle is synthesized by using RAFT mediated emulsion polymerization. Surface hydrophobicity/hydrophilicity and polymer composition are tunable.

Janus hollow particles with two compositions distinctly compartmentalized onto the interior and exterior surfaces of the shell, are promising in selective loading materials and controlled release. An amphiphilic Janus hollow particle is synthesized by multi-stage seeded emulsion polymerization after removal of the carboxylated polymer core from the core/shell latex by alkali treatment [181]. The core is formed by dispersion polymerization of the monomer mixture of butyl acrylate (BA), methyl methacrylate (MMA)

and methacrylic acid (MAA). By another swelling polymerization of the monomer mixture of styrene and MMA, a triple-layered core-shell latex is formed with the hydrophilic core and hydrophobic shell. The interlayer with a moderate polarity such as PMMA is key to form the core/shell structure. Otherwise, an acorn-like structure is formed by polymerization of styrene. Onto the interior surface of the shell, PAA moiety is present, rendering the pH responsive performance. Another Janus hollow particle is synthesized by one-step emulsion polymerization when using toluene as the oil phase [182]. The stabilizer of poly(vinylpyrrolidone) onto the PS core is conducive to form a homogeneous silica layer by sol-gel process of TEOS. The oil phase is composed of monomers of DVB, glycidyl methacrylate (GMA), St, toluene and the initiator of BPO. The oil phase is fed for the swelling in the presence of SDS. After the polymerization, the highly crosslinked polymer of P(DVB-GMA-St) tends to separate from the PS solution in toluene. Meanwhile, the newly formed polymer penetrates the open pore within the silica shell to release internal stress. The lobe is thus formed. After simple evaporation of toluene from the PS containing oil phase, the hollow structure is generated while PS is precipitated onto the interior surface of the silica shell. This strategy is promising to generate Janus hollow structures in one-pot after two-step phase separations.

## 5.2. Inorganic particle seeded synthesis

### 5.2.1. By seeded emulsion polymerization

When an inorganic particle is employed as the seed, polymerization of the monomers occurs onto the inorganic particle surface. Competition among the interfacial tension drives the phase separation and gives diverse morphologies. By the emulsion polymerization of styrene onto the modified silica particle surface, snowman and acorn-like morphologies are achieved depending on the grafting density of MPS (Fig. 11a) [183]. The particle surface modification is performed by adsorption of an oxyethylene-based macromonomer or covalent grafting of a trialkoxysilane derivative, favoring the formation of PS nodules at the silica surface. The number ratio between the silica seed and the growing nodule is key to control morphology of the composite particles. When the ratio is around 1:1, a dumbbell-like or snowman-like particle is obtained. The Janus particle serves as a building block to generate colloidal assemblies. The approach is general and applicable for smaller seed particles, such as the MPS-functionalized silica nanoparticle with a diameter below 60 nm [184]. Poly(styrene-co-butyl acrylate) (P(St-co-BA)) nanoparticles with diameters in the range of 25–60 nm are

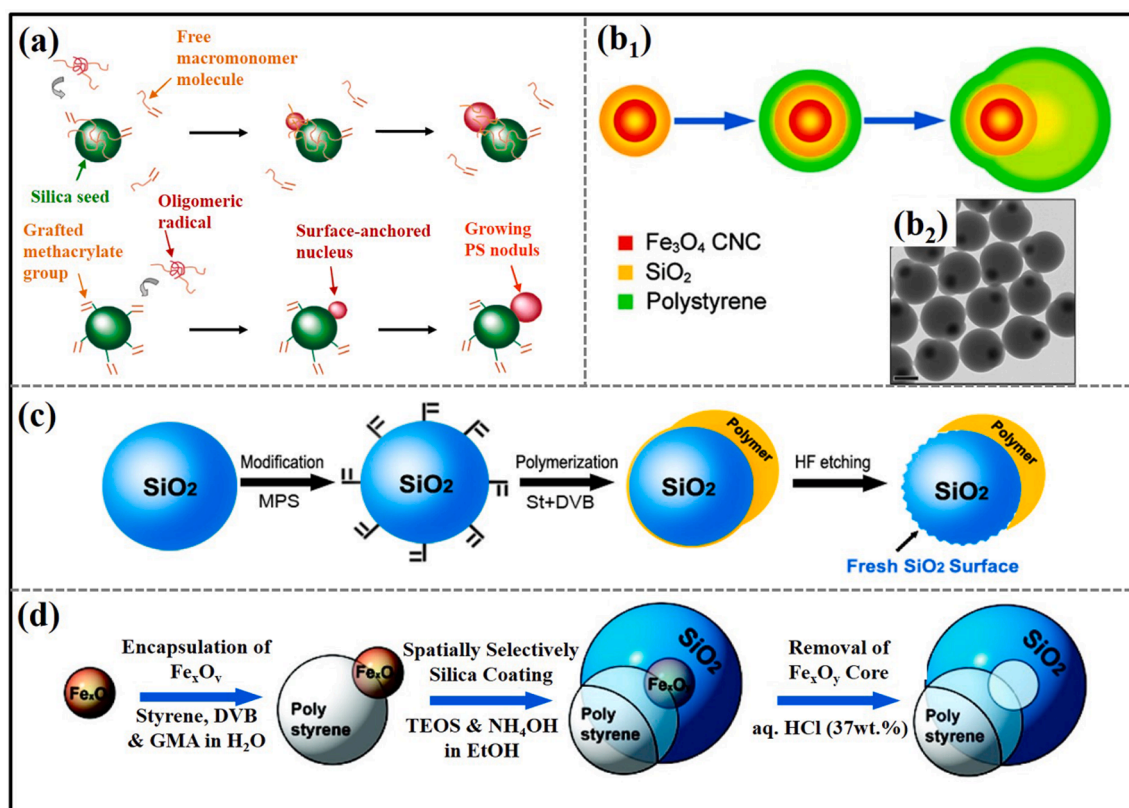


**Fig. 11.** (a) Janus particles by physicochemical association with a macromonomer or covalent grafting onto the functionalized silica by seeded emulsion polymerization. Adapted with permission from Ref. [183]. Copyright 2005 American Chemical Society. (b<sub>1</sub>) Schematic synthesis of the organic/inorganic core-shell particle and (b<sub>2</sub>) the TEM image. Adapted with permission from Ref. [185]. Copyright 2007 American Chemical Society. (c) Schematic synthesis of the Janus particle by seeded emulsion polymerization in combination with a wet etching. Adapted with permission from Ref. [186]. Copyright 2010 The Royal Society of Chemistry. (d) Synthesis of the mushroom-like Janus particle. Adapted with permission from Ref. [187]. Copyright 2010 American Chemical Society.

synthesized *via* emulsion polymerization. Sodium styrene sulfonate is used as the ionic comonomer, SDS as the surfactant and divinyl benzene (DVB) as the crosslinking agent. Dumbbell- and snowman-like P(St-co-BA)/silica composite Janus nanoparticles with silica and polymer nodules smaller than 60 nm are obtained by introducing MPS functionalized silica nanoparticle as the seed in the emulsion polymerization. The silica seed with MPS grafted onto the surface is capable of stabilizing the growing latex particles thus assisting an accelerated polymerization. Particles with dumbbell-like and snowman-like morphologies are favored at the equal number of the seed and the newly formed nodule. A silica coated magnetic core/shell particle can be used as the seed for the surface polymerization of styrene. A series of spherical and non-spherical magnetite-polystyrene ( $\text{Fe}_3\text{O}_4$ -PS) colloids are synthesized with the superparamagnetic cores concentrically or eccentrically positioned inside the PS shell (Fig. 11b) [185]. The Janus colloids serve as active components in sensors and actuators, microelectromechanical systems, and photonic devices. The composite spheres with concentric and eccentric superparamagnetic cores demonstrate interesting assembly behavior when subjected to a magnetic field. The concentric particles form linear chains, while the eccentric particles give a zigzag chain under the similar magnetic conditions.

It is noted that although the abovementioned Janus particles are asymmetric in shape, the whole exterior surface is coated with the same composition. The compositions are not distinctly compartmentalized. As an example, when the grafting density of MPS on the silica particle surface is high, the other part of the silica particle is covered with a thin layer of polymer shell after the polymerization induced surface de-wetting. Although the particle appears asymmetric in shape, the particle is only dispersed in solvents after washing the surfactant from the particle surface. This implies that the particle is not amphiphilic. In order to break this dilemma, a new strategy is proposed to generate the fresh hydrophilic silica surface with silanol group after removal of the thin polymer layer [186]. With diluted aqueous HF or  $\text{NH}_4\text{F}$ , the thin polymer layer can be easily fractured and detached from the silica surface under sonication while etching silica thereby. A fresh silica surface is exposed while the thick polymer shell remains intact and adhered onto the particle at the opposite side (Fig. 11c). The derived composite particle keeps the original asymmetric shape and becomes well dispersible both in water and solvents. The particle is strict Janus in terms of amphiphilicity and anisotropic shape. Functional materials can be

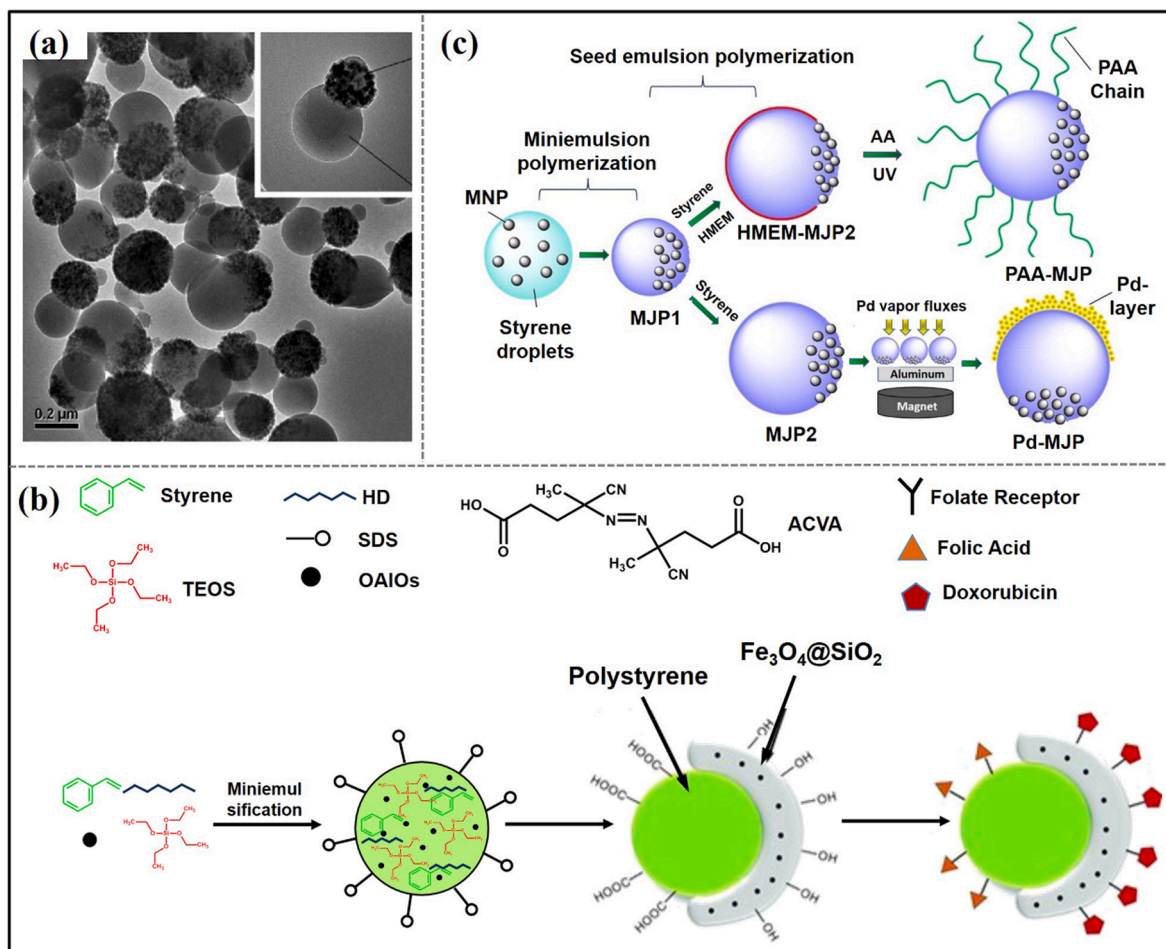


**Fig. 12.** (a) TEM image of the  $\text{Fe}_3\text{O}_4$ @silica/PS Janus composite particle. Adapted with permission from Ref. [190]. Copyright 2011 American Chemical Society. (b) Schematic synthesis of the magnetic Janus particle with dual functionalities for drug delivery. Adapted with permission from Ref. [191]. Copyright 2013 Wiley. (c) Schematic synthesis of the magnetic Janus particle by mini-emulsion polymerization and a subsequent seed emulsion polymerization. Adapted with permission from Ref. [193]. Copyright 2015 American Chemical Society.

**Table 4**  
Janus materials synthesized by seeded swelling polymerization.

Composition	Synthetic Method	Shape	Size	Property/Application	Ref.
PS/PMMA	SSP <sup>a</sup>	Dimple, acorn, spherical (tunable)	Tunable	Colloidal stabilizer	[134]
PS/PMMA	SSP + SIP <sup>b</sup>	Spherical, snowman-like	Tunable	Nonionic surfactant	[135,136]
PS/P(MMA-CMS)-b-PDM		Hemispherical	5.1 $\mu\text{m}$	Thermal responsive	[137]
PMMA/P(S-BIEM)-g-PDM		Mushroom-like	4.8 $\mu\text{m}$	pH- and temperature responsive	[138,139]
PS/PMMA	SSP + Solvent evaporation	Acorn to 'ball in bowl' strawberry-like	Tunable	Amphiphilicity	[140]
IA-Chol/H <sub>2</sub> pdcA-PDMS		Dumbbell-shaped (tunable)	Tunable	Amphiphilicity	[141]
PS/P2VP				Tunable	pH-responsive switchablesurfactants
gPDMS-b-gPS		Snowman-like, mushroom-like, and unclosed core-shell (tunable)	Tunable	Amphiphilicity	[143]
PEO-b-PMAAz		Snowman-like	~70 nm (long)	Light-triggered reversible self-engulfing	[144]
MNPs and PS-b-PAA nanocomposites		Sphere	~ 180 nm	Imaging, magnetolytic therapy	[145]
EVA/PLLA, EVA/PLGA, PMMA/PLGA		Snowman-like	100–120 $\mu\text{m}$	Theranostic	[146]
PS/PMMA		Sphere	3–15 $\mu\text{m}$	All-color-dual wavelength microlasers	[147]
PMMA-PA		Mushroom- and bowl-like	Tunable	Optically active	[148]
PS/P nBMA	SSP	Snowman-like and confetti-like	Tunable	Amphiphilicity	[149]
PS/P(S-NaSS)/PnBMA	SSP + Solvent evaporation	Golf ball-like	Tunable	Amphiphilicity	[150]
PS-PBA	SSP	Dumbbell- or peanut-shaped	Tunable	Amphiphilicity	[151,152]
PS/PEHMA/n-paraffin		Tunable	Tunable	Amphiphilicity	[153]
PS-co-PVA and PTA bulbs		Sphere	2 $\mu\text{m}$	Magnetic-responsive	[154]
PGMA/PSMA		Tunable	1.46 $\mu\text{m}$	Catalytic	[155]
Pd NP- and Fe <sub>2</sub> O <sub>3</sub> NP-patchy JMP		Sphere	~ 2 $\mu\text{m}$	Catalytic activity and magnetic responsive	[156]
PS-Br-PA	Dispersion polymerization + SSP	Sphere	~ 2 $\mu\text{m}$	Amphiphilicity	[157]
PS/PBMA	SSP	Dumbbell-like	Tunable	Surfactant	[158,159]
PS/tBA	Dispersion polymerization + SSP	Dumbbell and multilobe (tunable)	Tunable	Amphiphilicity	[160]
PS-PA	SSP + click reaction	Tunable	Tunable	Solid surfactant	[161]
PS/PDVB-PAA	SSP + Interfacial polymerization	Hemispherical, crescent-moon (tunable)	Tunable	Amphiphilicity	[162]
PS-PNIPAM	SSP	Dumbbell-like	Tunable	Responsive	[163]
P(p-nBA/PFS)-P(MMA/nBA)		Acorn-shaped	115 nm	Amphiphilicity	[164]
PAN/PS		Snowman-like	100 nm (PS)	Solid surfactant	[165]
silica@PDVB			Tunable	Solid emulsifier	[166]
silica@PDVB/PS			~ 430 nm	Dye degradation	[167]
PS/PDVB-silica			677 nm	Magnetic responsive	[168]
PS/PVBC		Sphere	3.05 $\pm$ 0.09 $\mu\text{m}$	Bioactive	[169]
PAA-PTPM-PTMPT	SSP + click reaction	Spherical- and worm-like	Tunable	Amphiphilicity	[170]
PS/poly(St-co-TMSPA)	SSP	Dumbbell	Tunable	photonic crystal	[172]
P(St-DVB-AA)@SiO <sub>2</sub> /PS		Snowman-like	Tunable	Solid surfactant	[174]
P(StDVB-AA)/P(MPS-St)		Raspberry-like to snowman-like (tunable)	Tunable	Solid surfactant	[175]
PS <sub>PAA</sub> /PMMA <sub>PVP</sub>		Core-shell	~ 2 $\mu\text{m}$	One-dimensional particle array	[176]
PS@SiO <sub>2</sub>		Dumbbell	Depending on PS	N/A <sup>c</sup>	[177]
PS@Titania		Dumbbell	Tunable	Solid surfactant	[178]
P(MMA-MAA)-PBMA		Sphere	Tunable	Pickering stabilizer	[179]
P(BA-co-MMA)		Dumbbell	25 nm	Stabilizer	[180]
PA/PBMM		Acorn-like	Tunable	Amphiphilicity	[181]
P(DVB-GMA-St)@SiO <sub>2</sub> @PS, P(DVB-GMA-St)@MPS-SiO <sub>2</sub> @PS		Elephant trunk-like and acorn-like	Tunable	Amphiphilicity	[182]
Silica-polystyrene		Dumbbell or snowman-like (tunable)	Tunable	Particulate surfactant	[183]
P(St-co-BA)/silica	SSP	Dumbbell- and snowman-like	< 60 nm	Amphiphilicity	[184]
Fe <sub>3</sub> O <sub>4</sub> @SiO <sub>2</sub> @PS		snowman-like	Tunable	Superparamagnetic	[185]
silica/polymer	SSP + selectively etching	Anisotropic	Tunable	Amphiphilicity	[186]
Fe <sub>x</sub> O <sub>y</sub> @PSD-SiO <sub>2</sub>	SSP	Mushroom	Tunable		[187]

(continued on next page)

Table 4 (continued)

Composition	Synthetic Method	Shape	Size	Property/Application	Ref.
silica/Fe <sub>x</sub> O <sub>y</sub> /P(St-co-DVB)		Mushroom	Tunable	Drug delivery, catalysis, or multifunctional sensor	
PS/silica	Mini-emulsion	Mushroom	Tunable	Amphiphilicity	[188]
Fe <sub>3</sub> O <sub>4</sub> @silica/PS	polymerization	Snowman-like	~ 0.5 μm	Biomedical	[189]
PS/Fe <sub>3</sub> O <sub>4</sub> @SiO <sub>2</sub>		Core-shell	200 nm (PS)	Superparamagnetic, amphiphilic	[190]
PS-SiO <sub>2</sub>		Snowman-like	~ 80 nm	Drug delivery	[191]
Fe <sub>3</sub> O <sub>4</sub> -PS-Pd	Mini-emulsion polymerization + vapor deposition	Sphere	Tunable	Magnetic field	[192]
				Magnetic, catalysis	[193]

a: Seeded swelling polymerization.

b: Surface initiated polymerization.

c: Not available.

preferentially grown against the silanol group at the fresh surface, deriving functional Janus particles. The synthesis is scalable for producing large quantity of strict Janus particles. Similarly, a mushroom-like Janus particle of silica/Fe<sub>x</sub>O<sub>y</sub>/P(St-co-DVB) is fabricated by selectively coating the Fe<sub>x</sub>O<sub>y</sub>/polymer snowman-like particle from the Fe<sub>x</sub>O<sub>y</sub> side (Fig. 11d) [187]. After dissolution of Fe<sub>x</sub>O<sub>y</sub>, the mushroom-like Janus particle of silica/polymer is generated with a hollow interior cavity. The Janus hollow material is promising as a carry for drug delivery and catalysis. The Janus composite particle of silica/Fe<sub>x</sub>O<sub>y</sub>/P(St-co-DVB) is capable of stabilizing emulsions such as toluene/water and vegetable oil/water systems. The functional Janus materials can be easily derived by selective functionalization of both hemispheres of the parent Janus particle, which are promising in phase transfer catalysis [188].

### 5.2.2. By mini-emulsion polymerization

Mini-emulsion polymerization is effective to prepare smaller Janus particles of polymer-inorganic nanocomposites, where the inorganic particles are incorporated within a polymer matrix. The process can be completed in one step. In the mini-emulsion polymerization, both nucleation and growth of the particle occur in the confined small droplet. For example, Janus asymmetric particle of PS/silica nanocomposite is synthesized via mini-emulsion polymerization [189]. The silica particle of 120 nm in diameter is partially modified with octadecyltrimethoxysilane (ODMS), while the other part remains hydrophilic. The modified silica particle is dispersed in the oil phase containing styrene and hexadecane. Sodium dodecyl sulfate (SDS), sodium bicarbonate and potassium persulfate are dissolved in water to form the aqueous phase. A mini-emulsion is formed by mixing the oil and aqueous phases under ultrasonication. An asymmetric droplet is formed with an oil droplet anchored onto the silica particle. After the polymerization at high temperature, the oily monomer droplet becomes solidified and connected with the silica particle, forming the asymmetric Janus particle of PS/silica. Free PS nanoparticles co-exist with the Janus particle, which can be separated by centrifugation. A magnetic responsive Janus particle of Fe<sub>3</sub>O<sub>4</sub>@silica/PS is fabricated by mini-emulsion polymerization of styrene and the sol-gel process of TEOS in the Fe<sub>3</sub>O<sub>4</sub> contained emulsion droplet containing styrene, hexane, AIBN, TEOS and MPS (Fig. 12a) [190]. The composite droplet lobe of Fe<sub>3</sub>O<sub>4</sub>/TEOS/MPS is anchored at the as-synthesized PS nanoparticle, which is partially encapsulated with silica. After a further sol-gel process by feeding aqueous NH<sub>4</sub>OH, the composite droplet lobe becomes solidified with the Fe<sub>3</sub>O<sub>4</sub> nanoparticles incorporated in the silica matrix. The Janus composite particle is achieved. The coupling agent of MPS plays a crucial role in controlling the morphology. The copolymerization of the monomers and polycondensation of TEOS are coupled with MPS. In the absence of MPS, the magnetic composite particle adopts an incomplete core/shell structure. The Janus composite particle displays the superparamagnetic performance, which is promising for biomedical applications such as nucleic acid extraction, protein purification, cancer diagnosis, and biosensors. If the hydrophobic initiator AIBN is replaced with a hydrophilic one of 4,4'-azobis(4-cyanovaleric acid), another Janus composite is generated with desired dual functionalities for drug delivery (Fig. 12b) [191]. The PS core is coated with carboxyl groups on one side, while the other side is covered with the silica composite layer containing iron oxide nanoparticle. The carboxyl group at the PS core surface and the silanol group at the silica shell are useful to conjugate functional materials for example folic acid and DOX, respectively. Along with the similar approach, a Janus magnetite particle with silica and PS onto the opposite sides is generated by sonochemical driven mini-emulsion polymerization [192]. PS at the Janus particle surface could induce functionalization by grafting PAA brush via polymerization, or by coating palladium nanoparticles via vapor deposition (Fig. 12c) [193].

Seeded swelling polymerization is simple and controllable, which is applicable to prepare those Janus materials of polymers and polymer/inorganic nanocomposites. Diverse morphologies can be easily adjusted for example by changing the seed/monomer ratio or by altering the seed shape. However, the method is not suitable for inorganic Janus materials. Table 4 lists the Janus materials prepared by seeded swelling polymerization.

## 6. Properties and applications

Janus materials with precisely controlled composition, architecture, and function represent new emerging materials and have shown promising applications in various fields. As functional solid surfactants, Janus materials provide powerful tools to manipulate interfaces [194-197]. The Janus materials are exclusively located at emulsion interfaces, providing an easy way to manipulate the

disperse phase with a magnet when the Janus materials are paramagnetic. This unique performance is highly attractive for efficient separation of emulsified systems [198]. When decorated with catalytic species, Janus-type catalysts can promote the interfacial catalysis, which are easily recycled [199]. They are also useful as new building blocks toward functional superstructures [200]. Janus

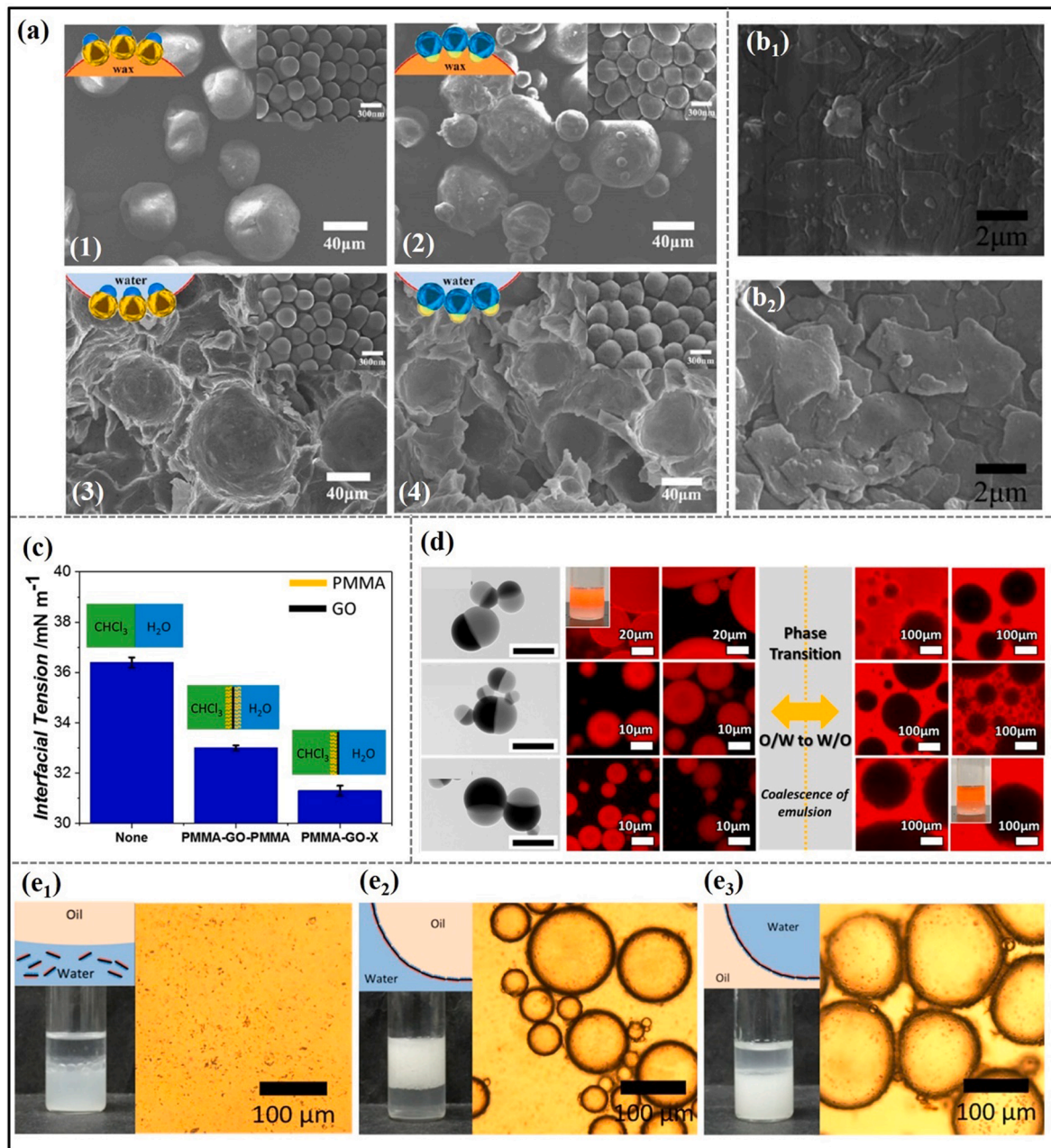


**Fig. 13.** (a) SEM images of the frozen droplets: (1–2) wax/water emulsions stabilized with the Janus particles of silica@PDVB and OTES-silica@PDVB-PAA, respectively; (3–4) water/wax emulsions stabilized with the Janus particles of silica@PDVB and OTES-silica@PDVB-PAA, respectively. Adapted with permission from Ref. [166]. Copyright 2015 American Chemical Society. (b<sub>1</sub>, b<sub>2</sub>) SEM images of the monolayer and multi-layer of the Janus nanosheet on the frozen paraffin droplet. Adapted with permission from Ref. [69]. Copyright 2011 Wiley. (c) Effect of the PMMA-GO-PMMA and PMMA-GO-X on the chloroform/water interfacial tension. Adapted with permission from Ref. [67]. Copyright 2017 American Chemical Society. (d) Fluorescence optical microscopy images of the Pickering emulsions stabilized by the Janus particle with different PS/P2VP volume ratios under various pH values. Adapted with permission from Ref. [142]. Copyright 2017 American Chemical Society. (e) Emulsifying the toluene/water mixture by using the Janus composite nanosheet of PNIPAM/silica/PDEAEMA under varied conditions: (e<sub>1</sub>) no emulsification at pH = 2 and T = 25 °C, (e<sub>2</sub>) a toluene/water emulsion formed at pH = 2 and T = 50 °C and (e<sub>3</sub>) a water/toluene emulsion formed at pH = 10 and T = 25 °C. Adapted with permission from Ref. [74]. Copyright 2015 American Chemical Society.

materials are promising in biomedical applications. Especially, they demonstrate unique ability to recognize cells and efficiently promote endocytosis, which is significant for biosensing and drug delivery [201-204]. In this section, we will exemplify several intriguing applications of the Janus materials which are easily tailored by the aforementioned methods.

### 6.1. Interfacial behavior

Amphiphilic Janus materials act as solid functional surfactants for emulsions, compatibilization agents for immiscible blends, separation of oil/water mixtures and special container. As solid surfactants, Janus materials display a higher desorption energy at interfaces than the corresponding isotropic particles with the Pickering effect. The Janus materials are exclusively anchored at the interface, making emulsions more stable. For example, a Janus dimer of PS-silica@NH<sub>2</sub> is strongly adsorbed at the oil/water interface, forming a closely packed monolayer [7]. The emulsion interface is robust to support the non-spherical shape of an emulsion droplet after the deformation. In comparison, the deformed droplet will be recovered into spherical shape when a homogeneous dimer with the same shape is used. The Janus particles adopt a well-defined orientation at the emulsion interface with the hydrophilic part facing toward the aqueous phase while the hydrophobic part toward the oil phase (Fig. 13a) [166]. Aspect size ratio of the two parts thus Janus balance of the Janus particles plays a key role in determining the emulsion type. When the hydrophilic lobe is bigger than the hydrophobic one, an oil-in-water emulsion is favored. The emulsion type is also related with the water/oil ratio. An oil-in-water emulsion is formed by using the silica/PDVB Janus particle at a high water/oil (W/O) ratio for example of 7:3. A water-in-oil emulsion is obtained at a low W/O ratio for example of 6:4. The emulsion phase inversion occurs around the W/O ratio of 6.2:3.8. Wettability of the silica/PDVB Janus particle can be reversed by modification. For example, by using Janus particle of OTES-silica@PDVB-PAA, the phase inversion occurs at a lower W/O ratio around 5.4:4.6. A bi-continuous emulsion is achieved during the phase inversion when the silica@PDVB/PS Janus particle is used [205]. A robust porous material is achieved by *in situ* interfacial polymerization of the bi-continuous emulsion. Both hydrophobic and hydrophilic surfaces form the corresponding continuous network along the channels. Phase inversion of the emulsion can be triggered by changing pH when using the responsive Janus particle [161]. Morphology of the Janus material can greatly affect the emulsion stability. Both elephant trunk-like hollow and acorn-like solid Janus particles are selected to compare the emulsification capability [182]. The emulsion stabilized with the hollow Janus particle is more stable. The hollow structure can gain additional interface than the solid particle, enhancing stability of the emulsion interface.

Janus nanoplates are superior as surfactants to stabilize the immiscible mixtures with more stability owing to restricted rotation at the interface [206]. A Janus nanosheet derived by crushing the Janus hollow silica sphere adopts the parallel lying mode at the oil-water interface, forming a monolayer at a low nanosheet content (Fig. 13b1). With increasing content of the Janus nanosheet, multi-layers are stacked at the interface (Fig. 13b2). The emulsion droplets become smaller progressively with increasing the Janus nanosheet content until reaching a plateau at the saturated coverage. It is applicable to emulsify non-aqueous immiscible mixtures for example of dimethylformamide/hexane mixtures [69]. The emulsion droplets keep stable with the spherical contour even after drying the oil phase, no coalescence or fracture is found. This is explained by jamming structure from the Janus nanosheet at the interface [81,129]. The chloroform/water interfacial tension is significantly lowered by using Janus PMMA-GO-X than the homogenous PMMA-GO-PMMA (Fig. 13c) [67], implying the Janus materials are more effective than the homogenous counterparts. A stable emulsion can be generated at a low concentration of the single-chain Janus particle. By using a tadpole-like single-chain polymer nanoparticle, a water/chlorobenzene emulsion is formed at an extremely low concentration of 0.0075%, much lower than the linear polymer counterpart [114].

Emulsification by using responsive Janus materials can be triggered by altering pH, temperature, light irradiation and magnetic field. A Janus particle of PS/P2VP is generated by solvent evaporation-induced phase separation, whose shape is tunable by changing the volume ratio of PS/P2VP [142]. The emulsion type can be reverted by regulating pH value in the aqueous phase (Fig. 13d). Upon loading paramagnetic iron oxide nanoparticles at the P2VP region, the composite Janus particle can be driven under a magnetic field. As the result, the dispersed oil droplets covered with the composite Janus particle can be withdrawn from the emulsion with a magnet. Afterwards, the Janus particle can be recycled after removal from the oil phase with a stronger magnet. The composite Janus particle makes both collecting the dispersed phase in emulsions and recycling easier, which is important for practical applications in many fields [168,192,207]. By using a light responsive Janus material for example spiropyran-containing Janus nanosheet, de-stabilization can be remotely triggered by UV irradiation [73]. Moreover, a dually responsive Janus material can be used to form emulsions, which can be triggered by multiple stimuli [74,82,120,207]. In the presence of PNIPAM/silica/PDEAEMA Janus nanosheet, the toluene and water are separated into two phases at  $T = 25\text{ }^{\circ}\text{C}$  and  $\text{pH} = 2$  with no emulsions forming. This is understandable that both polymers at the nanosheet are hydrophilic. At  $T = 50\text{ }^{\circ}\text{C}$  and  $\text{pH} = 2$ , the PNIPAM side becomes hydrophobic while the PDEAEMA side remains hydrophilic. The Janus nanosheet is amphiphilic. Consequently, a toluene-in-water stable emulsion is formed. An inverse emulsion of water-in-toluene is generated at  $T = 25\text{ }^{\circ}\text{C}$  and  $\text{pH} = 10$ , which is destabilized by heating to a high temperature at  $T = 50\text{ }^{\circ}\text{C}$  (Fig. 13e) [74]. Similarly, the emulsification and de-emulsification can be triggered by altering pH- and temperature when using the dually responsive Janus nanosheet of cPAA-*b*-PNIPAM [206].

The Janus materials are analogous to amphiphilic copolymers and can be used as functional compatibilizers for immiscible polymers. Janus nanoparticles with grafted polymer chains integrate the amphiphilicity of block copolymers and functionality of colloidal nanoparticles. Functional polymer blends are expected by using the functional Janus materials, which are exclusively anchored at the interfaces. Janus materials are superior as the compatibilizers over the molecular compatibilizers. In the case of copolymers, interfacial absorption degree and absorption dynamics are usually compromised since the two effects depending on molecular weight are adverse. Strict selection of copolymers with proper composition and molecular weight is prerequisite for the optimized effect. In contrast, Janus materials are tolerant against compositions in polymer blends, and display a much broad window

for the optimized compatibilization effect. Müller and coworkers have reported the first example by using Janus nanoparticle as compatibilizer in a polymer blend [96]. The Janus nanoparticle with PS and PMMA chains compartmentalized at the opposite sides is generated by disassembly of the partially crosslinked supramolecular structure of polystyrene-*block*-polybutadiene-*block*-poly(methyl methacrylate) triblock terpolymer (SBM) [96]. The Janus nanoparticle is located at the interface of the two polymer phases under macroscopic processing conditions at high temperature and shearing (Fig. 14a) [208]. The domains become smaller with increasing amount of the Janus nanoparticle. The Janus nanoparticle is also used in the blend of poly(2,6-dimethyl-1,4-phenylene ether) (PPE) and poly(styrene-*co*-acrylonitrile) (SAN) by the industry scale blending processing [209]. Morphology of the polymer blend is tuned by varying amount and composition of the Janus nanoparticle. A bi-continuous morphology is achieved in the PMMA/PS blend after demixing upon solvent removal [210]. Size of the dispersed domain is decreased with the Janus particle loading, while the phase inversion occurs by altering ratio of the PS/PMMA. A bi-continuous morphology is achieved around the equal fraction of the compositions, where a densely packed monolayer of the Janus nanoparticle is formed at the interface to stabilize the morphology. The snowman-like Janus composite particle with polybutadiene (PB) and polyisoprene (PI) rubber brushes at the two lobes has demonstrated a highly efficient compatibilization in the rubber blend of PB/PI. The interface between the two rubbers keeps stable after a thermal annealing, implying that interfacial stability is greatly enhanced by the Janus nanoparticle [211]. Janus nanosheets are more effective to enhance microstructural stability in polymer blends [212,213]. The example Janus nanosheet containing reactive epoxide (EP) group is derived by grafting butadiene acrylonitrile rubber (NBR) and 3-glycidyloxypropyltrimethoxysilane (GPTS) onto the opposite sides of the Janus silica nanosheet [212]. The EP/NBR Janus nanosheet demonstrates superior compatibilization for the blend of epoxy resin and nitrile-butadiene rubber blend (EP/LNBR) with synchronously improved strength and toughness. All the EP/NBR Janus nanosheets are present at the interface between the two polymers (Fig. 14b1). The Janus nanosheets are preserved at the interface after etching NBR with good solvents (Fig. 14b2), implying they are covalently bound at the interface after the epoxide

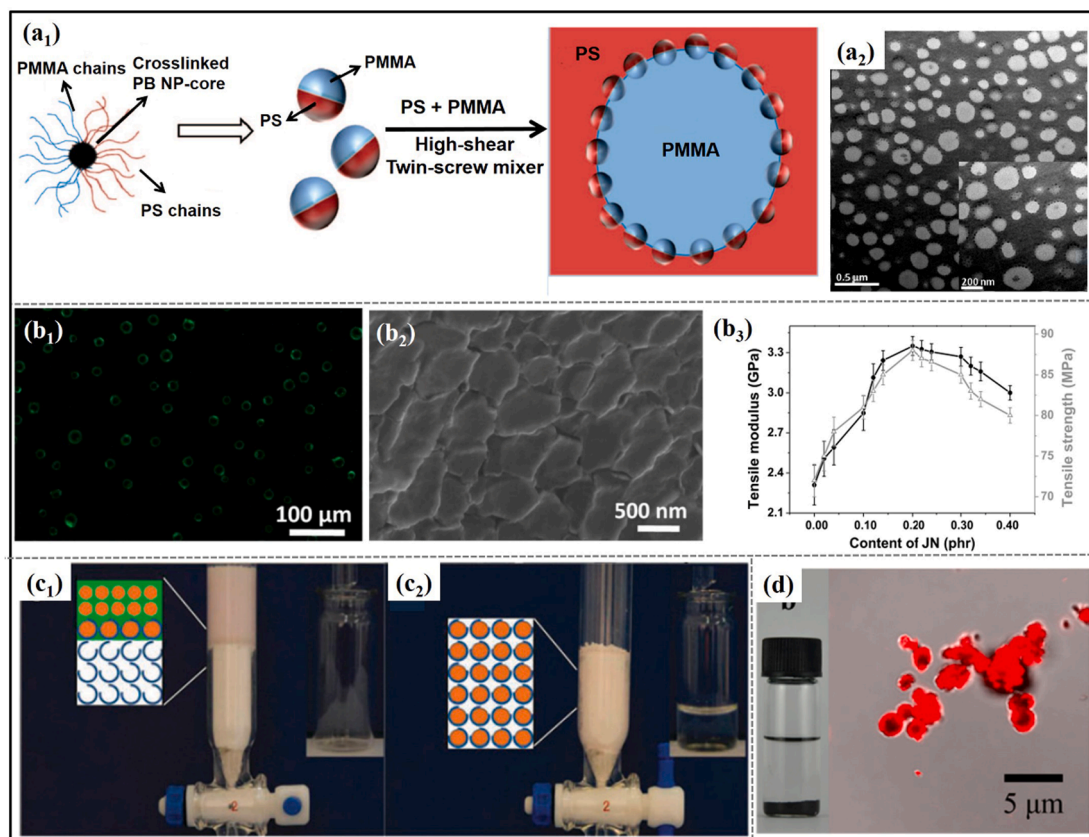


**Fig. 14.** (a<sub>1</sub>) Schematic structure of the Janus particle, (a<sub>2</sub>) TEM image of the Janus particles at the PS/PMMA interface. Adapted with permission from Ref. [208]. Copyright 2008 American Chemical Society. (b<sub>1</sub>) Fluorescence microscopy image of the EP/LNBR blend stabilized with 0.20% of EP/NBR Janus nanosheet, (b<sub>2</sub>) SEM image of the fracture surface after selective etching LNBR with good solvents, (b<sub>3</sub>) mechanical properties of the EP/LNBR depending on the EP/NBR Janus nanosheet content. Adapted with permission from Ref. [212]. Copyright 2019 American Chemical Society. (c<sub>1</sub>) A toluene/water emulsion flows through the Janus cage chromatography, clear aqueous phase elutes while toluene is absorbed, (c<sub>2</sub>) after the saturated absorption, the emulsion starts to elute. Adapted with permission from Ref. [13]. Copyright 2010 The Royal Society of Chemistry. (d) CLSM image of the PEG-octadecyl Janus cage after capturing oil. Adapted with permission from Ref. [55]. Copyright 2010 The Royal Society of Chemistry.

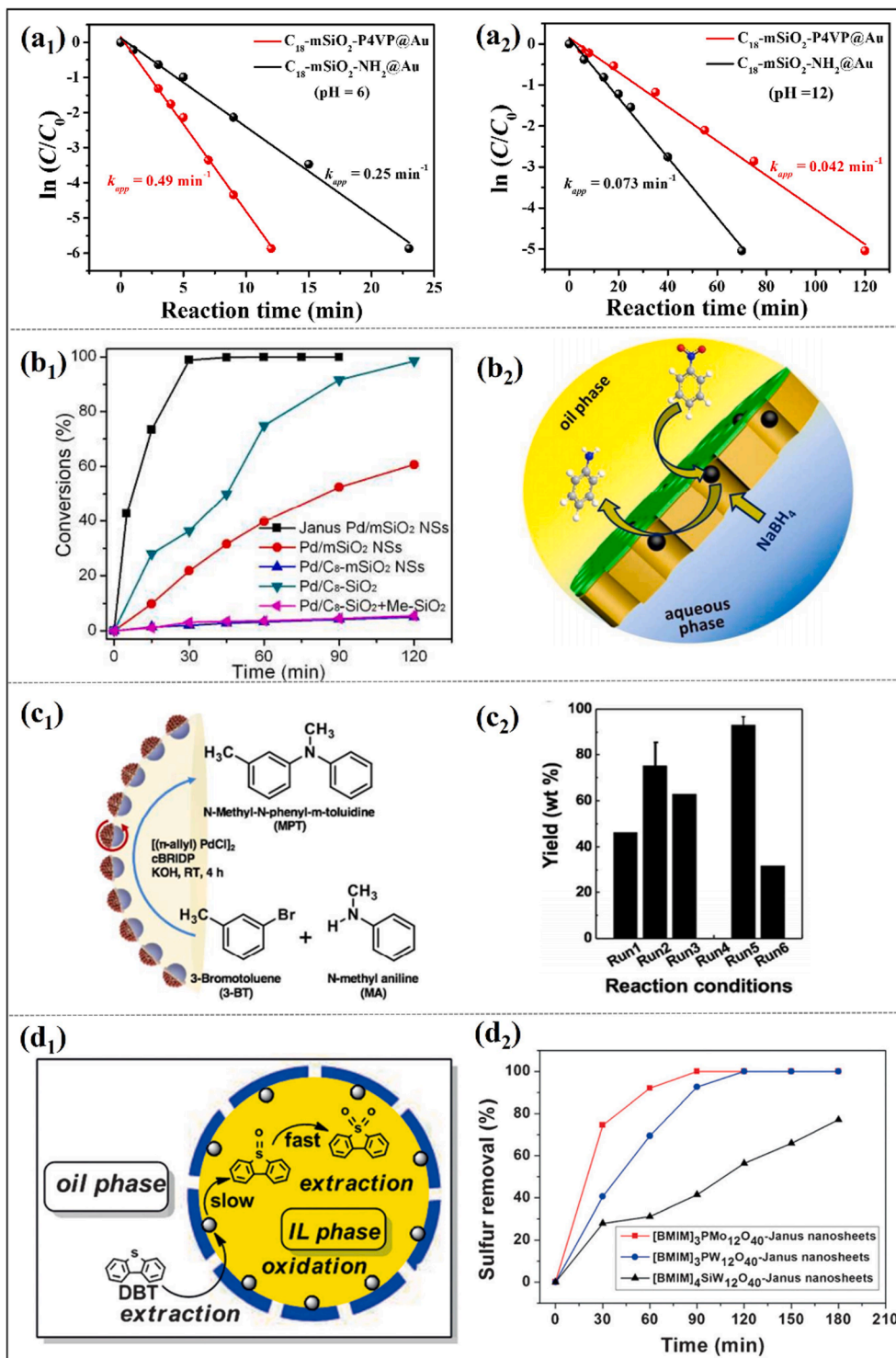


**Fig. 15.**  $\ln(C/C_0)$  of 4-NP with reaction time catalyzed by  $C_{18}$ -mSiO<sub>2</sub>-P4VP@Au and  $C_{18}$ -mSiO<sub>2</sub>-NH<sub>2</sub>@Au at varied pH values: (a<sub>1</sub>) 6, (a<sub>2</sub>) 12. Adapted with permission from Ref. [216]. Copyright 2020 The Royal Society of Chemistry. (b<sub>1</sub>) Conversion of nitrobenzene reduction by different catalysts, (b<sub>2</sub>) the illustrative reaction at the oil/water interface catalyzed by the Janus Pd/mSiO<sub>2</sub> nanosheet. Adapted with permission from Ref. [217]. Copyright 2018 The Royal Society of Chemistry. (c<sub>1</sub>) Schematic interfacial catalysis, (c<sub>2</sub>) yield of the amination of aryl bromide under different conditions. Run 5 denotes the presence of Pd NP decorated Janus catalyst and [(π-allyl)PdCl]<sub>2</sub>. Adapted with permission from Ref. [156]. Copyright 2018 The Royal Society of Chemistry. (d<sub>1</sub>) Illustrative interfacial catalysis, (d<sub>2</sub>) sulfur removal efficiency with various catalysts. Adapted with permission from Ref. [221]. Copyright 2017 Wiley.

groups at the Janus nanosheets are crosslinked with the EP matrix. At a saturated interfacial coverage with the EP/NBR Janus nanosheet around 0.2%, maximal mechanical properties are achieved owing to the most effective stress transfer between the two phases (Fig. 14b3). By using the Janus nanosheet of PMMA/epoxy in the blend of poly(vinylidene fluoride)/poly(L-lactic acid), an interconnected jamming structure is formed at the interface at the Janus nanosheet content around 0.5 wt%. No contraction is observed in the porous material after annealing at 190 °C for 30 min, implying the jamming structure is highly stable [213]. The synchronous enhancement of both strength and toughness of polymer blends by Janus nanomaterials may provide a new idea for highly effective recycling of polymer wastes with different compositions.

A Janus hollow cage with different wettability at the interior and exterior surfaces serves as a special container to separate oil/water mixtures. The chromatography column stacked by the Janus cage provides an easy and efficient way for oil/water separation. When a toluene-in-water emulsion flows through the column, toluene is selectively absorbed inside the cavity of the Janus cage and the clear aqueous phase elutes (Fig. 14c1) [13]. After the absorption reaches saturation, the Janus cages at the bottom are full with toluene (Fig. 14c2). The elute contains emulsions appearing opaque. When the thermal responsive polymer of PNIPAM is grafted onto the interior surface of the Janus cage, oily compounds can be selectively captured from the aqueous surroundings at high temperature [88]. At a lower temperature, the oily compounds are released. Similarly, the selective capture and release can be triggered by altering pH value when the interior surface is grafted with the pH responsive polymer of PDEAEMA [79]. In order to increase the collection rate, a coral-like structure is generated within the shell of the Janus cage of silica/alumina alloy [55]. The accelerated capture is attributed to the inward capillary force from the coral-like skeleton surface (Fig. 14d). The capture and release can be triggered when the skeleton surface is conjugated with desired functional materials for example thermal responsive PNIPAM or pH responsive PDEAEMA.

## 6.2. Heterogeneous catalysis

Although nanoscale catalysis has proved to be promising, inevitable aggregation and poor recyclability remain problems. Loading catalytic species at Janus nanostructures can significantly avoid the aggregation while making recycling easier. Various precious metal nanoparticles (i.e., Au, Pt, Pd) can anchor on the Janus skeleton (i.e., Janus nanoparticles, Janus nanosheets) by chemical interactions, yielding Janus-type catalysts. The precious metal nanoparticles are segregated by Janus skeleton thus greatly suppressing the aggregation. The recycling of Janus-type catalysts can be facilely achieved by centrifugation. In comparison, recycling of pure precious metal nanoparticles becomes difficult owing to their heavy aggregation after centrifugation. The Janus-type catalysts have exhibited extraordinary synergistic effects and excellent catalytic performances in self-propelled catalysis, interfacial catalysis, photocatalysis and electrocatalysis. Herein, we focus on the interfacial catalysis and recycling of the Janus-type heterogeneous catalysts. The catalysts are constructed by selective functionalization with catalytic species (i.e., Au, Ag, Pd, Co) and ion liquids (IL) at the Janus skeleton. The reduction of nitro-compounds is selected as the model reaction to evaluate the catalytic performance [156]. The reduction of nitrophenol (4-NP) to 4-aminophenol (4-AP) by the Au contained SiO<sub>2</sub> Janus porous microcapsule can be completed within 4 min. The catalytic activity is kept at very high level above 90% after recycles [214]. By selective loading catalytic NPs (Au, Ag) at the PAA regime of PAA/PS covered silica sphere, a hybrid hairy Janus catalyst is generated. Conversion of 4-NP to 4-AP is effectively catalyzed by the PAA/PS-Au Janus particle at a much lower catalyst content [49]. At the emulsion interface, the Au NP decorated Janus nanosheet shows much higher catalytic activity in the reduction of 4-NP than at the biphasic interface [215]. Compared with small molecule as the anchoring site for catalytic species, polymer such as P4VP is more efficient owing to a large number of anchoring sites in the polymer (Fig. 15a) [216]. Two Janus nanosheets of C<sub>18</sub>-mSiO<sub>2</sub>-P4VP and C<sub>18</sub>-mSiO<sub>2</sub>-NH<sub>2</sub> are used to derive the catalytic Janus mesoporous nanosheets by selective decoration of Au NPs at the hydrophilic side. Both catalytic Janus nanosheets could effectively stabilize the oil-in-water emulsions for the interfacial catalysis. The Janus particle of C<sub>18</sub>-mSiO<sub>2</sub>-P4VP after loading Au NPs exhibits remarkable higher catalytic activity owing to the densely loaded Au NPs at the P4VP chain. However, the catalytic activity becomes lower when P4VP is collapsed. Similarly, Pd NP functionalized Janus mesoporous nanosheet is highly efficient in the hydrogenation of nitrobenzene and the various substituted compounds [217]. Mass transfer is intensified through the transverse channels within the Janus nanosheets (Fig. 15b). By incorporating magnetic Fe<sub>2</sub>O<sub>3</sub> at the Ag NP functionalized Janus particle, the Janus catalyst is easily recycled with a magnet [156]. The Janus interfacial catalyst is advantageous in the heterogeneous catalysis, avoiding feeding additional phase transfer agents. The example amphiphilic Janus microparticle shows the same catalytic performance in the amination of aryl bromides at the emulsion interface as the commonly used phase transfer agent of tetra-*n*-butylammonium bromide (TBAB) [156]. When the Pd NP decorated Janus catalyst and [( $\pi$ -allyl)PdCl]<sub>2</sub> are simultaneously used, the yield is remarkably increased to 93% (Fig. 15c). The example Co cluster contained single-chain Janus nanoparticle shows much higher catalytic activity than the Janus nanosheet in the reduction of nitrobenzene to aniline at the emulsion interface [119]. This finding indicates that the functional single-chain Janus nanoparticles are more promising in heterogeneous catalysis.

Conjugation of ionic liquid moieties provides another effective way to achieve Janus-type catalysts. By the seeded emulsion polymerization and post-modification with the ionic liquid, the Janus particle of silica@PDVB/PS is further functionalized with the catalytic active species of PW<sub>12</sub>O<sub>40</sub><sup>3-</sup> [167]. 91.1 wt% of the methyl orange (MO) dye can be decomposed within 8 h in the toluene/water emulsion, while only 84.6 wt% of MO is degraded in the aqueous solution. The degradation products of MO are hydrophobic which are easily captured by the toluene phase, further promoting the degradation of MO. Poly(ionic liquid) (PIL) functionalized paramagnetic Janus particle exhibits the similar catalytic degradation of MO, which can be recycled by magnetic collection [218]. An amphiphilic Janus catalyst of HO-SiO<sub>2</sub>-IL-Ti(salen) is synthesized at a solid/liquid interface by the selective hydrophobic modification with a chiral salen Ti<sup>IV</sup> complex via the imidazolium ionic liquid (IL) linker [219]. The Janus HO-SiO<sub>2</sub>-Ti(salen) can effectively catalyze the asymmetric sulfoxidation at an emulsion interface with a high conversion of 99% and chemoselectivity of 97%. In comparison,

45% of conversion and 70% of chemoselectivity are achieved from the complex counterpart [219]. The IL-functionalized Janus particle (PA-PIL-JP) is highly active to catalyze the acylation reaction in the non-aqueous Pickering emulsion interface catalysis (FPIC) [220]. The IL-in-oil Pickering emulsion and the FPIC column are stabilized by PA-PILs-JP. The acylation of toluene to *p*-methylacetophenone with acetic anhydride is performed. The conversion of toluene in the FPIC column system is higher than in the Pickering emulsion system. The conversion is significantly increased in a smaller emulsion droplet. The Janus nanosheet tethered with IL moiety demonstrates excellent desulfurization, which is attractive to produce clean fuels [221]. In the conventional two-phase system

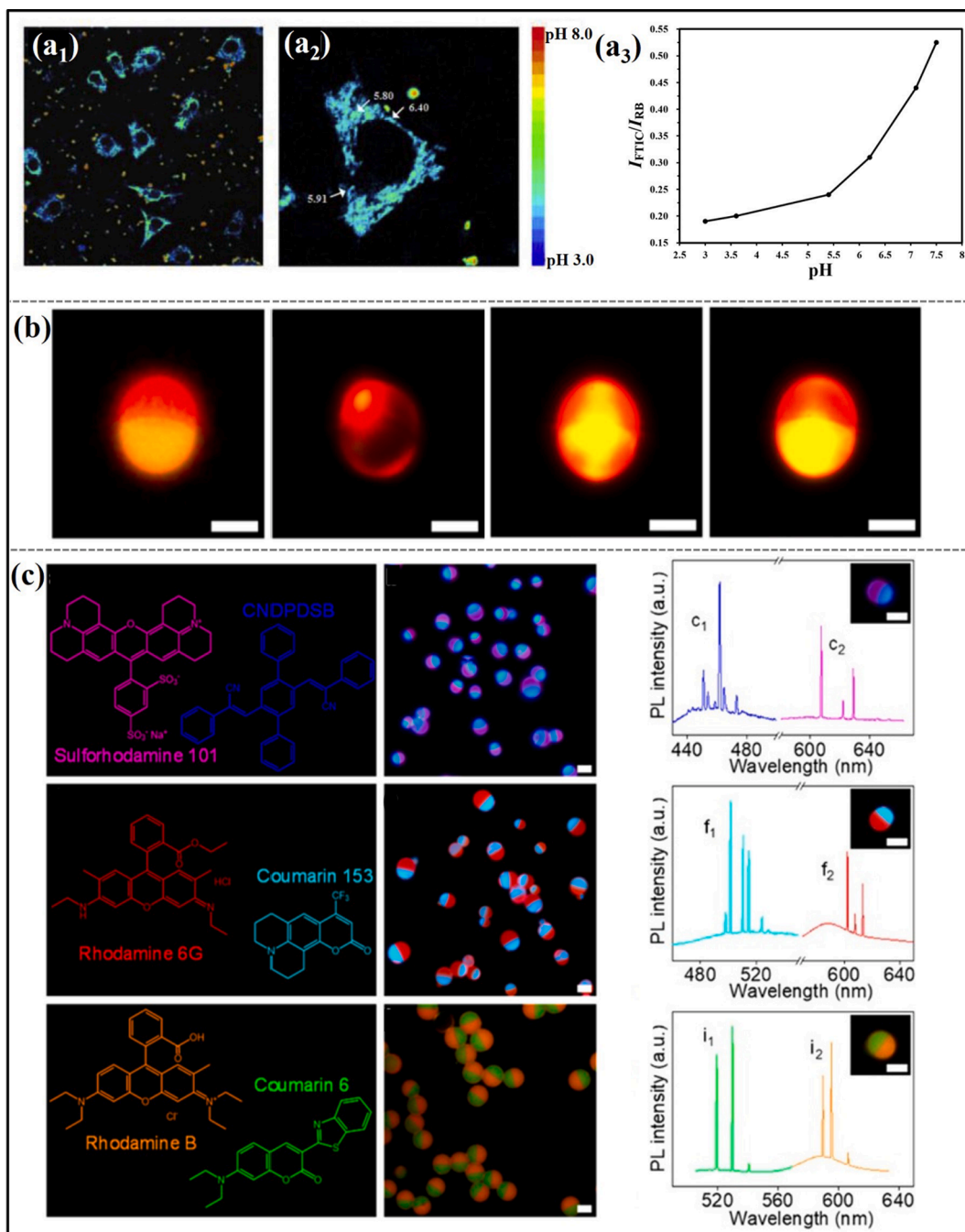


**Fig. 16.** (a<sub>1</sub>) The pseudocolored ratiometric image of the Janus probe-labeled SMMC-7721 cell, (a<sub>2</sub>) the single SMMC-7721 cell, (a<sub>3</sub>) pH titration of the Janus probe-labeled SMMC-7721 cell. Adapted with permission from Ref. [45]. Copyright 2019 The Royal Society of Chemistry. (b) PL images of the CNDPASDB-Rh101-doped Janus microspheres excited at UV light and focused laser at different positions. Scale bar: 5  $\mu$ m. (c) Molecular structures, PL images and normalized lasing spectra of the Janus microspheres with different dyes. Adapted with permission from Ref. [147]. Copyright 2019 American Chemical Society.

catalyzed by pure heteropolyacids (HPA), sulfur removal of the model compound of dibenzothiophene (DBT) is below 40%. The Janus catalyst can give an extremely high removal efficiency  $\sim 100\%$  by using  $\text{H}_3\text{PMo}_{12}\text{O}_{40}$  contained Janus catalyst. The high efficiency is related with the enhanced phase transfer and high contact area at the emulsion interface (Fig. 15d). By introducing the paramagnetic nanoparticle of  $\text{Fe}_3\text{O}_4$ , the NP/ $\text{PW}_{12}\text{O}_{40}^{3-}$ -based IL composite Janus nanosheet demonstrates superior catalytic performance in the esterification which is easily recycled by a magnet [94]. Similarly, the Janus silica cage of IL/PNIPAM composite exhibits thermal responsive desulfurization [54]. At a low temperature, the oxidation products are captured into the cage, facilitating the catalytic oxidation, which are released at a higher temperature [54]. The example Janus nanosheet is comprised of the hydrophobic groups ( $-\text{C}_8\text{H}_{17}$ ,  $-\text{C}_2\text{H}_4\text{Ph}$ ) and the hydrophilic groups ( $-\text{C}_3\text{H}_6\text{SO}_3\text{H}$ ,  $-\text{C}_3\text{H}_6\text{NH}_2$ ) at the opposite sides [222]. The Janus nanosheet displays a high catalytic activity in Knoevenagel condensation of a series of benzaldehydes with malononitrile in water and Fischer esterification of acetic acid with ethanol.

Another Janus nanosheet with molecular imprinted sites and thiol groups onto the two sides is employed for simultaneous removal of chlorophenols and heavy metals [77]. A catalytic Janus cage is achieved by incorporating the catalytic titania nanoparticle (i.e., P25). The photocatalytic decomposition is easily achieved within the cage upon UV irradiation after the organic compounds are captured inside the cage [223]. A Janus-type electrocatalyst is derived by pyrolysis the Ni and Fe precursors loaded graphene [224]. Nickel (Ni) and iron (Fe) single atoms are respectively loaded onto the inner and outer walls of a graphene hollow nanosphere. The single atom is coordinated with four N atoms *via* forming Ni-N<sub>4</sub> or Fe-N<sub>4</sub> planar configuration. A favorable electrocatalytic performance is demonstrated by the synergic effect at the Janus interface. The Ni-N<sub>4</sub>/GHS/Fe-N<sub>4</sub> Janus material exhibits excellent bifunctional electrocatalytic performance. The outer Fe-N<sub>4</sub> clusters are responsible for the high activity toward the oxygen reduction reaction (ORR), while the inner Ni-N<sub>4</sub> clusters show excellent activity toward the oxygen evolution reaction (OER). The Janus material is advantageous as an air-cathode over the benchmark Pt/C + RuO<sub>2</sub> air-cathode in rechargeable Zn-air battery with excellent energy efficiency and cycling stability. The work emphasizes the precise control of single-atom sites at carbon surface for the higher performance and more selective electrocatalysts. The Janus-type catalysts can be easily recycled by altering stimuli or using a magnet. What's more, catalysis of the Janus-type catalysts can be programmable by external stimuli for example altering temperature or pH value or under light irradiation. These merits make the Janus-type catalysts more attractive for practical applications.

### 6.3. Optical performances

Janus materials have exhibited intriguing optical properties and promising potentials in photonic crystals [225-227] and display [228-230]. As for a Janus optical probe, rheological property and molecular motion can be detected thereby [231]. Capping metal at one hemisphere of a microparticle provides an effective way to break the optical symmetry. The orientation can be tracked by using fluorescence and reflection. The torque acting on the particle can be measured by tracking the orientation and rotation, enabling the particle as a rotational viscometric probe to report on local Brownian, magnetic or biomechanical torques. Another example is light active Janus microparticle. One hemisphere emits a bright fluorescent signal, while an opaque metal darkens the other hemisphere. The particle is tumbling and blinking erratically by Brownian motion while they rotate literally. The fluctuating probe signals can be separated from optical and electronic backgrounds using principal components analysis or images analysis. Microrheological measurements are available at size and time scales, which are inaccessible by other traditional methods. The method is promising to improve sensitivity and reduce complexity for immunoassay procedures and intracellular chemical sensors [232]. A ratiometric fluorescent probe of Janus silica nanoparticle is synthesized against a Pickering emulsion interface, fluorescein isothiocyanate (FITC) and rhodamine B (RB) are selectively tethered onto opposite sides of the silica particle [45]. The Janus probe displays dual emission bands at 530 and 580 nm upon excitation at 488 nm. With increasing pH value, the ratiometric intensity ( $I_{530\text{nm}}/I_{580\text{nm}}$ ) of the probe is increased. Therefore, the pH change in cancer can be precisely measured by the probe (Fig. 16a). Similarly, pH of desired targets in a cell can be detected. A bicolor Janus microsphere is prepared by evaporation of a PS/PMMA emulsion droplet. The hydrophilic and hydrophobic dyes are selectively immobilized at the hydrophilic PMMA and hydrophobic PS hemispheres, respectively [147]. A dual-color micro-laser is gained from the Janus particle with tunable lasing performance by altering the Janus microstructure. The output color can be adjusted from red to yellow at different irradiation location when using the Janus microsphere with an equal PS/PMMA ratio. When the PMMA hemisphere is excited, the red emission from Rh101 appears. The yellow emission is observed when the PS hemisphere is exposed. When the PS/PMMA interface is irradiated, a dual-color emission is simultaneously achieved (Fig. 16b). Color of the lasing can be designed by encapsulating various dyes. An all-color micro-laser covering the whole visible spectra is achieved (Fig. 16c) [147]. In combination of emulsion polymerization and solvent evaporation induced phase separation, a new Janus particle is constructed with the chiral helical substituted polyacetylene. Significant circular dichroism effect is present from the one-handed helical polyacetylene [148].

### 6.4. Self-assembly towards superstructures

Self-assembly of Janus materials can be used to construct functional coatings and hierarchically structured superstructures. A cone-like PS particle is generated by squeezing the deformable PS particle at the triple-phase contact line by patchy emulsion interfacial polymerization. Under the protection of wax, the cone side of the PS particle is sulfonated to introduce sulfonic acid, which can induce the favorable growth of titania by sol-gel process of tetrabutyl titanate (TBT). Afterwards, the titania surface is modified with isopropyl tri-dioctylphosphatetitanate (NDZ-102) to introduce the hydrophobic group. Amine- group is further introduced to the flat bottom surface after the modification with 2-aminoethanethiol *via* Michael addition with the residual vinyl-group. The Janus composite particle is derived with the hydrophobic cone side and amine- group contained hydrophilic flat side [86]. A robust coating is fabricated

by self-assembly of the Janus particle while the amine group on the flat side is covalently connected with the epoxy resin intermediate layer upon crosslinking (Fig. 17a1-a2). Water contact angle on the coating is measured  $151 \pm 2^\circ$ . Moreover, the coating is highly adhesive for water (Fig. 17a3). Water droplets keep pinned when the substrate is turned downwardly. By changing size distribution of the cone-like Janus particles, wettability of the coating is tunable from highly adhesive to superhydrophobic. Another robust superhydrophobic coating is constructed with a strawberry-like Janus particle on the epoxy resin intermediate layer after crosslinking by the imidazolin group onto the bottom surface of the Janus particle [85]. The structured Janus particle with nanoscale roughness at the hydrophobic PS side is analogous to the micro-papillae at a lotus leaf surface, rendering the coating superhydrophobic performance. The water contact angle is measured over  $155^\circ$  with a small sliding angle below  $2^\circ$ . The superhydrophobic coating is robust to tolerate water flushing. The hierarchical rough structure and low surface energy are responsible for the superhydrophobic performance [233]. An anti-UV superhydrophobic coating is generated from a raspberry-like poly(vinylidene fluoride)/polystyrene (PVDF/PS) particle [234]. PVDF is responsible for the ultraviolet resistance. An anti-biofouling coating is achieved from the amphiphilic Janus particle with a spherical or a platelet-like shape [235]. The structure is composed of an inorganic core and hydrophilic/hydrophobic polymeric shell of poly(oligo(ethylene glycol) methylethermethacrylate) and polydimethylsiloxane (PDMS). Chemical composition and surface topography of the coating are tunable by the bi-functional Janus particle, rendering the anti-fouling performance. The chemical heterogeneity and surface roughness are also responsible for lower adhesion against bacteria under both static and dynamic conditions. Similarly, an anti-icing coating is formed with the synergistic effects of decreased area for icing and increasing unstable crystals at the edges of heterogeneities [236]. The heterogeneous surfaces formed by Janus particles exhibit the special “edge” morphologies. In the initial state, water is condensed on the hydrophilic portion of the surfaces, occupying relatively large hydrophilic clusters, which are pinned at the boundary between the hydrophilic and the hydrophobic regions. Cavities between the particles are free without water penetrated. Large ice crystal dendrites appear in the shape of the agglomeration of sector plates by the fast coalescence of water clusters upon freezing. A dry band is formed around the large crystals due to the evaporation of small drops in the vicinity of the large water clusters and the subsequent ice crystals. Ice adhesion becomes extremely low ca. 56 kPa. The composite Janus particles are promising as scalable building blocks toward ice-free coatings.

Janus particles with anisotropic composition and morphology act as building blocks toward superstructures. Morphology of the superstructures is highly dependent on solvents, concentration and Janus balance of the particles [237]. The example Janus cylinder

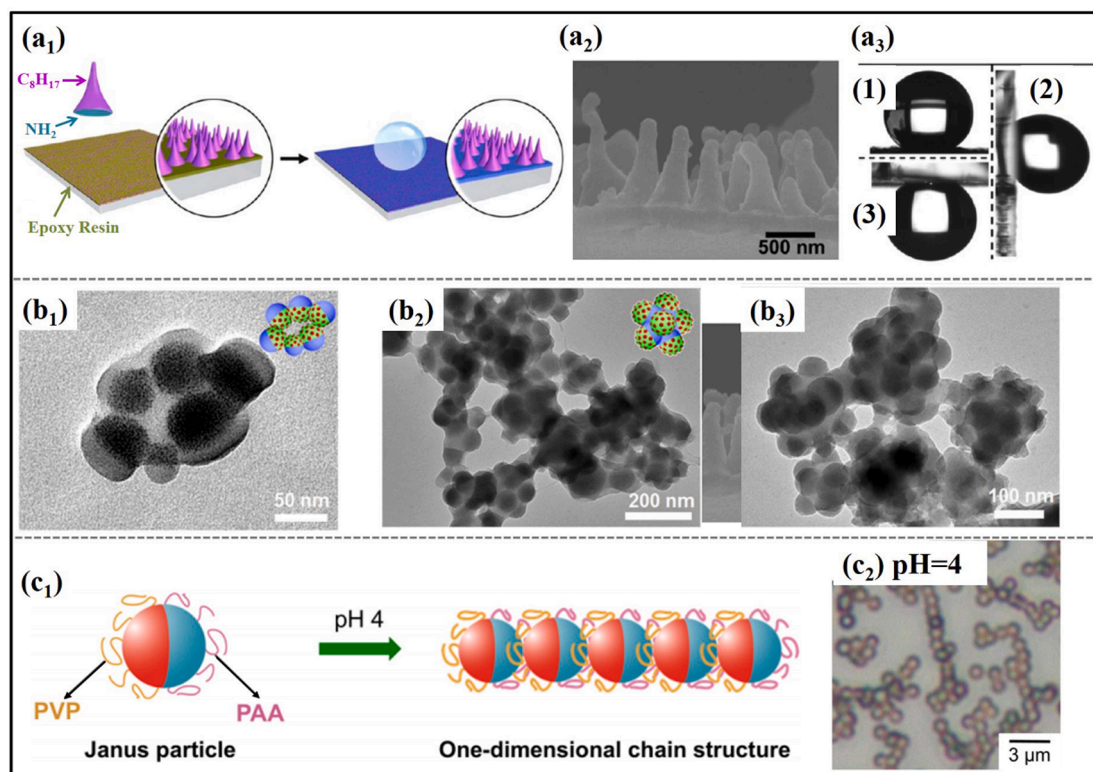


**Fig. 17.** (a<sub>1</sub>) Schematic fabrication of the highly adhesive coating, (a<sub>2</sub>) SEM image, (a<sub>3</sub>) Water droplet on the coating after tilting the substrate at varied angles: (1)  $0^\circ$ ; (2)  $90^\circ$ ; (3)  $180^\circ$ . Contact angle is measured  $151 \pm 2^\circ$ . Adapted with permission from Ref. [86]. Copyright 2015 American Chemical Society. TEM images of some superstructures after drying the Janus composite nanoparticle dispersions in the ethanol/chloroform mixtures with varied ethanol contents (%): (b<sub>1</sub>) 15%, (b<sub>2</sub>) 50%, (b<sub>3</sub>) 75%. Adapted with permission from Ref. [132]. Copyright 2015 American Chemical Society. (c<sub>1</sub>) Illustrative structure and (c<sub>2</sub>) TEM image of the chain-like superstructure by self-assembly of the Janus composite particle of PS<sub>PAA</sub>/PMMA<sub>PVP</sub> at pH = 4. Adapted with permission from Ref. [176]. Copyright 2015 American Chemical Society.

from the polystyrene-*block*-polybutadiene-*block*-poly(methyl methacrylate) (SBM) terpolymer can be well dispersed in the co-solvent of THF. In a selective solvent such as acetone, self-assembly occurs depending on solvent concentration. A fiber-like superstructure with the PS domain at the center is formed above the critical aggregation concentration. A fibrillar network is formed when a concentrated dispersion of the Janus cylinder is deposited on a surface [10]. The Janus particle of PS-P4VP/Au can form different superstructures by changing ethanol/chloroform ratio [132]. A loop is formed after drying the dispersion in a mixed solvent containing 15% of ethanol (Fig. 17b1). By increasing ethanol content to 50%, a network of raspberry-like spheres is formed with the PS domain facing inwardly and the P4VP/Au domain facing outwardly (Fig. 17b2). At 75% of ethanol, individual raspberry-like sphere is generated (Fig. 17b3). The morphological evolution is explained by the solubility difference of PS and P4VP in different solvents. Ethanol is a good solvent for P4VP but poor for PS. Increasing ethanol ratio should lead to the formation of raspberry-like spheres with PS domain as the core and many P4VP/Au domains on the PS core surface. A tadpole-like single-chain Janus nanoparticle (SCJNP) composed of a “tail” of poly(ethylene oxide) (PEO) and a “head” of crosslinked poly(2-cinnamoyloxyethylmethacrylate) (PCEMA) can self-assemble into a superparticle in the selective solvent of DMF/ethanol [11]. The superparticle can be dissociated into individual SCJNP under a gentle ultrasonication at 40 kHz for 10 min. Different structures covering spherical micelle, vesicle and large complex micelle are achieved in the mixed solvent of THF/water with varied ratios [115]. Janus Laponite disk can self-assemble into superstructures in the mixture of THF/methanol [64]. The Janus disk contains PS brush on one side and partially quaternized PDMAEMA on the other side. When methanol is fed to the THF dispersion, a bi-layered structure is achieved. The PS brush grafted sides are stacked while the other sides are exposed outwardly for the stabilization. A tubular superstructure is fabricated by self-assembly of a Janus particle with hydrophobic P2VN on one side and hydrophilic PEO/PAA on the opposite side. The superstructure can be unwrapped into trapezoidal or semicircular nanosheet under different ultrasonication time [105].

An example of unimolecular polymer Janus nanoparticle is synthesized from PS-*b*-P2VP-*b*-PEO by intramolecular crosslinking of the middle P2VP block using 1,4-dibromobutane (DBB) in DMF [102]. The Janus nanoparticles are individuals at a low concentration of 0.01 mg/mL, which are self-assembled into supermicelles with a patchy structure at a high concentration of 0.25 mg/mL. This

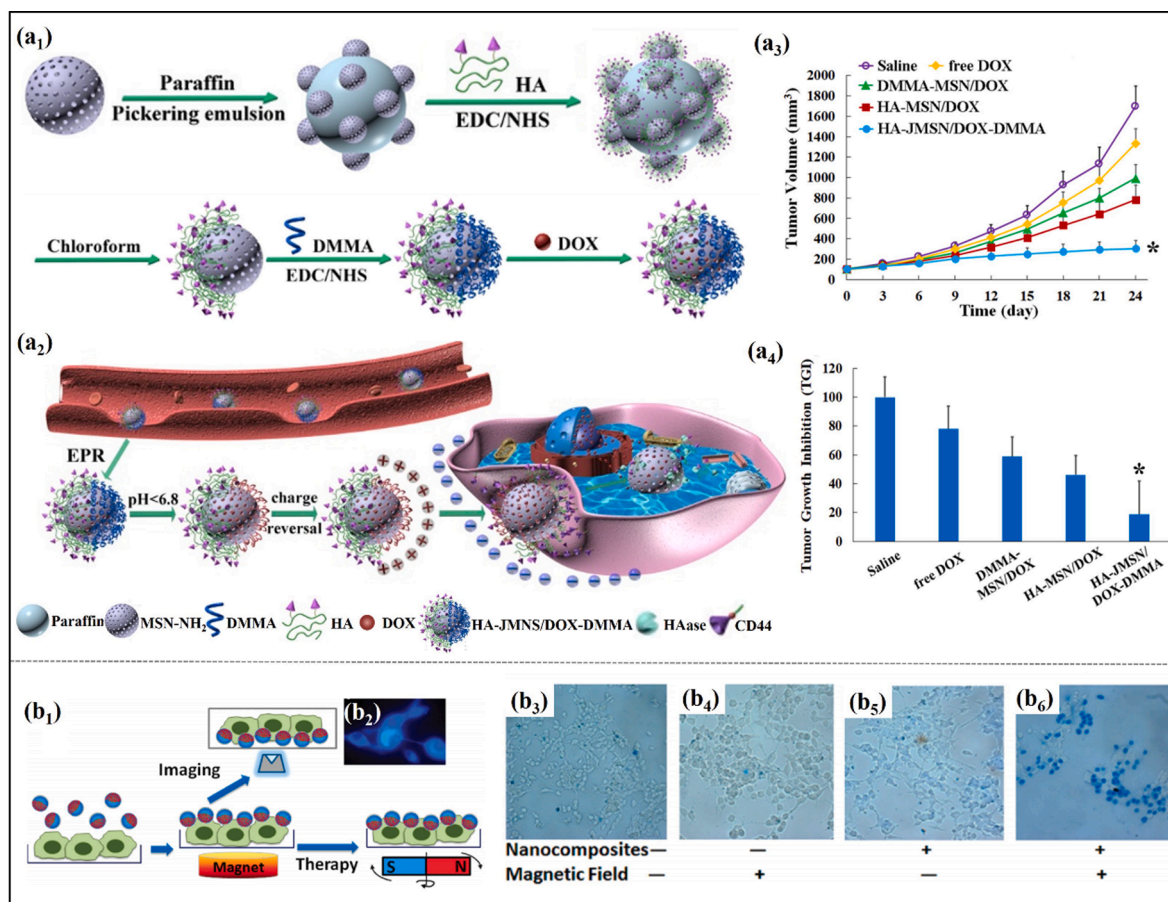


**Fig. 18.** (a<sub>1</sub>) Schematic preparation of HA-JMSN/DOX-DMMA, (a<sub>2</sub>) synergistic effect of pH-sensitive charge reversal and active targeting of HA-JMSN/DOX-DMMA for efficient tumor targeting delivery, (a<sub>3</sub>) tumor volume and (a<sub>4</sub>) tumor growth inhibition (TGI) of different treatment groups. Adapted with permission from Ref. [46]. Copyright 2019 American Chemical Society. (b<sub>1</sub>) Schematic magnetolytic therapy, (b<sub>2</sub>) fluorescent imaging of the cell coated with the Janus nanocomposite, (b<sub>3</sub>-b<sub>6</sub>) magnetolytic therapy on the tumor cell, - and + denote the absence and presence of the Janus nanocomposite and magnetic field. Adapted with permission from Ref. [145]. Copyright 2010 American Chemical Society.

finding provides the hint that determination of intramolecular crosslinking by light scattering should be cautious by consideration of the size-concentration dependence. The chemical interaction of Janus nanoparticle also determines the self-assembled superstructure [170]. A snowman-shaped Janus nanoparticle is achieved by seeded swelling polymerization of triethoxysilylpropylmethacrylate (TPM) against the PtBA particle, which derives the PAA-PTPM by selective hydrolysis of PtBA. A tri-segmental Janus nanoparticle of PAA-PTPM-TMPT is achieved by sol-gel process of 3-trimethoxysilylpropane-1-thiol (TMPT) against the PTPM lobe. The three lobes possess different compositions whose sizes can be adjusted independently. The Janus nanoparticles are flexible to achieve various superstructures. By utilizing hydrogen bonding as the attraction force, the PAA-PTPM-PTPM Janus nanoparticles can self-assemble into spherical- and wormlike micelles. Physical morphology is important in the colloidal self-assembly. The crucial parameter of curvature angle ( $\alpha$ ) determined by the relative lobe size is decisive for the self-assembled structures. For the dually responsive Janus composite particle of  $\text{PS}_{\text{PAA}}/\text{PMMA}_{\text{PVP}}$ , a chain-like structure is obtained by self-assembly *via* hydrogen bonding between the PAA and PVP stabilizers at pH = 4 when PAA is protonated (Fig. 17c) [176]. A string structure is formed from the poly(N-isopropylacrylamide-co-acrylic acid) microgel by coupling with ethylenediamine at pH = 4 [62]. A chain-like structure is formed by self-assembly of the Janus particle of  $\text{Fe}_3\text{O}_4@\text{SiO}_2@\text{PS}$  *via* the polar-polar interaction from the  $\text{Fe}_3\text{O}_4$  core under an external magnetic field [185]. The silica Janus particle can self-organize into a micellar cage with enzymes such as lipase from *Candida* sp. encapsulated. 5.6 times higher catalytic activity is demonstrated than the free enzyme in the example biphasic esterification of 1-hexanol with hexanoic acid [238]. The submicron sized Janus silica particle is synthesized by wax Pickering emulsion interface whose two sides are modified with 3-aminopropyltriethoxysilane and octadecyl trichlorosilane, respectively. The enzyme capsules are 5–50  $\mu\text{m}$  in diameter. The enzyme activity is increased with increasing the water/oil volume ratio and the Janus particle loading. The encapsulated enzyme can be easily recycled, which is promising to significantly reduce cost especially in the case of expensive enzymes.

### 6.5. Biomedical applications

The anisotropic Janus materials as new emerging functional materials are promising in biomedical applications, such as drug delivery, bio-imaging, and target therapy [203,239-241]. In this part, we will highlight the effects of composition and microstructure of the Janus materials in the biomedical applications. At the Pickering emulsion interface, a dually functionalized Janus nanoparticle (denoted HA-JMSN/DOX-DMMA) is constructed with HA and a charge reversal group of DMMA on the opposite sides of a mesoporous silica nanoparticle (MSN) with DOX loaded inside the MSN (Fig. 18a1) [46]. The Janus particle of HA-JMSN/DOX-DMMA can be remarkably accumulated at the tumor sites by the enhanced permeability and retention effect. In a weakly acidic micro-environment of tumor tissues, after the charge is reversed from negatively to positively, the Janus particle is capable of selectively attacking the cells upon recognition *via* electrostatic attraction. Owing to the over expression of CD44 receptor on the tumor cell membrane, the Janus particle is further engulfed by the tumor cell due to the interaction between HA and CD44 (Fig. 18a2). After entering the cell, hydrolysis of DMMA and digestion of HA open the pores, facilitating release of DOX which is accelerated at a lower pH value. The enhanced uptake of the Janus particle is originated from the synergistic effect of HA and DMMA. HA as a targeting ligand can greatly improve endocytosis of the Janus particle *via* the clathrin-mediated mode, whilst DMMA is conducive to internalization *via* the micropinocytosis mode. The therapeutic efficacy of HA-JMSN/DOX-DMMA is evaluated *in vivo* by using tumor bearing mice. Volume of the tumor is significantly decreased after the treatment with HA-JMSN/DOX-DMMA (Fig. 18a3). In comparison with the tumor growth inhibition (TGI) by free DOX (TGI of 77.97%), DMMA-MSN/DOX (TGI of 58.85%) and HA-MSN/DOX (TGI of 46.06%), HA-JMSN/DOX-DMMA shows the most efficient tumor inhibition with a TGI of 18.07% (Fig. 18a4).

A superparamagnetic Janus nanocomposite of polystyrene/ $\text{Fe}_3\text{O}_4@\text{SiO}_2$  is synthesized by mini-emulsion and sol-gel reaction. DOX is immobilized at the silica shell *via* the pH-sensitive hydrazone dynamic bonding, while folic acid (FA) is tethered at the PS surface *via* bisamine linker [191]. The tumor cell targeting and pH-induced drug delivery of the dually functionalized Janus nanocomposite are assessed by using the human MDA-MB-231 breast cell with the over expression of a folate receptor. The selective tumor targeting and internalization of super-paramagnetic Janus nanocomposites (SJNC) are greatly enhanced by the targeting ligand of FA. The pH sensitive hydrazone linker imparts the controlled release of DOX after internalization under acidic conditions. When two sides of the Janus mesoporous silica particle are asymmetrically decorated with the two targeting moieties of folic acid and triphenylphosphine (TPP), the derived Janus material is capable of targeting toward the tumor cells and mitochondria [242].

When a paramagnetic nanoparticle is incorporated within the Janus material, the Janus composite material is capable of imaging and magnetolytic performance. A Janus nanoparticle composed of pyrene labeled poly(styrene-*b*-allyl alcohol) ( $\text{PS}_{16}\text{-}b\text{-PAA}_{10}$ ) and a magnetic nanoparticle is prepared by evaporation induced phase separation in the microemulsion system [145]. The magnetic Janus nanoparticle shows efficient imaging and magnetolytic effects, allowing modulated damage of the cell membrane under a magnetic field (Fig. 18b1). The magnetic Janus nanoparticle can be quickly anchored at the cell which is easily visualized by fluorescent imaging (Fig. 18b2). The tumor cells are killed upon imposing a mechanical force on the cell membrane by spinning the magnetic field (Fig. 18b3-b6). The Janus mesoporous silica nanocarrier with iron oxide nanocube patches (denoted as IONCs-P-JMNC) is synthesized by interface evaporation assembly in the emulsion droplet [243]. Compared with the core-shell silica@iron, the iron oxide nanocube on the Janus particle could enhance dipolar energy and magnetic susceptibility owing to the anisotropic shape. 2.24 times augment of MRI  $r_2^*$  reflexivity is achieved by the IONCs-P-JMNC. The cumulated DOX release is 39.6% for 24 h without the magnetic field, which can be increased to 68.7% within 10 min under the magnetic field. In a single-step solvent evaporation emulsion, DOX and Paclitaxel (PTX) are concurrently incorporated within the magnetic polymer Janus particle [146]. The release of DOX and PTX is correlated with the polymer matrix. For instance, both drugs can be simultaneously released from the Janus particle of poly(ethyl vinyl acetate)/poly(D,L-lactide-co-glycolide) (PLGA/EVA), while a sequential release of DOX followed by PTX is achieved from the PMMA/PLGA.

Besides the target therapy and imaging, Janus materials with different active groups provide the starting materials to conjugate

various biomolecules [169]. An example Janus silica particle with amine- and vinyl- groups compartmentalized onto the two sides displays excellent dentin adhesion [244]. The amine- group of the Janus particle is capable to react with the carbonyl groups of the dentin, while the vinyl- group can anticipate the polymerization with the adhesive monomers giving a robust dentin bonding interface. Multiple functional Janus particles are promising for biological adhesives with tunable interfacial structures and performances.

## 7. Conclusion and perspectives

In summary, we have reviewed recent progress in the scalable synthesis strategies and promising applications of Janus materials of polymer/inorganic nanocomposites. The strategies are primarily based on the induced growth or confined self-assembly in a droplet and/or at an interface. Among them, Pickering emulsion interfacial synthesis has been extensively employed owing to the excellent controllability and relatively high yield of Janus particles. Proper wettability of particles is a prerequisite for forming the Pickering emulsions, and the particles should be large sufficiently to ensure a high desorption energy at the interface over the thermal energy. Interfacial materialization stands out as a straightforward means of producing nanoscale Janus materials. A wealthy of interfaces (i.e., liquid/liquid, liquid/solid and liquid/air) are suitable as the “factories” to synthesize Janus nanomaterials. This strategy is particularly advantageous as it facilitates combines the two synthetic approaches (i.e., Pickering emulsion interface and conventional emulsion interface stabilized with surfactants). This interfacial materialization is effective for large-scale fabrication of Janus nanomaterials with tunable shapes and microstructures. Confined self-assembly of block copolymers in emulsion droplets and/or unique templates represents a robust platform to yield Janus materials with tunable compositions and morphologies. Seeded emulsion polymerization is regarded as a simple and effective approach to large-scale production of Janus materials. Polymerization induced phase separation is crucial to govern the compartmentalization of polymers. Notably, it is of significance in achieving distinct compartmentalization by either post-modification or intensified phase separation for strict Janus materials to ensure the proper shape and composition distribution.

It is noteworthy that the asymmetric compositions and architectures of Janus materials render them a wide range of applications. As solid surfactants, emulsions by the Janus materials are more stable than molecular or polymeric surfactants. Composition, shape and Janus balance of the materials determine the type and microstructure of emulsions. The reversible emulsification and de-emulsification can be readily achieved by using responsive Janus materials. Miscibility of polymer blends is remarkably improved by introducing Janus particles as compatibilizers, facilitating the recycling of polymer wastes. Janus materials also provide ideal support for catalysts in heterogeneous catalysis, in particular at emulsion interface, where the improved mass transfer and a large contact area impart more effective catalysis. The Janus catalysts can be conveniently recycled via altering the external stimuli or applying the magnet. By incorporating different fluorescence dyes that distinctly compartmentalized at a Janus particle, the derived material could function as a probe possessing multiple emissions with tunable emission colors, which is particularly useful for display and detection of micro-environment. Functional coatings (e.g., superhydrophobic, anti-biofouling, and anti-icing) can be attained by chemical bonding the Janus particles onto the substrates of interest, where the exposed nanoscale coarsening surfaces are responsible for the markedly improved performance. Janus materials could also serve as building blocks toward diverse superstructures. Self-assembly of Janus materials enables the encapsulation of target species to form the capsule with tunable composition and microstructure, which is extremely useful for supporting functional materials and controlled releasing. As far as biomedical application is concerned, multi-functional Janus materials are capable of recognizing the targets for controlled release of drugs. It is also notable that the use of Janus materials also renders more efficient imaging and therapy.

Despite significant progress in the synthesis and applications of Janus materials, it remains challenging to develop robust methods to precisely tailor the shape and microstructure with desirable compositions and thus functionalities at the two specific sides. Future exploration should be concentrated on yet not limited to the following aspects.

First, a resilient and general strategy should be developed to enable large-scale production of inorganic, organic, and organic/inorganic composite Janus materials with controllable morphology and microstructure. For example, silica Janus nanosheets derived from interfacial materialization have demonstrated interesting performance. Yet, the irregular topology and large lateral size are the major obstacles for their exciting potential use in biomedicine. In principle, the lateral dimension can be further decreased to the critical size comparable with the nanosheet thickness at  $10^0$ - $10^1$  nm. The ability to reach such a critical size will open new avenue for the utility of Janus nanosheets, for example, as drug delivery vectors.

Second, although Janus nanoparticles engineered via self-assembly and disassembly of block copolymers could adopt a diversity of morphologies, spanning from spherical, cylindrical, to disc shapes, narrow molecular weight distribution and strict conditions (i.e., solvent, temperature, and concentration) are often required to attain them. Thus, it calls for the development of a simple way to mass-produce functional Janus nanomaterials from the copolymers or by polymerization of functional monomers. The ability to program or modulate the performance and composition of Janus materials will provide a powerful tool to precisely engineer interfaces and deliver materials of interest toward interfaces for smart devices.

Third, Janus-type catalysts for bio-catalysis (functioning as enzyme-like) and electrocatalysis merit intense interdisciplinary research efforts for producing green chemicals and clean fuels in the future. The Janus characteristic of catalysts (e.g., hydrophilic/hydrophobic, negatively charged/positively charged, electron-rich/electron-poor, bio-active/bio-inactive) may deliver fascinating synergistic effect and largely promote the catalytic reaction. For instance, the use of Janus electrocatalysts containing both metal-N species for oxygen reduction reaction (ORR) and metal oxides for oxygen evolution reaction (OER) may function as outstanding bi-functional electrocatalysts for both ORR and OER, which is highly desirable for metal-air batteries. In addition, functional single-chain Janus composite nanoparticles with tunable microstructures and synergistic effects of the constituents represents a new material for future research, as it promises new opportunity for use in catalysis, diagnosis, therapy, and functional superstructures.

Fourth, Janus materials have been primarily examined by means of electron microscopy and spectroscopy in the current state. Composition can be determined by selected-area electron diffraction (SAED) measurement, X-ray photoelectron spectroscopy (XPS), elemental mapping analysis, nuclear magnetic resonance spectroscopy, and synchrotron radiation technique. More systematical investigations into Janus materials and interfaces via a suite of advanced characterization tools may provide more critical insights into interfacial dynamics and thus the properties and performance of Janus materials.

Future research is envisioned to continue to witness much development in synthetic strategies that afford large-scale production of Janus materials of interest with precisely controlled compositions, morphologies, functionalities for a broader spectrum of applications, going beyond interfacial tailoring and functionalization, biomedical application, and catalysis.

### Declaration of Competing Interest

The authors declare that they have no known competing financial interests or personal relationships that could have appeared to influence the work reported in this paper.

### Acknowledgments

This work was supported by Tsinghua University Start-up Funding (53330100120), National Natural Science Foundation of China (52173207, 51833005) and Natural Science Foundation of Hunan Province (2020JJ5542).

### References

- [1] de Gennes PG. Soft matter. *Rev Mod Phys* 1992;64:645–8.
- [2] Cho I, Lee KW. Morphology of latex particles formed by poly(methyl methacrylate) seeded emulsion polymerization of styrene. *J Appl Polym Sci* 1985;30:1903–26.
- [3] Nie ZH, Li W, Seo M, Xu SQ, Kumacheva E. Janus and ternary particles generated by microfluidic synthesis: design, synthesis, and self-assembly. *J Am Chem Soc* 2006;128:9408–12.
- [4] Hou JS, Yang YY, Yu DG, Chen ZZ, Wang K, Liu YN, et al. Multifunctional fabrics finished using electrosprayed hybrid Janus particles containing nanocatalysts. *Chem Eng J* 2021;411:128474–84.
- [5] Tsyrenova A, Miller K, Yan J, Olson E, Anthony SM, Jiang S. Surfactant-mediated assembly of amphiphilic Janus spheres. *Langmuir* 2019;35(18):6106–11.
- [6] Jiang S, Granick S. A simple method to produce trivalent colloidal particles. *Langmuir* 2009;25(16):8915–8.
- [7] Kim JW, Lee D, Shum HC, Weitz DA. Colloid surfactants for emulsion stabilization. *Adv Mater* 2008;20:3239–43.
- [8] Seh ZW, Liu S, Zhang S, Bharathi MS, Ramanarayan H, Low M, et al. Anisotropic growth of titania onto various gold nanostructures: synthesis, theoretical understanding, and optimization for catalysis. *Angew Chem Int Ed* 2011;50:10140–3.
- [9] Kim J, Choi C-H, Yeom S-J, Eom N, Kang K-K, Lee C-S. Directed assembly of Janus cylinders by controlling the solvent polarity. *Langmuir* 2017;33(30):7503–11.
- [10] Walther A, Drechsler M, Rosenfeldt S, Harnau L, Ballauff M, Abetz V, et al. Self-assembly of Janus cylinders into hierarchical superstructures. *J Am Chem Soc* 2009;131:4720–8.
- [11] Walther A, Müller AHE. Janus particles. *Soft Matter* 2008;4(4):663. <https://doi.org/10.1039/b718131k>.
- [12] Walther A, Drechsler M, Müller AHE. Structures of amphiphilic Janus discs in aqueous media. *Soft Matter* 2009;5(2):385–90.
- [13] Liang FX, Liu JG, Zhang CL, Qu XZ, Li JL, Yang ZZ. Janus hollow spheres by emulsion interfacial self-assembled sol-gel process. *Chem Commun* 2011;47:1231–3.
- [14] Walther A, Hoffmann M, Müller AHE. Emulsion polymerization using Janus particles as stabilizers. *Angew Chem Int Ed* 2008;47:711–4.
- [15] Herrikhuyzen J, Portale G, Gielen JC, Christianen PCM, Sommerdijk NAJM, Meskers SCJ, et al. Disk micelles from amphiphilic Janus gold nanoparticles. *Chem Commun* 2008;14:697–9.
- [16] Isojima T, Lattuada M, Vander Sande JB, Hatton TA. Reversible clustering of pH- and temperature-responsive Janus magnetic nanoparticles. *ACS Nano* 2008;2(9):1799–806.
- [17] Paxton WF, Kistler KC, Olmeda CC, Sen A, Angelo SKS, Cao YY, et al. Catalytic nanomotors: autonomous movement of striped nanorods. *J Am Chem Soc* 2004;126:13424–31.
- [18] Valadares LF, Tao Y-G, Zacharia NS, Kitaev V, Galembeck F, Kapral R, et al. Catalytic nanomotors: self-propelled sphere dimers. *Small* 2010;6(4):565–72.
- [19] Tao AJ, Feng T, Russell TP. Self-assembly of nanomaterials at fluid interfaces. *The Eur Phys J E* 2016;39:57–69.
- [20] Xu WW, Wei ML, Serpe MJ. Janus microgels with tunable functionality, polarity, and optical properties. *Adv Opt Mater* 2017;5:1600614–22.
- [21] Liu SS, Wang CF, Wang XQ, Zhang J, Tian Y, Yin SN, et al. Tunable Janus colloidal photonic crystal supraballs with dual photonic band gaps. *J Mater Chem C* 2014;2:9431–8.
- [22] Yoshida M, Roh KH, Mandal S, Bhaskar S, Lim D, Nandivada H, et al. Structurally controlled bio-hybrid materials based on unidirectional association of anisotropic microparticles with human endothelial cells. *Adv Mater* 2009;21:4920–5.
- [23] Wu YJ, Lin XK, Wu ZG, Möhwald H, He Q. Self-propelled polymer multilayer Janus capsules for effective drug delivery and light-triggered release. *ACS Appl Mater Interfaces* 2014;6:10476–81.
- [24] Ma X, Hahn K, Sanchez S. Catalytic mesoporous Janus nanomotors for active cargo delivery. *J Am Chem Soc* 2015;137:4976–9.
- [25] Liang FX, Zhang CL, Yang ZZ. Rational design and synthesis of Janus composites. *Adv Mater* 2014;26:6944–9.
- [26] Zhou T, Wang B, Dong B, Li CY. Thermoresponsive amphiphilic Janus silica nanoparticles via combining “polymer single-crystal templating” and “grafting-from” methods. *Macromolecules* 2012;45(21):8780–9.
- [27] McConnell MD, Kraeutler MJ, Yang S, Composto RJ. Patchy and multi-region Janus particles with tunable optical properties. *Nano Lett* 2010;10(2):603–9.
- [28] Zhang LM, Yu JW, Yang MM, Xie Q, Peng HL, Liu ZF. Janus graphene from asymmetric two-dimensional chemistry. *Nat Commun* 2012;4:1443–9.
- [29] Ling XY, Phang IY, Acikgoz C, Yilmaz MD, Hempenius MA, Vancso GJ, et al. Janus particles with controllable patchiness and their chemical functionalization and supramolecular assembly. *Angew Chem Int Ed* 2009;48:7677–82.
- [30] Paunov VN, Cayre OJ. Supraparticles and “Janus” particles fabricated by replication of particle monolayers at liquid surfaces using a gel trapping technique. *Adv Mater* 2004;16:788–91.
- [31] Cayre O, Paunov VN, Velev OD. Fabrication of dipolar colloid particles by microcontact printing. *Chem Commun* 2003;18:2296–7.
- [32] Seidel P, Ravoo BJ. Preparation of microscale polymer Janus particles by sandwich microcontact printing. *Macromol Chem Phys* 2016;217:1467–72.
- [33] Kaufmann T, Gokmen MT, Wendeln C, Schneiders M, Rinnen S, Arlinghaus HF, et al. “Sandwich” microcontact printing as a mild route towards monodisperse Janus particles with tailored bifunctionality. *Adv Mater* 2011;23:79–83.
- [34] Ye S, Carroll RL. Design and fabrication of bimetallic colloidal “Janus” particles. *ACS Appl Mater Interfaces* 2010;2:616–20.

- [35] Choi J, Zhao Y, Zhang D, Chien S, Lo Y-H. Patterned fluorescent particles as nanoprobes for the investigation of molecular interactions. *Nano Lett* 2003;3(8):995–1000.
- [36] Jang B, Hong A, Kang HE, Alcantara C, Charreyron S, Mushtaq F, et al. Multiwavelength light-responsive Au/B-TiO<sub>2</sub> Janus micromotors. *ACS Nano* 2017;11(6):6146–54.
- [37] Lu A, Zhu HY, Xiao J, Chuu C, Han YM, Chiu M, et al. Janus monolayers of transition metal dichalcogenides. *Nat Nanotechnol* 2017;12:744–50.
- [38] Xuan MJ, Wu ZG, Shao JX, Dai LR, Si TY, He Q. Near infrared light-powered Janus mesoporous silica nanoparticle motors. *J Am Chem Soc* 2016;138:6492–7.
- [39] Pradhan S, Brown LE, Konopelski JP, Chen S. Janus nanoparticles: reaction dynamics and NOESY characterization. *J Nanopart Res* 2009;11:1895–903.
- [40] Nakahama K, Kawaguchi H, Fujimoto K. A novel preparation of nonsymmetrical microspheres using the langmuir-blodgett technique. *Langmuir* 2000;16(21):7882–6.
- [41] Kaewsaneha C, Tangboriboonrat P, Polpanich D, Eissa M, Elaissari A. Preparation of Janus colloidal particles via Pickering emulsion: an overview. *Colloids Surf A Physicochem Eng Aspects* 2013;439:35–42.
- [42] Hong L, Jiang S, Granick S. Simple method to produce Janus colloidal particles in large quantity. *Langmuir* 2006;22(23):9495–9.
- [43] Jiang S, Schultz MJ, Chen Q, Moore JS, Granick S. Solvent-free synthesis of Janus colloidal particles. *Langmuir* 2008;24(18):10073–7.
- [44] Wu CJ, Deng ZW, Shang B, Ikkala O, Peng B. A versatile colloidal Janus platform: surface asymmetry control, functionalization, and applications. *Chem Commun* 2018;54:12726–9.
- [45] Xing Y, Zhou Y, Fan Li, Yang Y, Zhang Y, Deng Xu, et al. Construction strategy for ratiometric fluorescent probe based on Janus silica nanoparticles as a platform toward intracellular pH detection. *Talanta* 2019;205:120021. <https://doi.org/10.1016/j.talanta.2019.06.021>.
- [46] Liu YJ, Dai R, Wei QY, Li WZ, Zhu G, Chi H, et al. Dual-functionalized Janus mesoporous silica nanoparticles with active targeting and charge reversal for synergistic tumor-targeting therapy. *ACS Appl Mater Interfaces* 2019;11:44582–92.
- [47] Berger S, Synytska A, Ionov L, Eichhorn K-J, Stamm M. Stimuli-responsive bicomponent polymer Janus particles by “grafting from”/“grafting to” approaches. *Macromolecules* 2008;41(24):9669–76.
- [48] Falireas PG, Vamvakaki M. pH-responsive polyampholytic hybrid Janus nanoparticles. *Polymer* 2017;130:50–60.
- [49] Kirillova A, Schliebe C, Stoychev G, Jakob A, Lang H, Synytska A. Hybrid hairy Janus particles decorated with metallic nanoparticles for catalytic applications. *ACS Appl Mater Interfaces* 2015;7:21218–25.
- [50] Razza N, Castellino M, Sangermano M. Fabrication of Janus particles via a “photo grafting-from” method and gold photoreduction. *J Mater Sci* 2017;52:13444–54.
- [51] Liu B, Zhang CL, Liu JG, Qu XZ, Yang ZZ. Janus non-spherical colloids by asymmetric wet-etching. *Chem Commun* 2009;45:3871–3.
- [52] Tan JSJ, Cao X, Huang YZ, Chen Z. Janus-like particles prepared through partial UV irradiation at the water/oil interface and their encapsulation capabilities. *Colloids Surf A Physicochem Eng Aspects* 2020;589:124460–71.
- [53] Zahna N, Kicckelbick G. Synthesis and aggregation behavior of hybrid amphiphilic titania Janus nanoparticles via surface-functionalization in Pickering emulsions. *Colloids Surf A Physicochem Eng Aspects* 2014;461:142–50.
- [54] Si Y, Ji X, Liang F, Jiang B, Yang Z. Responsive Janus cage reactor. *Chem Asian J* 2019;14(11):1917–20.
- [55] Zhang H, Wang Q, Jiang BY, Liang FX, Yang ZZ. Coral-like Janus porous spheres. *ACS Appl Mater Interfaces* 2016;8:33250–5.
- [56] Chen Xi, Xu J, Sun D, Jiang B, Liang F, Yang Z. Emulsion interfacial synthesis of polymer/inorganic Janus particles. *Langmuir* 2019;35(18):6032–8.
- [57] Wang ZP, Rutjes FPJT, van Hest JCM. pH responsive polymersome Pickering emulsion for simple and efficient Janus polymersome fabrication. *Chem Commun* 2014;50:14550–3.
- [58] Liu B, Wei W, Qu XZ, Yang ZZ. Janus colloids formed by biphasic grafting at a Pickering emulsion interface. *Angew Chem Int Ed* 2008;47:3973–5.
- [59] Zhang J, Jin J, Zhao H. Surface-initiated free radical polymerization at the liquid-liquid interface: a one-step approach for the synthesis of amphiphilic Janus silica particles. *Langmuir* 2009;25(11):6431–7.
- [60] Zhang J, Wang XJ, Wu DX, Liu L, Zhao HY. Bioconjugated Janus particles prepared by in situ click chemistry. *Chem Mater* 2009;21:4012–8.
- [61] Li D, He YJ, Wang S. On the rotation of the Janus CuO/CuS colloids formed at a Pickering emulsion interface. *J Phys Chem C* 2009;113:12927–9.
- [62] Suzuki D, Tsuji S, Kawaguchi H. Janus microgels prepared by surfactant-free Pickering emulsion-based modification and their self-assembly. *J Am Chem Soc* 2007;129:8088–9.
- [63] Nonomura Y, Komura S, Tsujii K. Adsorption of disk-shaped Janus beads at liquid-liquid interfaces. *Langmuir* 2004;20(26):11821–3.
- [64] Liu J, Liu G, Zhang M, Sun P, Zhao H. Synthesis and self-assembly of amphiphilic Janus laponite disks. *Macromolecules* 2013;46(15):5974–84.
- [65] Kirillova A, Stoychev G, Ionov L, Eichhorn KJ, Malinin M, Synytska A. Platelet Janus particles with hairy polymer shells for multifunctional materials. *ACS Appl Mater Interfaces* 2014;6:13106–14.
- [66] Luo D, Zhang FH, Zheng HT, Ren ZS, Jiang LL, Ren ZF. Electrostatic-attraction-induced high internal phase emulsion for large-scale synthesis of amphiphilic Janus nanosheets. *Chem Commun* 2019;55:1318–21.
- [67] de Leon AC, Rodier BJ, Luo Q, Hemmingsen CM, Wei P, Abbasi K, et al. Distinct chemical and physical properties of Janus nanosheets. *ACS Nano* 2017;11(7):7485–93.
- [68] Ma AY, Wang GL, Yang ZL, Bai LJ, Chen H, Wang WX, et al. Fabrication of Janus graphene oxide hybrid nanosheets by Pickering emulsion template for self-healing nanocomposite hydrogels. *Chem Eng J* 2020;385:123962–74.
- [69] Liang FX, Shen K, Qu XZ, Zhang CL, Wang Q, Li JL, et al. Inorganic Janus nanosheets. *Angew Chem Int Ed* 2011;50:2379–82.
- [70] Chen Y, Liang F, Yang H, Zhang C, Wang Q, Qu X, et al. Janus nanosheets of polymer inorganic layered composites. *Macromolecules* 2012;45(3):1460–7.
- [71] Chen Y, Yang H, Zhang C, Wang Q, Qu X, Li J, et al. Janus cages of bilayered polymer-inorganic composites. *Macromolecules* 2013;46(10):4126–30.
- [72] Yang H, Liang F, Wang X, Chen Y, Zhang C, Wang Q, et al. Responsive Janus composite nanosheets. *Macromolecules* 2013;46(7):2754–9.
- [73] Cao Z, Wang G, Chen Y, Liang F, Yang Z. Light-triggered responsive Janus composite nanosheets. *Macromolecules* 2015;48(19):7256–61.
- [74] Zhao Z, Liang F, Zhang G, Ji X, Wang Q, Qu X, et al. Dually responsive Janus composite nanosheets. *Macromolecules* 2015;48(11):3598–603.
- [75] Zhao ZG, Zhu FY, Qu XZ, Wu QH, Wang Q, Zhang GL, et al. pH-responsive polymeric Janus containers for controlled drug delivery. *Polym Chem* 2015;6:4144–53.
- [76] Ji XY, Zhang Q, Liang FX, Chen QN, Qu XZ, Zhang CL, et al. Ionic liquid functionalized Janus nanosheets. *Chem Commun* 2014;50:5706–9.
- [77] Liu JX, Wang P, Zhou MD, Ma Y, Niu XH, Pan GQ, et al. Tailored Janus silica nanosheets integrating bispecific artificial receptors for simultaneous adsorption of 2,6-dichlorophenol and Pb(II). *J Mater Chem A* 2019;7:16161–75.
- [78] Wang QG, Liu YJ, Qu XZ, Wang Q, Liang FX, Yang ZZ. Janus nanosheets by emulsion interfacial crosslinking of reactive surfactants. *Colloid Polym Sci* 2015;293:2609–15.
- [79] Wang QG, Liang FX, Wang Q, Qu XZ, Yang ZZ. Responsive composite Janus cages. *Chinese J Polym Sci* 2015;33:1462–9.
- [80] Jia F, Liang F, Yang Z. Janus mesoporous nanodisc from gelable triblock copolymer. *ACS Macro Lett* 2016;5(12):1344–7.
- [81] Sheng Li, Chen H, Fu W, Li Z. Janus silica hollow spheres prepared via interfacial biosilicification. *Langmuir* 2015;31(44):11964–70.
- [82] Chen H, Fu W, Li Z. Temperature and pH responsive Janus silica nanoplates prepared by the sol-gel process and postmodification. *Langmuir* 2020;36(1):273–8.
- [83] Nakanishi K, Takahashi R, Nagakane T, Kitayama K, Koheiya N, Shikata H, et al. Formation of hierarchical pore structure in silica gel. *J Sol-Gel Sci Technol* 2000;17:191–210.
- [84] Kamio E, Yonemura S, Ono T, Yoshizawa H. Microcapsules with macroholes prepared by the competitive adsorption of surfactants on emulsion droplet surfaces. *Langmuir* 2008;24(23):13287–98.
- [85] Yang HL, Liang FX, Chen Y, Wang Q, Qu XZ, Yang ZZ. Lotus leaf inspired robust superhydrophobic coating from strawberry-like Janus particles. *NPG Asia Mater* 2015;7:e176–81.
- [86] Zhao H, Liang F, Qu X, Wang Q, Yang Z. Cone-like Janus composite particles. *Macromolecules* 2015;48(3):700–6.
- [87] Wang Y, Zhang C, Tang C, Li J, Shen Ke, Liu J, et al. Emulsion interfacial synthesis of asymmetric Janus particles. *Macromolecules* 2011;44(10):3787–94.
- [88] Shi S, Zhang L, Zhang G, Song X, Sun D, Liang F, et al. Jellyfish-like Janus polymeric cage. *Macromolecules* 2020;53(6):2228–34.

- [89] Li J, Wang Y, Zhang C, Liang F, Qu X, Li J, et al. Janus polymeric cages. *Polymer* 2012;53(17):3712–8.
- [90] Shen Ke, Liang F, Liu J, Qu X, Zhang C, Li J, et al. Inward template synthesis of intact hollow spheres. *Polymer* 2011;52(20):4418–22.
- [91] Zhao LL, Zhu LJ, Chen Y, Wang Q, Li JL, Zhang CL, et al. Janus micro-reactors. *Chem Commun* 2013;49:6161–3.
- [92] Liu YJ, Liang FX, Wang Q, Qu XZ, Yang ZZ. Flexible responsive Janus nanosheets. *Chem Commun* 2015;51:3562–5.
- [93] Liu Y, Wang Q, Qu X, Liang F, Yang Z. Amine/acid composite Janus nanosheets. *Sci China Mater* 2015;58(2):126–31.
- [94] Xue D, Meng QB, Song XM. Magnetic-responsive Janus nanosheets with catalytic properties. *ACS Appl Mater Interfaces* 2019;11:10967–74.
- [95] Walther A, Müller AHE. Janus particles: synthesis, self-assembly, physical properties, and applications. *Chem Rev* 2013;113:5194–261.
- [96] Erhardt R, Böker A, Zettl H, Kaya H, Pyckhout-Hintzen W, Krausch G, et al. Janus micelles. *Macromolecules* 2001;34(4):1069–75.
- [97] Liu, Abetz V, Müller AHE. Janus cylinders. *Macromolecules* 2003;36(21):7894–8.
- [98] Walther A, André X, Drechsler M, Abetz V, Müller AHE. Janus discs. *J Am Chem Soc* 2007;129:6187–98.
- [99] Gröschel AH, Schacher FH, Schmalz H, Borisov OV, Zhulina EB, Walther A, et al. Precise hierarchical self-assembly of multicompartment micelles. *Nat Commun* 2012;3:710–9.
- [100] Gröschel AH, Walther A, Löbbling TI, Schmelz J, Hanisch A, Schmalz H, et al. Facile, solution-based synthesis of soft, nanoscale Janus particles with tunable Janus balance. *J Am Chem Soc* 2012;134:13850–60.
- [101] Zhang Z, Zhou CM, Dong HY, Chen DY. Solution-based fabrication of narrow-disperse ABC three-segment and  $\Theta$ -shaped nanoparticles. *Angew Chem Int Ed* 2016;55:6182–6.
- [102] Zhang W, He J, Bao H, Dong X. Polymeric Janus nanoparticles from triblock terpolymer micellar dimers. *RSC Adv* 2015;5(126):104223–7.
- [103] Hils C, Schmelz J, Drechsler M, Schmalz H. Janus micelles by crystallization-driven self-assembly of an amphiphilic, double-crystalline triblock terpolymer. *J Am Chem Soc* 2021;143:15582–6.
- [104] Danial M, Tran CMN, Young PG, Perrier S, Jolliffe KA. Janus cyclic peptide–polymer nanotubes. *Nat Commun* 2013;4:2780–802.
- [105] Cheng L, Zhang GZ, Zhu L, Chen DY, Jiang M. Nanoscale tubular and sheetlike superstructures from hierarchical self-assembly of polymeric Janus particles. *Angew Chem Int Ed* 2008;47:10171–4.
- [106] Voets IK, de Keizer A, de Waard P, Frederik PM, Bomans PHH, Schmalz H, et al. Double-faced micelles from water-soluble polymers. *Angew Chem Int Ed* 2006;45:6673–6.
- [107] Voets IK, Fokkink R, Hellweg T, King SM, Waard Pd, Keizer Ad, et al. Spontaneous symmetry breaking: formation of Janus micelles. *Soft Matter* 2009;5(5):999–1005.
- [108] Albert SK, Lee S, Durai P, Hu X, Jeong B, Park K, et al. Janus nanosheets with face-selective molecular recognition properties from DNA-peptide conjugates. *Small* 2021;17(12):2006110. <https://doi.org/10.1002/smll.v17.1210.1002/smll.202006110>.
- [109] Long S, Chen CY, Luo J, Dong HY, Wu LM, Chen DY. A one-pot approach using recyclable template to prepare dual-responsive yolk-shell or Janus-like nanoparticles. *Polym Chem* 2016;7:7170–6.
- [110] Deng R, Li H, Zhu J, Li B, Liang F, Jia F, et al. Janus nanoparticles of block copolymers by emulsion solvent evaporation induced assembly. *Macromolecules* 2016;49(4):1362–8.
- [111] Zhou P, Liang F, Liu Y, Deng R, Yang H, Wang Q, et al. Janus colloidal copolymers. *Sci China Mater* 2015;58(12):961–8.
- [112] Tang L, Liang FX, Wang Q, Qu XZ, Jiang BY, Yang ZZ. Polymer/metal segmental Janus nanoparticles. *Chinese J Polym Sci* 2017;35:799–808.
- [113] Zhou F, Xie M, Chen D. Structure and ultrasonic sensitivity of the superparticles formed by self-assembly of single chain Janus nanoparticles. *Macromolecules* 2014;47(1):365–72.
- [114] Xu FG, Fang ZH, Yang DG, Gao Y, Li HM, Chen DY. Water in oil emulsion stabilized by tadpole-like single chain polymer nanoparticles and its application in biphasic reaction. *ACS Appl Mater Interfaces* 2014;6:6717–23.
- [115] Li W, Kuo C-H, Kanyo I, Thanneeru S, He J. Synthesis and self-assembly of amphiphilic hybrid nano building blocks via self-collapse of polymer single chains. *Macromolecules* 2014;47(17):5932–41.
- [116] Fan WZ, Tong X, Farnia F, Yu B, Zhao Y. CO<sub>2</sub>-responsive polymer single-chain nanoparticles and self-assembly for gas-tunable nanoreactors. *Chem Mater* 2017;29:5693–701.
- [117] Xiang D, Chen Xi, Tang L, Jiang B, Yang Z. Electrostatic-mediated intramolecular cross-linking polymers in concentrated solutions. *CCS Chem* 2019;1(5):407–30.
- [118] Wang JW, Chen X, Lang FZ, Yang LP, Qiu D, Yang ZZ. Large scale synthesis of single-chain/colloid Janus nanoparticles with tunable composition. *Chem Commun* 2021;57:5834–7.
- [119] Xiang D, Jiang B, Liang F, Yan L, Yang Z. Single-chain Janus nanoparticle by metallic complexation. *Macromolecules* 2020;53(3):1063–9.
- [120] Lang F, Xiang D, Wang J, Yang L, Qiao Y, Yang Z. Janus colloidal dimer by intramolecular cross-linking in concentrated solutions. *Macromolecules* 2020;53(6):2271–8.
- [121] Ji XT, Zhang Y, Zhao HY. Amphiphilic Janus twin single-chain nanoparticles. *Chem Eur J* 2018;24:3005–12.
- [122] Jiang Li, Xie M, Dou J, Li H, Huang X, Chen D. Efficient fabrication of pure, single-chain Janus particles through their exclusive self-assembly in mixtures with their analogues. *ACS Macro Lett* 2018;7(11):1278–82.
- [123] Jing JY, Yao XH, Yang ZZ. Single polymer chain grafted Fe<sub>3</sub>O<sub>4</sub> composite Janus nanoparticle. *Acta Polym Sin* 2018;8:1066–72.
- [124] Yang L, Xu J, Wang J, Lang F, Liu B, Yang Z. Responsive single-chain/colloid composite Janus nanoparticle. *Macromolecules* 2020;53(6):2264–70.
- [125] Han S, Pensec S, Yilmaz D, Lorthioir C, Jestin J, Guigner JM, et al. Straightforward preparation of supramolecular Janus nanorods by hydrogen bonding of end-functionalized polymers. *Nat Commun* 2020;11:4760–5.
- [126] Choisset T, Canevet D, Sallé M, Lorthioir C, Bouteiller L, Woisel P, et al. Colored Janus nanocylinders driven by supramolecular coassembly of donor and acceptor building blocks. *ACS Nano* 2021;15(2):2569–77.
- [127] Moughton AO, Hillmyer MA, Lodge TP. Multicompartment block polymer micelles. *Macromolecules* 2012;45(1):2–19.
- [128] Higuchi T, Tajima A, Motoyoshi K, Yabu H, Shimomura M. Frustrated phases of block copolymers in nanoparticles. *Angew Chem Int Ed* 2008;47:8044–6.
- [129] Deng RH, Liang FX, Zhou P, Zhang CL, Qu XZ, Wang Q, et al. Janus nanodisc of diblock copolymers. *Adv Mater* 2014;26:4469–72.
- [130] Xu J, Wang Ke, Li J, Zhou H, Xie X, Zhu J. ABC triblock copolymer particles with tunable shape and internal structure through 3D confined assembly. *Macromolecules* 2015;48(8):2628–36.
- [131] Qiang XL, Steinhaus A, Chen C, Chakroun R, Gröschel AH. Template-free synthesis and selective filling of Janus nanocups. *Angew Chem Int Ed* 2019;58:7122–6.
- [132] Deng R, Liang F, Qu X, Wang Q, Zhu J, Yang Z. Diblock copolymer based Janus nanoparticles. *Macromolecules* 2015;48(3):750–5.
- [133] Deng R, Li H, Liang F, Zhu J, Li B, Xie X, et al. Soft colloidal molecules with tunable geometry by 3D confined assembly of block copolymers. *Macromolecules* 2015;48(16):5855–60.
- [134] Saito N, Kagari Y, Okubo M. Effect of colloidal stabilizer on the shape of polystyrene/poly(methyl methacrylate) composite particles prepared in aqueous medium by the solvent evaporation method. *Langmuir* 2006;22(22):9397–402.
- [135] Tanaka T, Nakatsuru R, Kagari Y, Saito N, Okubo M. Effect of molecular weight on the morphology of polystyrene/poly(methyl methacrylate) composite particles prepared by the solvent evaporation method. *Langmuir* 2008;24(21):12267–71.
- [136] Saito N, Nakatsuru R, Kagari Y, Okubo M. Formation of “snowman-like” polystyrene/poly(methyl methacrylate)/toluene droplets dispersed in an aqueous solution of a nonionic surfactant at thermodynamic equilibrium. *Langmuir* 2007;23(23):11506–12.
- [137] Ahmad H, Saito N, Kagawa Y, Okubo M. Preparation of micrometer-sized, monodisperse “Janus” composite polymer particles having temperature-sensitive polymer brushes at half of the surface by seeded atom transfer radical polymerization. *Langmuir* 2008;24(3):688–91.
- [138] Tanaka T, Okayama M, Kitayama Y, Kagawa Y, Okubo M. Preparation of “mushroom-like” Janus particles by site-selective surface-initiated atom transfer radical polymerization in aqueous dispersed systems. *Langmuir* 2010;26(11):7843–7.

- [139] Tanaka T, Okayama M, Minami H, Okubo M. Dual stimuli-responsive “mushroom-like” Janus polymer particles as particulate surfactants. *Langmuir* 2010;26(14):11732–6.
- [140] Wang Yi, Guo B-H, Wan X, Xu J, Wang X, Zhang Y-P. Janus-like polymer particles prepared via internal phase separation from emulsified polymer/oil droplets. *Polymer* 2009;50(14):3361–9.
- [141] Hsu C, Du Yi, Wang X. Janus and strawberry-like particles from azo molecular glass and polydimethylsiloxane oligomer. *Langmuir* 2017;33(40):10645–54.
- [142] Ku KH, Lee YJ, Yi G-R, Jang SG, Schmidt BVKJ, Liao K, et al. Shape-tunable biphasic Janus particles as pH-responsive switchable surfactants. *Macromolecules* 2017;50(23):9276–85.
- [143] Wang Q, Xiao AQ, Shen ZH, Fan XH. Janus particles with tunable shapes prepared by asymmetric bottlebrush block copolymers. *Polym Chem* 2019;10:372–8.
- [144] Hou X, Guan S, Qu T, Wu X, Wang D, Chen A, et al. Light-triggered reversible self-engulfing of Janus nanoparticles. *ACS Macro Lett* 2018;7(12):1475–9.
- [145] Hu SH, Gao XH. Nanocomposites with spatially separated functionalities for combined imaging and magnetolytic therapy. *J Am Chem Soc* 2010;132:7234–7.
- [146] Lim YGJ, Poh KCW, Loo SCJ. Hybrid Janus microparticles achieving selective encapsulation for theranostic applications via a facile solvent emulsion method. *Macromol Rapid Commun* 2019;40(7):1800801. <https://doi.org/10.1002/marc.v40.710.1002/marc.201800801>.
- [147] Wei C, Du YX, Liu YY, Lin XQ, Zhang C, Yao JN, et al. Organic Janus microspheres: a general approach to all-color dual-wavelength microlasers. *J Am Chem Soc* 2019;141:5116–20.
- [148] Zhang YJ, Kang L, Huang HJ, Deng JP. Optically active Janus particles constructed by chiral helical polymers through emulsion polymerization combined with solvent evaporation-induced phase separation. *ACS Appl Mater Interfaces* 2020;12:6319–27.
- [149] Okubo M, Fujibayashi T, Yamada M, Minami H. Monodisperse, snowman/confetti-shaped polymer particles by seeded dispersion polymerization. *Colloid Polym Sci* 2005;283:1041–5.
- [150] Fujibayashi T, Komatsu Y, Konishi N, Yamori H, Okubo M. Effect of polymer polarity on the shape of “golf ball-like” particles prepared by seeded dispersion polymerization. *Ind Eng Chem Res* 2008;47:6445–9.
- [151] Skelton TS, Chen Y, Bon SAF. Synthesis of “hard-soft” Janus particles by seeded dispersion polymerization. *Langmuir* 2014;30(45):13525–32.
- [152] Skelton TS, Chen Y, Bon SAF. Hierarchical self-assembly of “hard-soft” Janus particles into colloidal molecules and larger supracolloidal structures. *Soft Matter* 2014;10(39):7730–5.
- [153] Hosseinzadeh S, Saadat Y. Preparation of “hard-soft” Janus polymeric particles via seeded dispersion polymerization in the presence of n-paraffin droplets. *RSC Adv* 2015;5(44):35325–37.
- [154] Kim H, Cho J, Cho J, Park BJ, Kim JW. Magnetic-patchy Janus colloid surfactants for reversible recovery of Pickering emulsions. *ACS Appl Mater Interfaces* 2018;10:1408–14.
- [155] Tian L, Li B, Li X, Zhang QY. Janus dimers from tunable phase separation and reactivity ratios. *Polym Chem* 2020;11:4639–46.
- [156] Cho J, Cho J, Kim H, Lim M, Jo H, Kim H, et al. Janus colloid surfactant catalysts for in situ organic reactions in Pickering emulsion microreactors. *Green Chem* 2018;20(12):2840–4.
- [157] Chang F, van Ravensteyn BGP, Lacina KS, Kegel WK. Bifunctional Janus spheres with chemically orthogonal patches. *ACS Macro Lett* 2019;8(6):714–8.
- [158] Kim JW, Larsen RJ, Weitz DA. Synthesis of nonspherical colloidal particles with anisotropic properties. *J Am Chem Soc* 2006;128:14374–7.
- [159] Kim JW, Larsen RJ, Weitz DA. Uniform nonspherical colloidal particles with tunable shapes. *Adv Mater* 2007;19:2005–9.
- [160] Li YF, Chen SS, Demirci S, Qin SY, Xu ZH, Olson E, et al. Morphology evolution of Janus dumbbell nanoparticles in seeded emulsion polymerization. *J Colloid Interface Sci* 2019;543:34–42.
- [161] Bradley LC, Stebe KJ, Lee D. Clickable Janus particles. *J Am Chem Soc* 2016;138:11437–40.
- [162] Fan J-B, Liu H, Song Y, Luo Z, Lu Z, Wang S. Janus particles synthesis by emulsion interfacial polymerization: polystyrene as seed or beyond? *Macromolecules* 2018;51(5):1591–7.
- [163] Mock EB, Zukoski CF. Emulsion polymerization routes to chemically anisotropic particles. *Langmuir* 2010;26(17):13747–50.
- [164] Misra A, Urban MW. Acorn-shape polymeric nano-colloids: synthesis and self-assembled films. *Macromol Rapid Commun* 2010;31:119–27.
- [165] Tang C, Zhang C, Liu J, Qu X, Li J, Yang Z. Large scale synthesis of Janus submicrometer sized colloids by seeded emulsion polymerization Janus anisotropic hybrid particles with tunable size from patchy composite spheres. *Macromolecules* 2010;43(11):5114–20.
- [166] Sun Y, Liang F, Qu X, Wang Q, Yang Z. Robust reactive Janus composite particles of snowman shape. *Macromolecules* 2015;48(8):2715–22.
- [167] Zhao R, Yu X, Sun D, Huang L, Liang F, Liu Z. Functional Janus particles modified with ionic liquids for dye degradation. *ACS Appl Nano Mater* 2019;2(4):2127–32.
- [168] Yu X, Sun Y, Liang F, Jiang B, Yang Z. Triblock Janus particles by seeded emulsion polymerization. *Macromolecules* 2019;52(1):96–102.
- [169] Li BH, Wang M, Chen K, Cheng ZF, Chen GJ, Zhang ZX. Synthesis of bifunctional Janus particles. *Macromol Rapid Commun* 2015;36:1200–4.
- [170] Kang CJ, Hooncic A. Versatile triblock Janus nanoparticles: synthesis and self-assembly. *Chem Mater* 2019;31:1688–95.
- [171] Yu HK, Mao ZW, Wang DY. Genesis of anisotropic colloidal particles via protrusion of polystyrene from polyelectrolyte multilayer encapsulation. *J Am Chem Soc* 2009;131:6366–7.
- [172] Park JG, Forster JD, Dufresne ER. High-yield synthesis of monodisperse dumbbell-shaped polymer nanoparticles. *J Am Chem Soc* 2010;132:5960–1.
- [173] Forster JD, Park J-G, Mittal M, Noh H, Schreck CF, O’Hern CS, et al. Dufresne, assembly of optical-scale dumbbells into dense photonic crystals. *ACS Nano* 2011;5(8):6695–700.
- [174] Wang FW, Liu HR, Zhang Y, Liu HW, Ge XW, Zhang XY. Synthesis of snowman-like polymer-silica asymmetric particles by combination of hydrolytic condensation process with  $\gamma$ -ray radiation initiated seeded emulsion polymerization. *J Polym Sci Polym Chem* 2014;52:339–48.
- [175] Wang FW, Liu HR, Zhao LL, Zhang XY. Facile fabrication of polymer-inorganic hybrid particles with various morphologies by combination of hydrolytic condensation process with radiation seeded emulsion polymerization. *Colloid Polym Sci* 2014;292:1171–9.
- [176] Onishi S, Tokuda M, Suzuki T, Minami H. Preparation of Janus particles with different stabilizers and formation of one-dimensional particle arrays. *Langmuir* 2015;31(2):674–8.
- [177] Qiu JC, Chen ZT, Chi MF, Xia YN. Swelling-induced symmetry breaking: A versatile approach to the scalable production of colloidal particles with a Janus structure. *Angew Chem Int Ed* 2021;60:12980–4.
- [178] Liu B, Liu J, Liang F, Wang Q, Zhang C, Qu X, et al. Robust anisotropic composite particles with tunable Janus balance. *Macromolecules* 2012;45(12):5176–84.
- [179] Lotierzo A, Longbottom BW, Lee WH, Bon SAF. Synthesis of Janus and patchy particles using nanogels as stabilizers in emulsion polymerization. *ACS Nano* 2019;13(1):399–407.
- [180] Pham BTT, Such CH, Hawkett BS. Synthesis of polymeric Janus nanoparticles and their application in surfactant-free emulsion polymerizations. *Polym Chem* 2015;6:426–35.
- [181] Li C, Wu ZM, He YF, Song PF, Zhai WZ, Wang RM. A facile fabrication of amphiphilic Janus and hollow latex particles by controlling multistage emulsion polymerization. *J Colloid Interf Sci* 2014;426:39–43.
- [182] Hou H, Yu D, Tian Q, Hu G. Preparation, characterization, and properties of hollow Janus particles with tailored shapes. *Langmuir* 2014;30(7):1741–7.
- [183] Reculusa S, Legrand CP, Perro A, Duguet E, Lami EB, Mingotaud C, et al. Hybrid dissymmetrical colloidal particles. *Chem Mater* 2005;17:3338–44.
- [184] Bladé T, Malosse L, Duguet E, Lansalot M, Lami EB, Ravaine S. Synthesis of nanoscaled poly(styrene-co-n-butylacrylate)/silica particles with dumbbell- and snowman-like morphologies by emulsion polymerization. *Polym Chem* 2014;5:5609–16.
- [185] Ge JP, Hu YX, Zhang TR, Yin YD. Superparamagnetic composite colloids with anisotropic structures. *J Am Chem Soc* 2007;129:8974–5.
- [186] Zhang CL, Liu B, Tang C, Liu JG, Qu XZ, Yang ZZ. Large scale synthesis of Janus submicron sized colloid by wet etching anisotropic ones. *Chem Commun* 2010;46:4610–2.
- [187] Feyen M, Weidenthaler C, Schüth F, Lu AH. Regioselectively controlled synthesis of colloidal mushroom nanostructures and their hollow derivatives. *J Am Chem Soc* 2010;132:6791–9.
- [188] Passas-Lagos E, Schüth F. Amphiphilic Pickering emulsifiers based on mushroom-type Janus particles. *Langmuir* 2015;31(28):7749–57.

- [189] Qiang W, Wang Y, He P, Xu H, Gu H, Shi D. Synthesis of asymmetric inorganic/polymer nanocomposite particles via localized substrate surface modification and miniemulsion polymerization. *Langmuir* 2008;24(3):606–8.
- [190] Wang Y, Xu H, Ma Y, Guo F, Wang F, Shi D. Facile one-pot synthesis and morphological control of asymmetric superparamagnetic composite nanoparticles. *Langmuir* 2011;27(11):7207–12.
- [191] Wang F, Pauletti GM, Wang JT, Zhang JM, Ewing RC, Wang YL, et al. Dual surface-functionalized Janus nanocomposites of polystyrene/Fe<sub>3</sub>O<sub>4</sub>@SiO<sub>2</sub> for simultaneous tumor cell targeting and stimulus-induced drug release. *Adv Mater* 2013;25:3485–9.
- [192] Teo BM, Suh SK, Hattori TA, Ashokkumar M, Grieser F. Sonochemical synthesis of magnetic Janus nanoparticles. *Langmuir* 2011;27(1):30–3.
- [193] Yu XJ, Huang SB, Chen KM, Zhou ZM, Guo XH, Li L. Preparation of functional Janus particles with response to magnetic force. *Ind Eng Chem Res* 2015;54:2690–6.
- [194] Söz ÇK, Trosien S, Biesalski M. Janus Interface materials: a critical review and comparative study. *ACS Mater Lett* 2020;2:336–57.
- [195] Kirillova A, Marschelke C, Synytska A. Hybrid Janus particles: challenges and opportunities for the design of active functional interfaces and surfaces. *ACS Appl Mater Interfaces* 2019;11:9643–71.
- [196] Bradley LC, Chen W-H, Stebe KJ, Lee D. Janus and patchy colloids at fluid interface. *Curr Opin Colloid Inter Sci* 2017;30:25–33.
- [197] Liang F, Liu B, Cao Z, Yang Z. Janus colloids toward interfacial engineering. *Langmuir* 2018;34(14):4123–31.
- [198] Marschelke C, Fery A, Synytska A. Janus particles: from concepts to environmentally friendly materials and sustainable applications. *Colloid Polym Sci* 2020;298:841–65.
- [199] Wu Z, Li Li, Liao T, Chen X, Jiang W, Luo W, et al. Janus nanoarchitectures: from structural design to catalytic applications. *Nano Today* 2018;22:62–82.
- [200] Zhang J, Grzybowski BA, Granick S. Janus particle synthesis, assembly, and application. *Langmuir* 2017;33(28):6964–77.
- [201] Yáñez-Sedeño P, Campuzano S, Pingarrón JM. Janus particles for (bio)sensing. *Appl Mater Today* 2017;9:276–88.
- [202] Su H, Price CAH, Jing L, Tian Q, Liu J, Qian K. Janus particles: design, preparation, and biomedical applications. *Nano Today* 2019;4:100033–51.
- [203] Le TC, Zhai J, Chiu WH, Tran PA, Tran N. Janus particles: recent advances in the biomedical applications. *Int J Nanomed* 2019;14:6749–77.
- [204] Zhang YF, Huang K, Lin J, Huang P. Janus nanoparticles in cancer diagnosis, therapy and theranostics. *Biomater Sci* 2019;7:1262–75.
- [205] Sun DY, Si Y, Song XM, Liang FX, Yang ZZ. Bi-continuous emulsion using Janus particles. *Chem Commun* 2019;55:4667–70.
- [206] Liu Y, Xu X, Liang F, Yang Z. Polymeric Janus nanosheets by template RAFT polymerization. *Macromolecules* 2017;50(22):9042–7.
- [207] Xue D, Song X, Liang F. Ultrathin Janus nanodiscs. *RSC Adv* 2017;7(41):25450–4.
- [208] Walther A, Matussek K, Müller AHE. Engineering nanostructured polymer blends with controlled nanoparticle location using Janus particles. *ACS Nano* 2008;2(6):1167–78.
- [209] Bahrami R, Löbbling TI, Gröschel AH, Schmalz H, Müller AHE, Altstädt V. The impact of Janus nanoparticles on the compatibilization of immiscible polymer blends under technologically relevant conditions. *ACS Nano* 2014;8(10):10048–56.
- [210] Bryson KC, Löbbling TI, Müller AHE, Russell TP, Hayward RC. Using Janus nanoparticles to trap polymer blend morphologies during solvent-evaporation-induced demixing. *Macromolecules* 2015;48:4220–7.
- [211] Nie H, Zhang C, Liu Y, He A. Synthesis of Janus rubber hybrid particles and interfacial behavior. *Macromolecules* 2016;49(6):2238–44.
- [212] Hou Y, Zhang GL, Tang XP, Si Y, Song XM, Liang FX, et al. Janus nanosheets synchronously strengthen and toughen polymer. *Macromolecules* 2019;52:3863–8.
- [213] Guan J, Gui H, Zheng Y, You J, Li Y, Liang F, et al. Stabilizing polymeric interface by Janus nanosheet. *Macromol Rapid Commun* 2020;41(19):2000392. <https://doi.org/10.1002/marc.v41.1910.1002/marc.202000392>.
- [214] Kong X, Wu CC, Feng L, Qu JY, Liu PG, Wang XM, et al. Silica-based hierarchical porous Janus microcapsules: construction and support of Au nanoparticle catalyst inside. *Chem Commun* 2017;53:8054–7.
- [215] Xu XY, Liu YJ, Gao Y, Li HM. Preparation of Au@silica Janus nanosheets and their catalytic application. *Colloids Surf A Physicochem Eng Aspects* 2017;529:613–20.
- [216] Yang JY, Wang JL, Liu YJ, Li HM, Lin ZQ. Stimuli-responsive Janus mesoporous nanosheets towards robust interfacial emulsification and catalysis. *Mater Horiz* 2020;7:3242–9.
- [217] Yan S, Zou HB, Chen S, Xue N, Yang HQ. Janus mesoporous silica nanosheets with perpendicular mesochannels: affording highly accessible reaction interfaces for enhanced biphasic catalysis. *Chem Commun* 2018;54:10455–8.
- [218] Zhao Ruotong, Han Tianhao, Sun Dayin, Huang Liyan, Liang Fuxin, Liu Zhengping. Poly(ionic liquid)-modified magnetic Janus particles for dye degradation. *Langmuir* 2019;35(35):11435–42.
- [219] Zhang MJ, Tang ZY, Fu WQ, Wang WY, Tan R, Yin DH. An ionic liquid-functionalized amphiphilic Janus material as a Pickering interfacial catalyst for asymmetric sulfoxidation in water. *Chem Commun* 2019;55:592–5.
- [220] Tang Xiuping, Hou Yu, Meng Qing Bo, Zhang Guolin, Liang Fuxin, Song Xi-Ming. Heteropolyacids-functionalized Janus particles as catalytic emulsifier for heterogeneous acylation in flow ionic liquid-in-oil Pickering emulsion. *Colloids Surf A Physicochem Eng Aspects* 2019;570:191–8.
- [221] Xia LX, Zhang HR, Wei ZC, Jiang Y, Zhang L, Zhao J, et al. Catalytic emulsion based on Janus nanosheets for ultra-deep desulfurization. *Chem Eur J* 2017;23:1920–9.
- [222] Vafaezadeh Majid, Breuninger Paul, Löscher Philipp, Wilhelm Christian, Ernst Stefan, Antonyuk Sergiy, et al. Janus interphase organic-inorganic hybrid materials: novel water friendly heterogeneous catalysts. *ChemCatChem* 2019;11(9):2304–12.
- [223] Wu G, Zhao LL, Liang HZ, Yan YH, Tan H. Janus hollow polymeric hairy microspheres as efficient adsorbents and catalyst scaffolds. *Mater Chem Front* 2019;3:922–30.
- [224] Chen JY, Li H, Fan C, Meng QW, Tang YW, Qiu XY, et al. Dual single-atomic Ni-N<sub>4</sub> and Fe-N<sub>4</sub> sites constructing Janus hollow graphene for selective oxygen electrocatalysis. *Adv Mater* 2020;32:2003134–44.
- [225] Hu Yuandu, Wang Jianying, Li Chengnian, Wang Qin, Wang Hong, Zhu Jintao, et al. Janus photonic crystal microspheres: centrifugation-assisted generation and reversible optical property. *Langmuir* 2013;29(50):15529–34.
- [226] Liu SS, Wang CF, Wang XQ, Zhang J, Tian Y, Yin SN, et al. Tunable Janus colloidal photonic crystal supraballs with dual photonic band gaps. *J Mater Chem C* 2014;2:9431–8.
- [227] Forster Jason D, Park Jin-Gyu, Mittal Manish, Noh Heeso, Schreck Carl F, O'Hern Corey S, et al. Assembly of optical-scale dumbbells into dense photonic crystals. *ACS Nano* 2011;5(8):6695–700.
- [228] Nisisako T, Torii T, Takahashi T, Takizawa Y. Synthesis of monodisperse bicolored Janus particles with electrical anisotropy using a microfluidic co-flow system. *Adv Mater* 2006;18:1152–6.
- [229] Kim SH, Jeon SJ, Jeong WC, Park HS, Yang SM. Optofluidic synthesis of electroresponsive photonic Janus balls with isotropic structural colors. *Adv Mater* 2008;20:4129–34.
- [230] Fialkowski M, Bitner A, Grzybowski BA. Self-assembly of polymeric microspheres of complex internal structures. *Nat Mater* 2005;4:93–7.
- [231] Behrend CJ, Anker JN, McNaughton BH, Kopelman R. Microrheology with modulated optical nanoprobes (MOONs). *J Magn Mater* 2005;293:663–70.
- [232] Behrend CJ, Anker JN, Kopelman R. Brownian modulated optical nanoprobes. *Appl Phys Lett* 2004;84:154–6.
- [233] Yang TT, Li YY, Gui HG, Du DM, Du Y, Song XM, et al. Superhydrophobic coating derived from the spontaneous orientation of Janus particles. *ACS Appl Mater Interfaces* 2021;13:25392–9.
- [234] Wang YJ, Song SF, Yuan JF, Zhu L, Pan MW, Liu G. Architecture and performance of raspberry-like colloidal particle clusters via self-assembly of in situ generated Janus Pparticles. *Ind Eng Chem Res* 2018;57:8907–17.
- [235] Kirillova A, Marschelke C, Friedrichs J, Werner C, Synytska A. Hybrid hairy Janus particles as building blocks for antibiofouling surfaces *ACS Appl. Mater Interfaces* 2016;8:32591–603.
- [236] Kirillova A, Ionov L, Roisman IV, Synytska A. Hybrid hairy Janus particles for anti-icing and de-icing surfaces: synergism of properties and effects. *Chem Mater* 2016;8:6995–7005.

- [237] Cheng L, Hou GL, Miao JJ, Chen DY, Jiang M, Zhu L. Efficient synthesis of unimolecular polymeric Janus nanoparticles and their unique self-assembly behavior in a common solvent. *Macromolecules* 2008;41:8159–66.
- [238] Cao W, Huang RL, Qi W, Su RX, He ZM. Self-assembly of amphiphilic Janus particles into monolayer capsules for enhanced enzyme catalysis in organic media. *ACS Appl Mater Interfaces* 2015;7:465–73.
- [239] Yi Y, Sanchez L, Gao Y, Yu Y. Janus particles for biological imaging and sensing. *Analyst* 2016;141:3526–39.
- [240] Fan XS, Yang J, Loh XJ, Li ZB. Polymeric Janus nanoparticles: recent advances in synthetic strategies, materials properties, and applications. *Macromol Rapid Commun* 2019;40:1800203–21.
- [241] Tran LTC, Lesieur S, Faivre V. Janus nanoparticles: materials, preparation and recent advances in drug delivery. *Expert Opin Drug Deliv* 2014;11:1061–74.
- [242] López V, Villegas MR, Rodríguez V, Villaverde G, Lozano D, Baeza A, et al. Janus mesoporous silica nanoparticles for dual targeting of tumor cells and mitochondria. *ACS Appl Mater Interfaces* 2017;9:26697–706.
- [243] Zhang WT, Choi H, Yua B, Kim DH. Synthesis of iron oxide nanocube patched Janus magnetic nanocarriers for cancer therapeutic applications. *Chem Commun* 2020;56:8810–3.
- [244] Han B, Xia WD, Liu KN, Tian FC, Chen Y, Wang XY, et al. Janus nanoparticles for improved dentin bonding. *ACS Appl Mater Interfaces* 2018;10:8519–26.



**Yijiang Liu** received Master degree majoring in polymer chemistry and physics from Xiangtan University in 2009. In 2015, she received Ph.D degree in polymer physics and chemistry from Institute of Chemistry, Chinese Academy of Sciences (ICCAS) under supervision by Prof. ZZ Yang. Now, she is associate professor in Xiangtan University. Her research is focused on synthesis and performance of 2D Janus nanosheets, and polymer-based carbon materials and the electrochemical performance.



**Jialin Wang** is now postgraduate student in College of Chemistry, Xiangtan University. Her research concerns with synthesis and performance of Janus nanosheets and perovskite nanocrystals.



**Yue Shao** is currently a master student at Department of Chemical Engineering, Tsinghua University under the supervision by Prof. ZZ Yang. His research involves design and synthesis of Janus composites and the self-organized nanostructures.



**Renhua Deng** received Bachelor (2010) and Ph.D. (2015) from Huazhong University of Science and Technology (HUST) under the supervision of Prof. Jintao Zhu and Prof. Zhenzhong Yang. From 2016 to 2019, he worked as a research associate at University of Sheffield, Durham University, and the University of Bristol. He joined HUST as a professor in 2019. His research interests include the synthesis and self-assembly of block copolymer and inkjet printing of nanomaterials.



**Jintao Zhu** is professor in School of Chemistry and Chemical Engineering, HUST. He received Bachelor (2000) and Master degrees (2002) at Hunan University, and Ph.D. (2005) at Changchun Institute of Applied Chemistry, Chinese Academy of Science. After postdoctoral research at University of Alberta and University of Massachusetts at Amherst, he joined HUST as professor in 2009. His current research involves self-assembled polymers and nanoparticles for nanophotonics, healing materials, memory devices, and immunotherapy.



**Zhenzhong Yang** received Bachelor at Tsinghua University (1991), Master at Jilin University (1994) and Ph.D at ICCAS (1997). After postdoctoral research in polymer central laboratory of BASF at Ludwigshafen (1997-1998), he joined ICCAS as assistant professor. In 2003, he was promoted as full professor. In 2018, he moved to Department of Chemical Engineering, Tsinghua University. His research interests cover methodology of polymer composites with precisely tunable macroscopic morphology and microstructure/spatial compartmentalization of components thus performances. The composites include hollow spheres and capsules; mesoporous membranes. Currently, he focuses on methodology of Janus nanocomposites, performances, and practical applications.